

Causal Inference on Sequential Treatments via Tensor Completion

Chenyin Gao*

Han Chen†

Anru R. Zhang‡

Shu Yang§

Abstract

Marginal Structural Models (MSMs) are popular for causal inference of sequential treatments in longitudinal observational studies, which however are sensitive to model misspecification. To achieve flexible modeling, we envision the potential outcomes to form a three-dimensional tensor indexed by subject, time, and treatment regime and propose a tensorized history-restricted MSM (HRMSM). The semi-parametric tensor factor model allows us to leverage the underlying low-rank structure of the potential outcomes tensor and exploit the pre-treatment covariate information to recover the counterfactual outcomes. We incorporate the inverse probability of treatment weighting in the loss function for tensor completion to adjust for time-varying confounding. Theoretically, a non-asymptotic upper bound on the Frobenius norm error for the proposed estimator is provided. Empirically, simulation studies show that the proposed tensor completion approach outperforms the parametric HRMSM and existing matrix/tensor completion methods. Finally, we illustrate the practical utility of the proposed approach to study the effect of ventilation on organ dysfunction from the Medical Information Mart for Intensive Care database.

Keywords: Gradient descent, Penalized estimation, Tucker decomposition, Non-asymptotic error, Sieve approximation

1 Introduction

Randomized trial studies have been recognized as the gold standard for learning causality due to the randomization of treatments that ensure the patients exposed to one treatment resemble those exposed to another in all possible pre-treatment covariates. However, inferring causality in longitudinal studies becomes more challenging due to the presence of sequential treatments and time-varying confounding. As explained by J. M. Robins et al. (2000), standard regression methods, whether or not adjusting for confounders, are fallible when coping with sequential treatments. In response, *Marginal Structural Models* (MSMs) (J. M. Robins, 2000) and *Structural Nested Mean Models* (SNMMs) (J. M. Robins, 1994) have been proposed for causal inference in longitudinal studies, targeting different causal questions. MSMs are tailored to estimate the population-level (or marginal) causal effects, whereas SNMMs allow causal effects to be dynamically influenced by time-varying confounders. In particular, MSMs are well-suited for assessing the average impact of treatments on populations, which is the primary focus of our paper. However, these frameworks are often stringently parametric, as the standard estimation (e.g., G-computation (J. Robins, 1986)) typically relies on specific model assumptions for the outcomes, making them sensitive to model misspecification. In addition, they require a fixed time horizon setting and do not scale well to a

*Department of Statistics, North Carolina State University, Raleigh, NC

†Department of Statistical Science, Duke University, Durham, NC

‡Departments of Biostatistics & Bioinformatics and Computer Science, Duke University, Durham, NC

§Department of Statistics, North Carolina State University, Raleigh, NC

prolonged time horizon. There are several advanced, flexible machine learning methods built on encoder-decoder architectures to capture long-range, complex dependencies between outcomes and time-varying confounders (e.g., counterfactual recurrent network (CRN) Bica et al. (2020), G-Net (Li et al., 2021), and Causal Transformer (CT) (Melnichuk et al., 2022)). However, most of them only account for the instantaneous treatment effect (i.e., the effect of the current treatment on the current outcome). For example, CT uses an adversarial objective to produce time-varying representations that are balanced only on the current treatment assignment, which neglects the lagged treatment effect often widely seen in medical practice and, therefore, impedes their deployment when a delayed treatment effect is present.

As causal inference is essentially a missing data analysis, it can be closely related to a problem of matrix or tensor completion, which aims at recovering the underlying low-rank or approximately low-rank structure from the observed samples. In the longitudinal observational studies with sequential treatments, we develop a novel tensorized history-restricted Marginal Structural Model (HRMSM), an extension of MSMs assuming the sequential treatments only influence the outcomes on a short-term basis (Neugebauer et al., 2007). In practice, such as in critical care settings like MIMIC-III, clinical interventions often have effects that are most pronounced in the short term due to rapidly changing patient states. Our new perspective conceptualizes the potential outcomes as a three-dimensional tensor, with each tensor mode corresponding to the subject, time, and treatment regime (see Figure 1 for an illustration). Thus, the sequential treatment effect estimation problem is formulated as a tensor completion problem, allowing for the use of tensor structural information such as low rankness. In this paper, we substantiate the low rankness by the tensor factor model, i.e., the Tucker decomposition (Tucker, 1966). Hence, our proposal is model-free, utilizing the data-adaptive latent factors to recover the missing potential outcomes (i.e., counterfactuals) and making it less susceptible to model misspecification. Furthermore, our model scales well to a large sample size and a prolonged time horizon. For instance, if the outcomes remain stable across subjects over time, the latent factors associated with time can be exploited to enhance the precision of the estimated causal effects (Abadie et al., 2010).

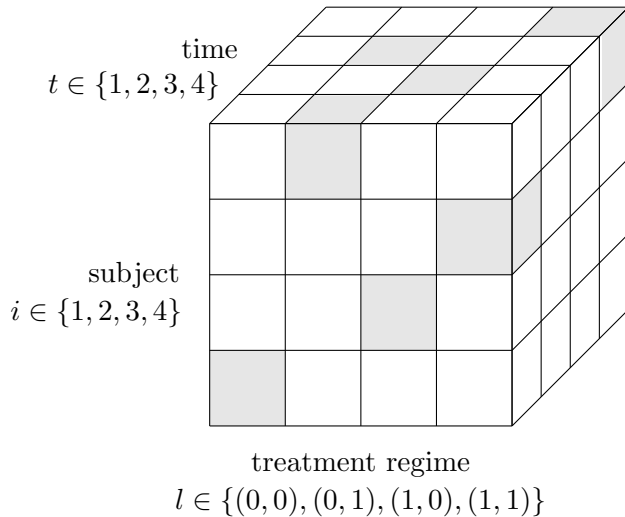


Figure 1: A illustration of potential outcomes tensor: a (subject \times time \times treatment regime) tensor of dimension $\mathbb{R}^{4 \times 4 \times 2^2}$ with $N = 4$, $T = 4$ and $k = 2$; the gray cells represent the observed entries, whereas the white cells represent the missing entries.

Tensor completion is one of the most actively studied problems in tensor-related literature and

has attracted broad attention in a wide range of applications (Xu & Yin, 2013; Semerci et al., 2014; Xie et al., 2016; Mandal & Parkes, 2019). Despite the intrinsic connection between causal inference and missing data analysis, most tensor completion methods cannot be directly employed as they often assume that the missingness occurs completely at random (Liu et al., 2012; Jain & Oh, 2014; Barak & Moitra, 2016; Xia et al., 2021; Cai et al., 2021) or specially designed (Zhang, 2019). However, the sequential treatment assignment in longitudinal studies can be an endogenous process, as its value may be affected by some time-dependent prognostic factors, rendering the independent Bernoulli missingness implausible. To properly handle the treatment endogeneity, we adopt sequential ignorability in Assumption 3, where treatment is sequentially randomized given the historical information. Under the assumption of sequential ignorability, an inverse probability of treatment weighted (IPTW) tensor completion algorithm is proposed to impute the counterfactuals; see Section 3.2.2 for more details. Certainly, other types of ignorability assumptions are available to handle treatment endogeneity. One possible assumption is latent ignorability, where the potential outcomes are conditional independent of the treatments given the observable and the latent factors. Therefore, the relationships between the subject-specific latent factors can be leveraged to impute the other missing outcomes (Agarwal & Syrgkanis, 2022; Agarwal et al., 2023). Typically, they require that subject-specific latent factors satisfy the well-supported condition, which stipulates that the latent factors associated with one subject are expressible as a linear combination of other subjects. This concept is akin to the incoherence condition usually required for tensor completion, where each tensor entry contains a similar amount of information, enabling the recovery of any missingness from the observed tensor. However, the latent ignorability assumption might not be reasonable in our context, as this independence is ascertained given all time-related latent factors, including the future ones.

Intuitively, the tensor completion problem can be solved with well-studied matrix completion algorithms by unfolding tensors into matrices (Tomioka et al., 2010; Gandy et al., 2011; Liu et al., 2012). Yet, such unfolding-based methods might discard the multi-way structure of the tensor and therefore lose additional correlational information among modes. To directly explore the tensor structures, Yuan & Zhang (2016, 2017) propose to use tensor nuclear norm minimization, which is guaranteed to be more efficient. However, the computation of tensor nuclear norm minimization is NP-hard in general, which may prevent its usage for real-data applications. One possible remedy is to restrict the feasible solutions in a sub-class of tensors, e.g., a class of low multi-linear rank tensors. Followed by a low-rank tensor space optimization algorithm, a polynomial-time computable estimator can be obtained (Xia & Yuan, 2017; Xia et al., 2021; Cai et al., 2021; Zhen & Wang, 2024). Furthermore, most works consider the low-rank completion based on the outcomes tensor only, whereas much fewer works focus on incorporating the baseline covariates to assist tensor completion with exceptions including Acar et al. (2011), T. Zhou et al. (2017), Ibriga & Sun (2022) and J. Zhou et al. (2021). In our paper, we incorporate the baseline covariates into the proposed tensorized HRMSM using the sieve approximation to capture their relationship with the potential outcomes, motivated by the semi-parametric tensor factor model in E. Y. Chen et al. (2020). Hence, instead of searching for the optimum in the unrestricted low-rank tensor space, we minimize the weighted loss function via the projected gradient descent optimizer in the covariate-relevant functional space with dimensions endowed by the order of sieve basis, which is faster and more stable.

Our contributions are summarized as follows: 1) we propose a tensorized HRMSM framework based on the Tucker decomposition for modeling the potential outcomes, which does not rely on stringent parametric assumptions, allows the incorporation of the baseline covariates for tensor completion, and scales well to a large sample size and an infinite time horizon setting; 2) theoretically, we provide a non-asymptotic upper bound on the Frobenius norm error for the completed

potential outcomes tensor, taking into account that the uncertainty in estimating the IPTW; and 3) empirically, we provide several synthetic experiments and a real-data application to highlight the benefits of the proposed framework comparing with existing competitors.

The rest of the paper is organized as follows. Section 2 layouts the longitudinal observational study and a set of essential assumptions. Section 3 illustrates the low-rank tensor completion paradigm and describes the proposed tensorized HRMSM in detail. Section 4 establishes the theoretical properties of our proposed method under the potential outcomes framework. A number of experiments are presented in Section 5 with a real-data application in Section 6. All the technical proofs and details are provided in the Appendix.

2 Causal inference with sequential treatments

2.1 Notation and causal assumptions

Let $X_{i,0}$ be a d_0 -vector of pre-treatment covariates, and $(X_{i,t}, Y_{i,t}, A_{i,t})$ be the vector of time-varying covariates, an outcome variable and a binary treatment for subject $i = 1, \dots, N$ at time $t = 1, \dots, T$. Next, we use the colon in the indices to select a slice (both ends inclusive) of a vector; e.g., $a_{1:T} = (a_1, a_2, \dots, a_T)$. Following J. M. Robins (2000), let $X_{i,t}^{a_{1:T}}$ and $Y_{i,t}^{a_{1:T}}$ be the potential time-varying covariates and the potential outcome at t had the subject i followed the treatment trajectory $a_{1:T} \in \mathbb{A}_T$, where \mathbb{A}_T includes all the possible treatment histories over T time points. The full data for subject i is summarized by $\mathbb{V}_{i,t} = \{(X_{i,0}, X_{i,1:t}^{a_{1:T}}, Y_{i,1:t}^{a_{1:T}}) : a_{1:T} \in \mathbb{A}_T\}$, and $\mathbb{V}_{i,t}$ is null for $t \leq 0$ by convention. By the nature of the data collection procedure, in which $X_{i,t-1}$ actualizes before $A_{i,t}$, and $A_{i,t}$ actualizes before $Y_{i,t}$, we assume $X_{i,1:t}^{a_{1:T}} = X_{i,1:t}^{a_{1:t}}$ and $Y_{i,t}^{a_{1:T}} = Y_{i,t}^{a_{1:t}}$, that is, the future treatments will not affect the present variables. Also, as many treatments influence each subject on a short-term basis, the entire treatment history prior to an event occurrence may not be all relevant (Feldman et al., 2004; Heron & Smyth, 2010). Following Neugebauer et al. (2007), we assume that the potential outcomes at time t depends on the current treatment a_t and the previous $(k-1)$ treatment assignments for $k \geq 2$.

Assumption 1 (k -history restricted potential outcomes). $Y_{i,t}^{a_{1:t}} = Y_{i,t}^{a_{(t-k+1):t}}$, where $k > 0$ is a integer, for all $a_{1:t}$, $i = 1, \dots, N$ and $t = 1, \dots, T$.

The fundamental problem in causal inference is that not all potential outcomes can be observed for a particular subject. Thus, the identification of causal effects requires further assumptions. Following van der Laan et al. (2005), we make the following assumptions.

Assumption 2 (Causal consistency). $X_{i,1:t} = X_{i,1:t}^{A_{i,1:t}}$ and $Y_{i,t} = Y_{i,t}^{A_{i,1:t}}$ for $i = 1, \dots, N$ and $t = 1, \dots, T$.

Assumption 3 (Sequential treatment randomization).

$$A_{i,t} \perp \left\{ \left(X_{i,0}, X_{i,1:t}^{(A_{1:(t-1)}, a_{t:T})}, Y_{i,1:t}^{A_{1:(t-1)}, a_{t:T}} \right) : a_{t:T} \in \mathbb{A}_{T-t+1} \right\} \mid H_{i,t},$$

where $H_{i,t} = (X_{i,0:(t-1)}, A_{i,1:(t-1)}, Y_{i,1:(t-1)})$, for $i = 1, \dots, N$ and $t = 1, \dots, T$.

Assumption 4. Let $e(H_{i,t}) = \mathbb{P}(A_{i,t} = 1 \mid H_{i,t})$ and there exists a constant $\delta < 0.5$ such that we have $0 < \delta < e(H_{i,t}) < 1 - \delta < 1$ for $t = 0, \dots, T$ almost surely.

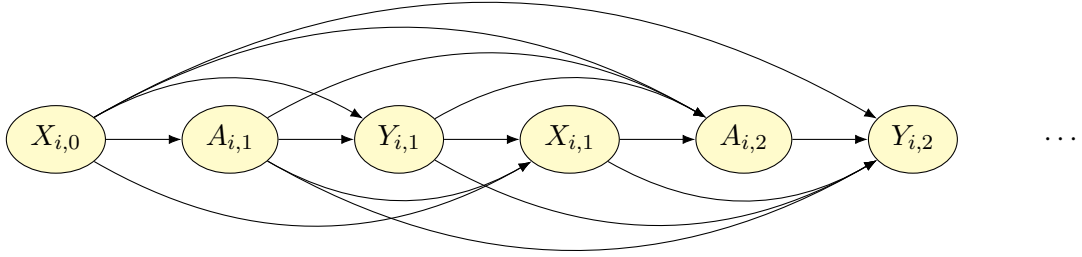


Figure 2: A directed acyclic graph illustrates the data-generating process of $(X_{i,0:T}, A_{i,1:T}, Y_{i,1:T})$ for individual i under Assumption 3.

Assumption 2 is necessary to consistently map the observed data with the potential outcomes without any interference between subjects. Assumption 3 implies that the treatment assignment at any time t is randomized among the subjects sharing the same value of the observed history accrued up to time t , also known as treatment ignorability or no unmeasured confounders. In the observational studies, Assumption 3 holds if the observed history contains all predictors of treatment assignment and outcome; see an example of a causal graph satisfying Assumption 3 in Figure 2. Assumption 4 is also known as the uniform overlap condition (Rosenbaum & Rubin, 1983), which ensures an adequate overlap between the treatment and control covariate distributions and allows each subject to have probability at least δ of receiving either treatment at each time point t . The parameter δ will play an important role in our main theoretical results. To provide some intuition, the potential outcomes under any treatment regime will have a positive probability of being observed. Thus, the recovery of any unobserved potential outcomes will be possible.

2.2 Marginal structural models

Marginal structural models (MSMs) are first established in J. Robins (1986) and rapidly become one of the most important types of models for causal inference in the presence of time-varying confounding. The MSMs impose parametric structural models for $Y_{i,t}^{a_{1:t}}$, which describe the marginal effect of time-varying treatments and possibly adjust for baseline treatment modification effects. Under Assumptions 1-4, we have

$$\mathbb{E}\{Y_{i,t}^{a_{(t-k+1):t}} \mid X_{i,0}\} = \mu(a_{(t-k+1):t}, X_{i,0}), \quad (1)$$

where $\mu(\cdot)$ is an unknown function of the past k treatments $a_{(t-k+1):t} \in \mathbb{A}_k$ and the baseline covariate $X_{i,0}$, termed as the history-restricted MSM (HRMSM), where \mathbb{A}_k includes all the possible treatment regimes over k time points (Neugebauer et al., 2007). Unlike the traditional MSMs, HRMSM only considers the treatments assigned between time $t - k + 1$ and t , instead of the entire treatment history $a_{1:t}$.

Let the time-specific IPTW estimating function be $\Psi(H_t \mid \mu, \eta_t)$ with a parametric structural model $\mu(a_{(t-k+1):t}, X_{i,0}; \eta_t)$ characterized by a fix-dimensional unknown parameter η_t . Under Assumptions 1-4, the IPTW can be used to consistently estimate η_t as in

$$\Psi(H_{i,t} \mid \mu, \eta_t) = w_{i,t} \frac{\partial \mu(A_{(t-k+1):t}, X_{i,0}; \eta_t)}{\partial \eta_t} \{Y_{i,t} - \mu(A_{(t-k+1):t}, X_{i,0}; \eta_t)\}, \quad (2)$$

with weights $w_{i,t} = \left[\prod_{j=t-k+1}^t e(H_{i,j})^{A_{i,j}} \{1 - e(H_{i,j})\}^{1-A_{i,j}} \right]^{-1}$. Therefore, the weight $w_{i,t}$ can be perceived as the inverse probability that subject i received his own observed treatment regime

$A_{i,(t-k+1):t}$ given his accrued history information $H_{i,t}$. By accounting for the statistic endogeneity of the treatment process $A_{i,t}$ with time-dependent confounders $X_{i,t}$, one can estimate the potential outcomes under any series of treatment regimes and establish a valid causal relationship. Example 1 is provided for an illustration.

Example 1. Suppose that $X_{i,0} \in \mathbb{R}^d$, $\mathbb{E}\{Y_{i,t}^{a_{(t-k+1):t}} | X_{i,0}\} = X_{i,0}^\top \eta_1 + \text{cum}(a_{(t-k+1):t})\eta_2 + t\eta_3$, where $\text{cum}(a_{(t-k+1):t})$ is the number of active treatments of the regimes $a_{(t-k+1):t}$, the HRMSM can be posited by $\mu(a_{(t-k+1):t}, X_{i,0}; \eta) = \{X_{i,0}^\top, \text{cum}(a_{(t-k+1):t}), t\}\eta$ with $\eta = (\eta_1, \eta_2, \eta_3)$ for $t = 1, \dots, T$.

Despite the appealing strengths of the HRMSM, its estimation error heavily hinges on the outcome model specification, which is usually restrictive and error-prone in practice. Although many other robust variants of MSMs have been formulated (Van der Laan et al., 2003; Mortimer et al., 2005; Yu & van der Laan, 2006), most of them exploit the latent factors over time in a stringent manner and thus do not scale well to large T . On the other hand, flexible machine learning techniques such as tensor completion tools have been proposed to handle missing data. Given the close relationship between causal inference and missing data analysis, one is motivated to see whether a flexible and efficient estimation can be achieved via low-rank tensor completion.

3 Tensor completion to causal inference

3.1 Preliminaries

Before we delve into the details of tensor completion, we introduce some basic notations, preliminaries, and tensor algebra, which can be helpful for our subsequent illustration. We use lowercase letters, e.g., x, y , to denote scalars, and the bold lowercase letters, e.g., \mathbf{x}, \mathbf{y} , are used to denote vectors. For any two vectors $\mathbf{x} \in \mathbb{R}^{p_1}, \mathbf{y} \in \mathbb{R}^{p_2}$, let $\mathbf{x} \otimes \mathbf{y} \in \mathbb{R}^{p_1 \times p_2}$ denotes their outer product. The bold uppercase letter such as \mathbf{X}, \mathbf{Y} are used to denote matrices, and the calligraphic letters \mathcal{X}, \mathcal{Y} are used to denote higher-order tensors. For any two tensors, say $\mathcal{X}, \mathcal{Y} \in \mathbb{R}^{p_1 \times p_2 \times p_3}$, let $\mathcal{X} \odot \mathcal{Y}$ denotes their entry-wise product $(\mathcal{X}\mathcal{Y})_{i_1, i_2, i_3} = \mathcal{X}_{i_1, i_2, i_3}\mathcal{Y}_{i_1, i_2, i_3}$, and $\langle \mathcal{X}, \mathcal{Y} \rangle$ denotes their inner product $\langle \mathcal{X}, \mathcal{Y} \rangle = \sum_{i_1, i_2, i_3} \mathcal{X}_{i_1, i_2, i_3}\mathcal{Y}_{i_1, i_2, i_3}$. Fibers and slices are two subarrays of tensors formed by fixing a subset of the indices. In particular, we define the fibers by $\mathcal{X}_{:, i_2, i_3} \in \mathbb{R}^{p_1}, \mathcal{X}_{i_1, :, i_3} \in \mathbb{R}^{p_2}, \mathcal{X}_{i_1, i_2, :} \in \mathbb{R}^{p_3}$, and the slices by $\mathcal{X}_{i_1, :, :} \in \mathbb{R}^{p_2 \times p_3}, \mathcal{X}_{:, i_2, :} \in \mathbb{R}^{p_1 \times p_3}, \mathcal{X}_{:, :, i_3} \in \mathbb{R}^{p_1 \times p_2}$.

Then, we introduce the unfolding (or the matricization) operator $\mathcal{M}_k(\cdot)$ that transforms tensors to matrices on mode- k . For example, after unfolding the tensor \mathcal{X} on its first mode, we have $\mathcal{M}_1(\mathcal{X}) \in \mathbb{R}^{p_1 \times p_2 p_3}$, where $[\mathcal{M}_1(\mathcal{X})]_{i_1, i_2 + p_2(i_3-1)} = \mathcal{X}_{i_1, i_2, i_3}$. Also, we introduce the mode- k tensor-matrix products. For example, let $\mathbf{U}_1 \in \mathbb{R}^{r_1 \times p_1}$, the mode-1 tensor-matrix multiplication is $\mathcal{X} \times_1 \mathbf{U}_1 \in \mathbb{R}^{r_1 \times p_2 \times p_3}$, where $(\mathcal{X} \times_1 \mathbf{U}_1)_{i_1, i_2, i_3} = \sum_{j_1=1}^{p_1} \mathcal{X}_{j_1, i_2, i_3} \mathbf{U}_{i_1, j_1}$. General mode- k matricization and mode- k tensor-matrix products can be defined in a similar manner. The multi-linear rank of \mathcal{X} is defined as the vector $(r_1, r_2, r_3) = \{\text{rank}(\mathcal{M}_1(\mathcal{X})), \text{rank}(\mathcal{M}_2(\mathcal{X})), \text{rank}(\mathcal{M}_3(\mathcal{X}))\}$. For any (r_1, r_2, r_3) multi-linear rank tensor \mathcal{X} in general, it can be factorized by the Tucker decomposition (Tucker, 1966) into a small core tensor $\mathcal{G} \in \mathbb{R}^{r_1 \times r_2 \times r_3}$ and three matrices $\mathbf{U}_i \in \mathbb{R}^{p_i \times r_i}$ with orthogonal columns, denoted as

$$\mathcal{X} = \mathcal{G} \times_1 \mathbf{U}_1 \times_2 \mathbf{U}_2 \times_3 \mathbf{U}_3 = [\mathcal{G}; \mathbf{U}_1, \mathbf{U}_2, \mathbf{U}_3], \quad (3)$$

where \mathcal{G} can be considered as the principal components with \mathbf{U}_i being the mode- i loading matrices. Next, as tensors are generalizations of matrices, several important matrix norms can be generalized under the tensor formulation (Landsberg, 2012; Hogben, 2013). Let the spectral norm of a tensor \mathcal{X} be $\|\mathcal{X}\| = \max\{\langle \mathcal{X}, \mathbf{a} \otimes \mathbf{b} \otimes \mathbf{c} \rangle : \mathbf{a} \in \mathbb{R}^{p_1}, \mathbf{b} \in \mathbb{R}^{p_2}, \mathbf{c} \in \mathbb{R}^{p_3}, \|\mathbf{a}\| = \|\mathbf{b}\| = \|\mathbf{c}\| = 1\}$, where we

use $\|\cdot\|$, with a little abuse of notations, to denote the spectral norm of a tensor and a matrix and the Euclidean norm of a vector. Likewise, the nuclear norm is $\|\mathcal{X}\|_* = \max\{\langle \mathcal{X}, \mathcal{Y} \rangle : \mathcal{Y} \in \mathbb{R}^{p_1 \times p_2 \times p_3}, \|\mathcal{Y}\| = 1\}$. Besides, let $\|\mathcal{X}\|_F = \sqrt{\langle \mathcal{X}, \mathcal{X} \rangle}$ and $\|\mathcal{X}\|_{\max} = \max_{i_1, i_2, i_3} |\mathcal{X}_{i_1, i_2, i_3}|$ be the Frobenius norm and max norm of a tensor, respectively; see Kolda & Bader (2009) for a more comprehensive review. We use c_0, C_0 to denote generic positive constants, whose actual values may vary from line to line.

3.2 Tensor and model formulation

3.2.1 Low-rank tensorized HRMSM with baseline covariates

To address these concerns, we envision the potential outcomes for N subjects at T times to form an $N \times T \times K$ tensor of three modes with entries $\mathcal{Y}_{i,t,l} = Y_{i,t}^{l(b)}$, where $K = 2^k$ and $l_{(b)}$ converts l from decimal to binary. Likewise, $\{a_{i,(t-k+1):t}\}_{(10)} = l$ is for decimal conversion. Take $k = 5$ as an example, we have $(3)_{(b)} = 00011$ and $(00101)_{(10)} = 5$. Therefore, the potential outcomes can be represented as a tensor of three modes, i.e., subject \times time \times treatment regime. Next, we assume that \mathcal{Y} admits the Tucker decomposition in (3) with noises, and the low-rank tensorized HRMSM is formulated by

$$\mathcal{Y} = \mathcal{Y}^* + \mathcal{E} = [\mathcal{G}^*; \mathbf{U}_1^*, \mathbf{U}_2^*, \mathbf{U}_3^*] + \mathcal{E}, \quad (4)$$

where $\mathcal{G}^* \in \mathbb{R}^{r_1 \times r_2 \times r_3}$, $\mathbf{U}_1^* \in \mathbb{R}^{N \times r_1}$, $\mathbf{U}_2^* \in \mathbb{R}^{T \times r_2}$, $\mathbf{U}_3^* \in \mathbb{R}^{K \times r_3}$, and all entries of \mathcal{E} are independent mean-zero sub-Gaussian random variables with $\text{var}(\mathcal{E}_{i,t,l}) \leq \sigma^2$. Various causal estimands can be easily formulated with the potential outcomes tensor \mathcal{Y} to assess the treatment effects. Let the causal estimand of our interest be the average treatment effect (ATE) between treatments $l_{(b)}$ and $l'_{(b)}$, defined as $\tau_{\text{ATE}}^{l,l'} = (NT)^{-1} \mathbb{E}[\sum_{i=1}^N \sum_{t=1}^T \{Y_{i,t}^{l(b)} - Y_{i,t}^{l'(b)}\}]$. It can be readily formulated by $\tau_{\text{ATE}}^{l,l'} = \mathcal{Y}^* \times_1 N^{-1} \mathbf{1}_N \times_2 T^{-1} \mathbf{1}_T \times_3 \{e_l(K) - e_{l'}(K)\}$ with the tensor representation, where $e_l(K)$ is a K -dimensional zero vector except its l -entry being 1.

Intuitively, the Tucker decomposition can be interpreted as the cluster heterogeneity or latent factors along each mode of \mathcal{Y} . For starters, the heterogeneity among subjects may be attributed to r_1 hidden factors, e.g., genetic or demographic factors. Second, the temporal variability may be dictated by a few time categories since diagnosis (e.g., early, middle, and late stages). Lastly, the variation of the sequential treatment regimes may be summarized into a few key factors, such as the number of cumulated treatments in the past. These latent factors, \mathbf{U}_1 , \mathbf{U}_2 , and \mathbf{U}_3 , are constructed in a data-adaptive way, making them more flexible and robust. For instance, suppose that \mathcal{Y}^* depends on some unknown function of the covariates X_0 . Our tensorized HRMSM can still accurately approximate the potential outcomes through the inferred factors \mathbf{U}_1 , without knowing the specific functional form, whereas the traditional MSMs are fallible if misspecified; see our simulation studies for more empirical evidence. To clarify our choice of tensor decomposition, we briefly compare Tucker decomposition with two widely used alternatives: the Canonical Polyadic (CP) and Tensor Train (TT) decompositions. CP decomposition imposes a common rank across all modes, which is overly restrictive for our data, where the latent structures underlying patients, time points, and treatment regimes differ substantially in complexity. TT decomposition is most suitable for higher-order tensors whose modes themselves admit an inherent sequential ordering. In our case, although the time mode has its own internal index order, the tensor is third-order and the three modes (time, treatment regimes, subjects) do not possess a meaningful sequence among the modes, so this requirement is not satisfied. In contrast, Tucker decomposition offers the flexibility of assigning different ranks to each mode and produces interpretable mode-specific latent factors.

These properties make Tucker decomposition well aligned with both the structure of our tensor representation and the scientific goals of our analysis.

Besides, the individual baseline covariates, such as age, gender, race, and general health status stored in $\mathbf{X}_0 \in \mathbb{R}^{N \times d_0}$ may assist tensor completion as it provides the covariate characteristic on the subject mode, leading to a covariate-assisted tensorized HRMSM; see Figure 3 (left). For concreteness, we assume the latent components associated with the subject-mode loading matrix \mathbf{U}_1^* can be partially explained by the matrix \mathbf{X}_0 , or more generally by $G^*(\mathbf{X}_0)$ based on an unknown function $G^* : \mathbb{R}^{N \times d_0} \rightarrow \mathbb{R}^{N \times r_1}$. Equivalently, we have $\mathbf{U}_1^* = G^*(\mathbf{X}_0) + \mathbf{\Gamma}$, where $\mathbf{\Gamma}$ is the residual component of \mathbf{U}_1^* after accounting for $G^*(\mathbf{X}_0)$, and $\{G^*(\mathbf{X}_0)\}^\top \mathbf{\Gamma} = 0$. Since both $G^*(\mathbf{X}_0)$ and $\mathbf{\Gamma}$ have orthonormal columns, we have $(\mathbf{U}_1^*)^\top \mathbf{U}_1^* = I_N$ by construction. This semi-parametric model is found in the matrix/tensor factor analysis literature (Bai & Li, 2012; Fan et al., 2016; E. Y. Chen et al., 2020). The key idea for estimating the unknown $G^*(\mathbf{X}_0)$ relies on the sieve approximation (X. Chen, 2007). Let $\Phi(\mathbf{X}_0) \in \mathbb{R}^{N \times d_\Phi}$ be the user-specified basis functions (e.g., B-spline, polynomial series), where each row corresponds to the subject and each column corresponds to a sieve basis. Let $\mathbf{B} \in \mathbb{R}^{d_\Phi \times r_1}$ be the unknown sieve coefficients matrix and $\mathbf{R} \in \mathbb{R}^{N \times r_1}$ be the residual matrix, we have $G^*(\mathbf{X}_0) = \Phi(\mathbf{X}_0)\mathbf{B} + \mathbf{R}$. Importantly, the error terms $\mathbf{\Gamma}$ and \mathbf{R} arise due to different reasons and cannot be absorbed into one single term, where $\mathbf{\Gamma}$ represents the system error unexplained by \mathbf{X}_0 while \mathbf{R} represents the approximation error originating from the sieve basis approximation. Thus, the proposed covariate-assisted tensorized HRMSM does not

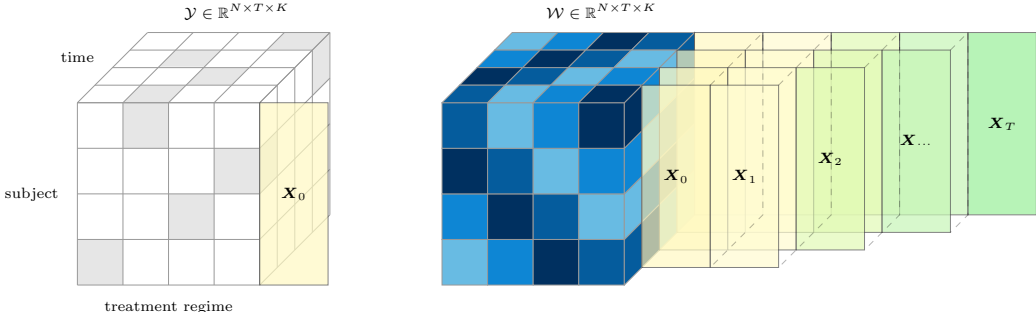


Figure 3: (Left) The potential outcomes tensor $\mathcal{Y} \in \mathbb{R}^{N \times T \times K}$ coupled with baseline covariates \mathbf{X}_0 ; (Right) The weight tensor $\mathcal{W} \in \mathbb{R}^{N \times T \times K}$ coupled with baseline covariates \mathbf{X}_0 and time-varying covariates $\mathbf{X}_{1:T}$; the gray cells represent the observed entries and the shades of blue cells represent the weight intensities.

involve restrictive parametric assumptions. We modify the running example in Example 1 for an illustration.

Example 2. Suppose that $X_{i,0} \in \mathbb{R}^d$, $\mathbb{E}\{Y_{i,t}^{a(t-k+1):t} \mid X_{i,0}\} = X_{i,0}^\top \eta_1 + (X_{i,0}^2)^\top \eta_2 + t\eta_3 + \text{cum}(a_{(t-k+1):t})\eta_4 + \text{cum}(a_{(t-k+1):t})X_{i,0}^\top \eta_5$, where $X_{i,0}^2$ is the coordinate-wise square of $X_{i,0}$. Let the basis function be constructed via polynomials up to the 2-nd order as $\Phi(X_{i,0}) = \{1, X_{i,0}^\top, (X_{i,0}^2)^\top\}^\top$. Then, we have

$$\mathbb{E}\left\{Y_{i,t}^{a(t-k+1):t} \mid X_{i,0}\right\} = \mathbb{E}(\mathcal{Y}_{i,t,l} \mid X_{i,0}) = \mathcal{G} \times_1 \Phi(X_{i,0})^\top \times_2 (1, t) \times_3 \{1, \text{cum}(l_{(b)})\},$$

where

$$\mathcal{G}_{1,:,:} = \begin{pmatrix} 0 & \eta_4 \\ \eta_3 & 0 \end{pmatrix}, \quad \mathcal{G}_{1+j,:,:} = \begin{pmatrix} \eta_{1,j} & \eta_{5,j} \\ 0 & 0 \end{pmatrix}, \quad \mathcal{G}_{1+d+j,:,:} = \begin{pmatrix} \eta_{2,j} & 0 \\ 0 & 0 \end{pmatrix}, \quad j = 1, \dots, d,$$

and therefore is encompassed by our tensorized HRMSM in (4).

3.2.2 Tensor completion and inverse probability treatment weighting

Due to the fundamental problem in the causal inference that only the potential outcomes under the actualized treatment can be observed, only $N \times T$ realizations of the potential outcomes are observed. To link our setup to the tensor completion literature, we define the observation pattern tensor as Ω , where $\Omega_{i,t,l} = 1$ if $l = \{A_{i,(t-k+1):t}\}_{(10)}$ and zero otherwise. Hence, only the potential outcomes $\mathcal{Y}_{i,t,l}$ whose associated subjects have actually received the treatment regime $l_{(b)}$ are observed. Despite recent advances in the tensor completion literature (Xia et al., 2021; Cai et al., 2021), most of them typically assume uniform missingness, that is, each entry of the observation pattern Ω follows independent and identical Bernoulli distributions. However, this assumption is unrealistic in causal inference with observational studies where the missingness of potential outcomes is tied to the actual treatment uptake, and the time-varying confounders can affect the treatment assignment.

Let \mathcal{W} be the propensity weight tensor with entries $\mathcal{W}_{i,t,l} = \mathbb{P}\{A_{i,(t-k+1):t} = l_{(b)} \mid H_{i,t}\}^{-1}$, which is the inverse product of a series of propensity scores. To obtain consistent causal estimation via tensor completion, the IPTW can be used to create a pseudo-population, where the missingness occurs randomly. In particular, we propose to recover the potential outcomes tensor by minimizing the following weighted loss function:

$$\min_{\mathcal{G}, \mathbf{U}_{1,X}, \mathbf{U}_2, \mathbf{U}_3} L(\mathcal{G}; \mathbf{U}_{1,X}, \mathbf{U}_2, \mathbf{U}_3; \mathcal{W}) = \min_{\mathcal{G}, \mathbf{U}_{1,X}, \mathbf{U}_2, \mathbf{U}_3} \frac{1}{2} \|\sqrt{\mathcal{W}} \odot \mathbf{P}_\Omega(\mathcal{Y} - [\mathcal{G}; \mathbf{U}_{1,X}, \mathbf{U}_2, \mathbf{U}_3])\|_F^2, \quad (5)$$

where $\sqrt{\mathcal{W}}$ is the entry-wise square root of \mathcal{W} , $\mathbf{U}_{1,X}$ lies in the column space of $\Phi(\mathbf{X}_0)$ and $\mathbf{P}_\Omega(\cdot)$ is the projection operator of any tensor onto the subspace of tensors whose entries vanish if $\Omega_{i,t,l} = 0$.

In practice, the weight tensor \mathcal{W} is often unknown and is replaced by the estimated weight tensor $\widehat{\mathcal{W}}$, yielded by the inverse product of the estimated propensity scores. As the time-varying confounders for each time point t are coupled with the weight tensor \mathcal{W} along the subject mode; see Figure 3 (right), the collected historical information $H_{i,t}$ can be utilized to assist in reasoning about the sequential treatment mechanism, i.e., the propensity weights; see Remark 1 for an example of weight tensor estimation.

Remark 1. *The most popular propensity score estimation is to use maximum likelihood estimation (MLE) at each time period. However, the dimension of $H_{i,t}$ keeps increasing as time t proceeds, which may lead to unstable estimation. Toward this end, a regularized maximum likelihood estimation can be adopted with a proper penalty, e.g., the Lasso penalty and smoothly clipped absolute deviation (SCAD) penalty. The penalized negative log-likelihood under the logistic modeling $e(H_{i,t}; \alpha_t)$ is*

$$\begin{aligned} \widehat{\alpha}_t &= \min_{\alpha_t = (\alpha_{0,t}, \alpha_{1,t})} \frac{1}{N} \sum_{i=1}^N \{\log(1 + e^{\alpha_{0,t} + \alpha_{1,t} H_{i,t}}) - A_{i,t}(\alpha_{0,t} + \alpha_{1,t} H_{i,t})\} + p_{\lambda_\alpha}(|\alpha_{1,t}|) \\ &= L_w(\alpha_t) + p_{\lambda_\alpha}(|\alpha_{1,t}|), \end{aligned} \quad (6)$$

where $L_w(\alpha_t)$ can be replaced with other loss function, e.g., the generalized quasi-likelihood function (Ning et al., 2020) and the covariate imbalance loss function (Lee et al., 2021), and $p_{\lambda_\alpha}(\cdot)$ is some penalization function gauged by the tuning parameter λ_α . Hence, the estimated weight tensor

$\widehat{\mathcal{W}} = (\widehat{\mathcal{W}}_{i,t,l}) \in \mathbb{R}^{N \times T \times K}$ is

$$\widehat{\mathcal{W}}_{i,t,l} = \left[\prod_{j=t-k+1}^t e(H_{i,j}; \widehat{\alpha}_j)^{A_{i,j}} \{1 - e(H_{i,j}; \widehat{\alpha}_j)\}^{1-A_{i,j}} \right]^{-1},$$

where $l = \{A_{i,(t-k+1):t}\}_{(10)}$.

3.2.3 Algorithm details

For implementing the minimization problem in (5) with \mathcal{W} replaced by $\widehat{\mathcal{W}}$, we will use the projected gradient descent (PGD) algorithm to find the optimal solution $(\widehat{\mathcal{G}}, \widehat{\mathbf{U}}_{1,X}, \widehat{\mathbf{U}}_2, \widehat{\mathbf{U}}_3)$. The idea of PGD is to repeatedly update the current solution in the opposite direction of the partial gradients of the function $L(\cdot)$ while projecting the updated solution onto a restricted space to satisfy any desired constraints. In particular, we first compute the partial gradients of $L(\cdot)$ on $(\mathcal{G}, \mathbf{U}_{1,X}, \mathbf{U}_2, \mathbf{U}_3)$ at each iteration step I :

$$\begin{aligned} \frac{\partial L}{\partial \mathcal{G}} &= \nabla L \times_1 \mathbf{U}_{1,X}^\top \times_2 \mathbf{U}_2^\top \times_3 \mathbf{U}_3^\top, \quad \frac{\partial L}{\partial \mathbf{U}_{1,X}} = \mathcal{M}_{(1)}(\nabla L)(\mathbf{U}_3 \otimes \mathbf{U}_2)\mathcal{M}_{(1)}(\mathcal{G})^\top, \\ \frac{\partial L}{\partial \mathbf{U}_2} &= \mathcal{M}_{(2)}(\nabla L)(\mathbf{U}_3 \otimes \mathbf{U}_{1,X})\mathcal{M}_{(2)}(\mathcal{G})^\top, \quad \frac{\partial L}{\partial \mathbf{U}_3} = \mathcal{M}_{(3)}(\nabla L)(\mathbf{U}_2 \otimes \mathbf{U}_{1,X})\mathcal{M}_{(3)}(\mathcal{G})^\top, \end{aligned}$$

where $\nabla L = \nabla L(\mathcal{X}) = \widehat{\mathcal{W}} \odot \Omega \odot (\mathcal{X} - \mathcal{Y})$ and $\mathcal{X} = \mathcal{G} \times_1 \mathbf{U}_{1,X} \times_2 \mathbf{U}_2 \times_3 \mathbf{U}_3$. Next, we update $(\mathcal{G}^{(I)}, \mathbf{U}_{1,X}^{(I)}, \mathbf{U}_2^{(I)}, \mathbf{U}_3^{(I)})$ by subtracting $\eta \cdot \partial L / \partial (\mathcal{G}^{(I)}, \mathbf{U}_{1,X}^{(I)}, \mathbf{U}_2^{(I)}, \mathbf{U}_3^{(I)})$, which moves the current iterate towards the opposite direction of partial gradients with step size η , denoted by $(\mathcal{G}^{(I+1)}, \mathbf{U}_1^{(I+1)}, \mathbf{U}_2^{(I+1)}, \mathbf{U}_3^{(I+1)})$. Since the PGD is an iterative optimization algorithm for finding a local minimum, large step sizes may overstep the local minima. Therefore, the choice of the step size η lies at the heart of the PGD as it should not exceed the inverse Lipschitz constant of the gradient. In practice, we employ a line search strategy to adaptively set η during optimization. However, the updated $\mathbf{U}_1^{(I+1)}$ might not lie in the column space of $\Phi(\mathbf{X}_0)$ as desired, and thus an extra projection operator is included at each iterative step, which projects $\mathbf{U}_1^{(I+1)}$ onto the restricted tensor space, denoted by $\mathbf{U}_{1,X}^{(I+1)}$. For theoretical reasons in Section 4, the updated $\mathbf{U}_2^{(I+1)}$ and $\mathbf{U}_3^{(I+1)}$ are projected to the Stiefel manifold to enforce column orthogonality. A summary of the full algorithm is provided in Algorithm 1.

Besides, it is recognized that the direct rank computation of (r_1, r_2, r_3) is a NP-hard problem (Kolda & Bader, 2009), and we propose to tune (r_1, r_2, r_3) based on minimizing the BIC criterion:

$$\begin{aligned} \text{BIC} &= \log \left\{ \|\sqrt{\widehat{\mathcal{W}}} \odot \mathbf{P}_\Omega(\mathcal{Y} - \mathcal{G}^{(I_{\max})} \times_1 \mathbf{U}_{1,X}^{(I_{\max})} \times_2 \mathbf{U}_2^{(I_{\max})} \times_3 \mathbf{U}_3^{(I_{\max})})\|_F^2 \right\} \\ &\quad + \frac{\log(NTK)}{(NTK)} \{r_1 r_2 r_3 + (N - r_1)r_1 + (T - r_2)r_2 + (K - r_3)r_3\}, \end{aligned} \tag{7}$$

where $r_1 r_2 r_3 + (N - r_1)r_1 + (T - r_2)r_2 + (K - r_3)r_3$ is the degrees of freedom for any (r_1, r_2, r_3) multi-linear rank tensor in $\mathbb{R}^{N \times T \times K}$ (Zhang, 2019, Proposition 1); see Section A1.1.2 of the Supplemental Material for more details.

4 Statistical guarantee

We first consider the following conditions which can be helpful to obtain the upper bound for the estimation tensor error in tensor completion.

Algorithm 1: Projected gradient descent for minimizing (5)

- 1 **Input:** The observed outcome tensor \mathcal{Y} , estimated weight tensor $\widehat{\mathcal{W}}$, the observation pattern Ω , the basis functions $\Phi(\mathbf{X}_0)$, the multi-linear rank (r_1, r_2, r_3) , maximal number of iterations I_{\max} , and step-size η .
- 2 *Initialization:* Use the standard projected higher-order SVD (HOSVD) for initialization,

$$\begin{aligned}\mathbf{U}_k^{(0)} &= \text{HOSVD}_{r_k}\{\mathcal{M}_{(k)}(\mathcal{Y}_w)\}, \quad \mathbf{U}_{1,X}^{(0)} = \mathbf{P}_{\Phi(\mathbf{X}_0)}\mathbf{U}_k^{(0)}, \\ \mathcal{G}^{(0)} &= \mathcal{Y}_w \times_1 \mathbf{U}_{1,X}^{(0)\top} \times_2 \mathbf{U}_2^{(0)\top} \times_3 \mathbf{U}_3^{(0)\top},\end{aligned}$$

where $\text{HOSVD}_r(\cdot)$ returns the orthonormal matrix comprised the top r left singular vectors of a matrix, $\mathcal{Y}_w = \mathcal{Y} \odot \Omega \odot \widehat{\mathcal{W}}$, and

$$\mathbf{P}_{\Phi(\mathbf{X}_0)} = \Phi(\mathbf{X}_0)\{\Phi(\mathbf{X}_0)\top\Phi(\mathbf{X}_0)\}^{-1}\Phi(\mathbf{X}_0)\top$$

is the projection matrix onto the sieves spaces spanned by the basis function $\Phi(\mathbf{X}_0)$.

- 3 **for** $I = 1, \dots, I_{\max}$ **do**

4

$$\begin{aligned}\mathbf{U}_1^{(I)} &= \mathbf{U}_{1,X}^{(I-1)} - \eta \frac{\partial L(\mathcal{G}^{(I-1)}, \mathbf{U}_{1,X}^{(I-1)}, \mathbf{U}_2^{(I-1)}, \mathbf{U}_3^{(I-1)})}{\partial \mathbf{U}_{1,X}}, \quad \mathbf{U}_{1,X}^{(I)} = \mathbf{P}_{\Phi(\mathbf{X}_0)}\mathbf{U}_1^{(I)}, \\ \mathbf{U}_k^{(I)} &= \mathbf{U}_k^{(I-1)} - \eta \frac{\partial L(\mathcal{G}^{(I-1)}, \mathbf{U}_{1,X}^{(I-1)}, \mathbf{U}_2^{(I-1)}, \mathbf{U}_3^{(I-1)})}{\partial \mathbf{U}_k}, \quad \mathbf{U}_k^{(I)} = \mathbf{P}_{\mathbf{U}_k}\mathbf{U}_k^{(I)}, \quad k = 2, 3, \\ \mathcal{G}^{(I)} &= \mathcal{G}^{(I-1)} - \eta \frac{\partial L(\mathcal{G}^{(I-1)}, \mathbf{U}_{1,X}^{(I-1)}, \mathbf{U}_2^{(I-1)}, \mathbf{U}_3^{(I-1)})}{\partial \mathcal{G}}.\end{aligned}$$

5 Estimated potential outcomes tensor $\widehat{\mathcal{Y}} = \mathcal{G}^{(I_{\max})} \times_1 \mathbf{U}_{1,X}^{(I_{\max})} \times_2 \mathbf{U}_2^{(I_{\max})} \times_3 \mathbf{U}_3^{(I_{\max})}$

Assumption 5. (a) The estimated weight tensor $\widehat{\mathcal{W}}$ satisfies

$$\frac{\sup_{t=1, \dots, T} |\widehat{\mathcal{W}}_{i,t,l} - \mathcal{W}_{i,t,l}|}{\sqrt{TN^{-1} \log(N + T + K)}} \rightarrow 0.$$

(b) The number of the basis functions d_{Φ} , and the residual component $\mathbf{\Gamma}$ satisfy

$$\frac{\sqrt{T d_{\Phi}^{-\tau}} \vee \sqrt{NT} \|\mathbf{\Gamma}\|}{\sqrt{(N \vee T) \log(N + T + K)}} \rightarrow 0,$$

where τ controls the smoothness of the unknown function $G^*(\mathbf{X}_0)$.

Assumption 5(a) states that the estimation error of the weight tensor should be bounded. Take the logistic modeling in Remark 1 for an example. Let \mathcal{J}_t denote the indices of true nonzero coefficients for the logistic model $e(H_{i,t}; \alpha_t)$. If the parameter α_t can be estimated with root- N consistency, then we have $\sup_{t=1, \dots, T} |\mathcal{J}_t| / \sqrt{T \log(N + T + K)} \rightarrow 0$, which essentially limits the number of true nonzero coefficients, $|\mathcal{J}_t|$, under correct model specification; see Lemma A3. Assumption 5(b) requires that the covariates \mathbf{X}_0 retain significant explanatory power for the unknown function

$G^*(\mathbf{X}_0)$. This assumption is crucial for establishing the upper bound induced by the projection matrix $\mathbf{P}_{\Phi(\mathbf{X}_0)}^\perp$; see Lemma A4.

Now, we can study the upper bound for the estimation error in tensor completion. Denote the weighted loss function (5) concisely by $L(\mathcal{X}; \widehat{\mathcal{W}}) = \sum_{\Omega_{i,t,l}=1} \widehat{\mathcal{W}}_{i,t,l} (\mathcal{Y}_{i,t,l} - \mathcal{X}_{i,t,l})^2$. To proceed with our claims on the statistical properties, we request the following assumptions on the true potential outcomes tensor \mathcal{Y}^* to bypass the ill-concentrated tensors.

Assumption 6. Suppose $\mathcal{Y}^* = \mathcal{G}^* \times_1 \mathbf{U}_1^* \times_2 \mathbf{U}_2^* \times_3 \mathbf{U}_3^*$ and $\mathbf{U}_k^*, k = 1, 2, 3$ have orthonormal columns, there exist some constants μ_0 and L_0 such that $\mathcal{Y}^* \in \mathfrak{C}(r_1, r_2, r_3, \mu_0, L_0)$, where

$$\begin{aligned} & \mathfrak{C}(r_1, r_2, r_3, \mu_0, L_0) \\ &= \left\{ \mathcal{X} = \mathcal{G} \times_1 \mathbf{U}_1 \times_2 \mathbf{U}_2 \times_3 \mathbf{U}_3, \quad \mu(\mathcal{X}) \leq \mu_0, \quad \max_{k \in \{1, 2, 3\}} \|\mathcal{M}_k(\mathcal{G})\| \leq L_0 \sqrt{\frac{NTK}{\mu_0^{3/2} (r_1 r_2 r_3)^{1/2}}} \right\}, \end{aligned}$$

where $\mu(\mathcal{X}) = \max\{\mu(\mathbf{U}_1), \mu(\mathbf{U}_2), \mu(\mathbf{U}_3)\}$, $\mu(\mathbf{U}_1) = N\|\mathbf{U}_1\|_{2,\infty}^2/r_1$, $\mu(\mathbf{U}_2) = T\|\mathbf{U}_2\|_{2,\infty}^2/r_2$, and $\mu(\mathbf{U}_3) = K\|\mathbf{U}_3\|_{2,\infty}^2/r_3$.

By enforcing \mathcal{Y}^* in the restricted tensor space $\mathfrak{C}(r_1, r_2, r_3, \mu_0, L_0)$, the loading matrices \mathbf{U}_k should satisfy the incoherence condition, which is commonly assumed in the matrix/tensor completion literature (Candès & Recht, 2009; Ma & Ma, 2017; Yuan & Zhang, 2017; Cao et al., 2020; Xia et al., 2021; Cai et al., 2021). Intuitively, the incoherence condition indicates that each tensor entry contains a similar amount of information so missing any of them will not prevent us from being able to reconstruct the entire tensor. In particular, small $\mu(\mathcal{X})$ implies that the energy of tensor \mathcal{X} is balanced across all modes, which is essential for establishing the restricted strong convexity in Lemma A2. In addition, we also require an upper bound on the spectral norm of each matricization of the core tensor \mathcal{G} , which is useful to diminish the estimation error lying in the orthogonal space of the sieve basis functions $\Phi(\mathbf{X}_0)$. Encouragingly, Algorithm 1 can easily incorporate the conditions in Assumption 6 by including multiple projection steps to ensure that $(\mathcal{G}^{(I)}, \mathbf{U}_{1,X}^{(I)}, \mathbf{U}_2^{(I)}, \mathbf{U}_3^{(I)})$ lie in the restricted domain $\mathfrak{C}(r_1, r_2, r_3, \mu_0, L_0)$ throughout the iterations.

By the definition of $\widehat{\mathcal{Y}}$ that minimizes the weighted loss function, we have $L(\widehat{\mathcal{Y}}; \widehat{\mathcal{W}}) \leq L(\mathcal{Y}^*; \widehat{\mathcal{W}})$, where

$$\begin{aligned} & \sum_{\Omega_{i,t,l}=1} \widehat{\mathcal{W}}_{i,t,l} (\mathcal{Y}_{i,t,l} - \widehat{\mathcal{Y}}_{i,t,l})^2 - \sum_{\Omega_{i,t,l}=1} \widehat{\mathcal{W}}_{i,t,l} (\mathcal{Y}_{i,t,l} - \mathcal{Y}_{i,t,l}^*)^2 \\ &= \sum_{\Omega_{i,t,l}=1} \widehat{\mathcal{W}}_{i,t,l} (\mathcal{Y}_{i,t,l} - \widehat{\mathcal{Y}}_{i,t,l})^2 - \sum_{\Omega_{i,t,l}=1} \mathcal{W}_{i,t,l} (\mathcal{Y}_{i,t,l} - \widehat{\mathcal{Y}}_{i,t,l})^2 \end{aligned} \tag{8}$$

$$+ \sum_{\Omega_{i,t,l}=1} \mathcal{W}_{i,t,l} (\mathcal{Y}_{i,t,l} - \widehat{\mathcal{Y}}_{i,t,l})^2 - \sum_{\Omega_{i,t,l}=1} \mathcal{W}_{i,t,l} (\mathcal{Y}_{i,t,l} - \mathcal{Y}_{i,t,l}^*)^2 \tag{9}$$

$$+ \sum_{\Omega_{i,t,l}=1} \mathcal{W}_{i,t,l} (\mathcal{Y}_{i,t,l} - \mathcal{Y}_{i,t,l}^*)^2 - \sum_{\Omega_{i,t,l}=1} \widehat{\mathcal{W}}_{i,t,l} (\mathcal{Y}_{i,t,l} - \mathcal{Y}_{i,t,l}^*)^2 \tag{10}$$

$$= I_1 + I_2 + I_3 \leq 0,$$

where the terms I_1 and I_3 are bounded under Assumption 5(a) by estimating $\mathcal{W}_{i,t,l}$ with vanishing error. The boundary of (10) is challenging and is proved in the Appendix with details. Thus, we establish the statistical guarantee for our proposed tensor completion in Theorem 1.

Theorem 1. *Under Assumptions 1-6, and other regularity conditions, if $\hat{\mathcal{Y}}$ minimizes the objective function in (5), we have*

$$\begin{aligned} \frac{\|\mathcal{Y}^* - \hat{\mathcal{Y}}\|_F^2}{NT} &\leq \frac{CL_0^2 \log(N+T+K)}{p_{\min} N} \\ &\vee \frac{C' k^2 (r_1 \wedge d_\Phi) r_2 r_3}{\max\{(r_1 \wedge d_\Phi), r_2, r_3\} p_{\min}^2} \frac{(N \vee T)}{NT} \log(N+T+K) \left\{ \sigma^2 \left(\frac{p_{\max}}{p_{\min}} \right)^2 \vee L_0^2 \right\}, \end{aligned}$$

with probability greater than $1 - 7(N+T+K)^{-2}$ for some constants C , C' , C'' and C''' , where $p_{\min} = \delta^k \leq \mathbb{P}(A_{i,t-k+1:t} = a_{(t-k+1):t} \mid H_{i,t}) \leq (1-\delta)^k = p_{\max}$.

Theorem 1 shows that the upper bound converges to zero as N and T grow if the estimation errors for $G^*(\mathbf{X}_0)$ and \mathcal{W} are sufficiently small for well-conditioned $\mathcal{Y}^* - \hat{\mathcal{Y}}$. Here, we provide an interpretation of each term in the right-hand side of the tensor estimation error. First, one can show that a deterministic upper bound for $\sum_{\Omega_{i,t,l}=1} \mathcal{W}_{i,t,l} (\mathcal{Y}_{i,t,l}^* - \hat{\mathcal{Y}}_{i,t,l})^2$ under any realization of the observation pattern Ω , or equivalently the treatment mechanism, which is controlled by the spectral norm of the weighted error tensor \mathcal{E}_Ω^w . Combining it with the restricted strong convexity condition, it yields the *second* error term; however, to legitimately use the restricted strong convexity condition, one requires a lower bound on $\|\mathcal{Y}^* - \hat{\mathcal{Y}}\|_F^2$, which is not necessarily satisfied for every \mathcal{Y}^* and $\hat{\mathcal{Y}} \in \mathfrak{C}(r_1, r_2, r_3, \mu_0, L_0)$ (Hamidi & Bayati, 2019). In fact, the required lower bound plays a similar role as the incoherence condition on $\mathcal{Y}^* - \hat{\mathcal{Y}}$ (Xia et al., 2021). Hence, failing to attain the lower bound will give us another upper bound for $\|\mathcal{Y}^* - \hat{\mathcal{Y}}\|_F^2$, which is the *first* term on the right-hand side.

Remark 2 (Comparison with matrix completion on panel data). *The proposed tensorized HRMSM can be used to draw causal inferences on panel data with staggered entries. Under the staggered adoption design, it is common to assume that the potential outcomes are only influenced by the contemporaneous treatment, which rules out the dynamic treatment effects and focuses on estimating two potential outcomes matrices $Y(0)$ and $Y(1)$. By setting $k = 1$, our tensorized HRMSM reduces to this setup, and a close analog can be drawn upon the matrix completion approach in Athey et al. (2021), which exploits the low rankness via the matrix nuclear norm regularization. In fact, the first and the second error terms in Theorem 1 are comparable to the first two terms in Theorem 2, Athey et al. (2021). However, Athey et al. (2021) impute the potential outcomes matrices $Y(0)$ and $Y(1)$ separately, whereas we stack these two matrices into a tensor and employ the Bernstein-type inequality to bound the tolerance quantity ϑ . Consider a special case where $N \asymp T$, our tolerance term satisfies $\vartheta \asymp N$, which is of a smaller order than that in Athey et al. (2021), i.e., $\vartheta \asymp N^{3/2}$. An empirical experiment demonstrates that our method achieves stable numerical results regardless of the time that subjects are first exposed to the treatment; see Section A1.2.1 in the Supplementary Material for more details.*

Remark 3 (On Global vs. Algorithmic Consistency.). *Theorem 1 establishes the consistency of the global minimizer \hat{Y} . However, due to the non-convex nature of the optimization problem, the proposed algorithm cannot guarantee convergence to the global optimum. In practice, good empirical performance is often observed as demonstrated in our numerical analysis. Similar gaps between theoretical and computational guarantees are common in the tensor and nonconvex optimization literature (e.g., Wang & Li (2020); Y. Zhou et al. (2024); H. Zhou et al. (2013)). A more rigorous analysis linking algorithmic convergence and statistical consistency is left for future work.*

5 Simulation studies

We assess the effectiveness of the tensorized HRMSMs in recovering the potential outcomes tensor with fixed multi-linear ranks under Gaussian noises through extensive Monte Carlo simulations. Specifically, we compare the covariate-assisted tensorized HRMSM with the parametric HRMSM in Neugebauer et al. (2007), the matrix factor model in Fan et al. (2016) based on the unfolded tensor $\mathcal{M}_{(1)}(\mathcal{Y})$, the *vanilla* tensorized HRMSM without incorporating any baseline covariates, and CT, as empirical evidence indicates its superiority over other state-of-the-art methods (Melnichuk et al., 2022). For the HRMSM, we postulate time-specific linear models $\mu(a_{(t-k+1):t}, X_{i,0}; \eta_t) = (a_{(t-k+1):t}, X_{i,0}^\top)^\top \eta_t$; The matrix factor model and the *vanilla* tensorized HRMSM are included to demonstrate the usefulness of the tensor representation and covariate assistance. For a fair comparison, we minimize an IPTW version of their target loss functions, where the weights adjust for the time-varying confounding. The performance of the first four methods is evaluated by the normalized tensor mean squared error of the difference between the recovered tensor $\hat{\mathcal{Y}}$ and the ground truth \mathcal{Y}^* as $\ell_2(\hat{\mathcal{Y}}) = \|\hat{\mathcal{Y}} - \mathcal{Y}^*\|_F^2 / \|\mathcal{Y}^*\|_F^2$; for CT, however, the difference is computed based on 10 randomly sampled paths only, due to the high computational cost associated with its pathwise prediction mechanism. All simulation results are based on 100 data replications.

In what follows, the tensor estimation error is investigated under a set of simulation designs. Specifically, Section 5.1 studies the impact of different model formulations of $\{\mathcal{Y}_{i,t,l}, e(H_{i,t})\}$; Section 5.2 examines the effects of the covariate-orthogonal loadings Γ . For now, we assume the true multi-linear ranks are known, and a BIC-based tuning procedure is shown to be effective at the hyperparameter tuning in Section A1.1.2 of the Appendix.

5.1 Effect of outcome and propensity score models

We assess the robustness of our proposed model under various outcome and propensity score models. For starter, the baseline covariate $\mathbf{X}_0 \in \mathbb{R}^{N \times d_0}$ and the time-dependent covariate counterfactuals $X_{i,t}^{a_{(t-2):t}}$ are simulated as $X_{i,0} \stackrel{i.i.d.}{\sim} \mathcal{N}(0, 1)$, $X_{i,t}^{a_{(t-2):t}} = \text{cum}(X_{i,0}) + \eta_1 a_{i,t} + \eta_2 a_{i,t-1} + \eta_3 a_{i,t-2}$, where $\text{cum}(X_{i,0})$ is the sum of all the entries of $X_{i,0}$, $d_0 = 20$, and $\eta_m = 2^{-m}$, $m = 1, 2, 3$. For $a_{i,(t-k+1):t} \in \mathbb{A}_k$, we consider two data-generating procedures for $\mathcal{Y}_{i,t,l}$, labeled by (M1) and (M2). In particular, (M1) is a simple linear model of $X_{i,0:t}$ and $a_{i,(t-k+1):t}$ for $\mathcal{Y}_{i,t,\{a_{i,(t-k+1):t}\}(10)}$, whereas (M2) is a complex additive model, which includes the sieve basis functions of $X_{i,0}$ and several quadratic terms; see Section A1.1 of the Appendix for the detailed definitions of (M1) and (M2). Next, we consider two sequential treatment assignment mechanisms for $A_{i,t}$ depending on the time-varying confounders $(X_{i,t}, X_{i,t-1})$:

$$(A1) \quad \mathbb{P}(A_{i,t} = 1 | H_{i,t}) = e(H_{i,t}) = \exp(X_{i,t} + X_{i,t-1}) / \{1 + \exp(X_{i,t} + X_{i,t-1})\},$$

$$(A2) \quad \mathbb{P}(A_{i,t} = 1 | H_{i,t}) = e(H_{i,t}) = \exp(2X_{i,t} + 2X_{i,t-1}) / \{1 + \exp(2X_{i,t} + 2X_{i,t-1})\},$$

where (A2) is prone to assign treatments on the previously treated subjects, leading to a wider range of possible propensity scores and therefore a smaller δ than (A1). The penalized likelihood estimation in (6) with SCAD penalty is used for estimating the propensity score at each time point.

Figure 4 displays the normalized tensor error $\ell_2(\hat{\mathcal{Y}})$ versus N and T for various estimators when $k = 5$. We observe that the benchmark HRMSM achieves the best performance when the generative model of $\mathcal{Y}_{i,t,l}$ is correctly specified by $\mu(a_{(t-k+1):t}, X_{i,0}; \eta_t)$. However, as several quadratic terms are involved in (M2), the estimation accuracy of HRMSM is negatively affected due to its incorrect parameterization, whereas our flexible tensor representation is able to capture the complex relationship between the potential outcomes and covariates, time, and treatments.

More importantly, we observe that the estimation error of the tensorized HRMSMs (both the *vanilla* and covariate-assisted) are favorably affected by the sample size N , which aligns with our theoretical bounds in Theorem 1. In addition, the normalized error is not greatly positively impacted by the time points T , which can be attributed to the increasingly time-specific propensity score estimations when T grows. However, the tensorized HRMSMs can still significantly improve the performance over the matricized minimization, especially for larger T . By contrast, CT suffers from cumulative prediction bias, likely due to its autoregressive attention mechanism through which small local errors propagate and accumulate over time. Besides, it also subject to confounding bias as the produced time-varying representations are only balanced on current treatment assignment, which do not account for the lagged treatment effect. As the latent factors of potential outcomes tensor over the first mode is explainable by the baseline covariate \mathbf{X}_0 in both (M1) and (M2), additional information can be harnessed by the covariate-assisted tensorized HRMSM to compensate the efficiency loss due to increased variability of IPTWs in (A2).

5.2 Effect of covariate-independent component

In this subsection, we assess the effectiveness of our proposed framework when the strength of the covariate-independent components varies. In particular, the sequential treatment assignment for $A_{i,t}$ follows (A1) and the generative model of $\mathcal{Y}_{i,t,l}$ is similar to (M2) except that the covariate-orthogonal noises $\Gamma_{i,j}$ are added, where $\Gamma_{i,j}$ controls the amplitude of the covariate-orthogonal part.

In this case, the potential outcome tensor still admits the low-rank formulation except that the tensor factors of the first mode is changed to include the extra covariate-independent component $\Gamma_{i,j}$. Consider three ways for generating the $\Gamma_{i,j}$:

- 1) $\Gamma_{i,j} = 0$, encoded by none covariate-orthogonal noises;
- 2) $\Gamma_{i,j} \sim \mathcal{N}(0, 5^2)$, encoded by weak covariate-orthogonal noises; and
- 3) $\Gamma_{i,j} \sim \mathcal{N}(0, 20^2)$, encoded by strong covariate-orthogonal noises.

Figure 4 displays the normalized mean squared error $\ell_2(\hat{\mathcal{Y}})$ under varying strength of $\Gamma_{i,j}$ (none, weak or strong) versus N and T . Similar to the phenomenons observed in Figure 4, the covariate-assisted tensorized HRMSM can improve the estimation accuracy upon the *vanilla* tensorized HRMSM regardless of whether the magnitude of $\Gamma_{i,j}$ is strong or not. In particular, the merits of employing the covariate-assisted tensorized HRMSM are more accentuated when the noises induced by $\Gamma_{i,j}$ are amplified. The substantial performance improvement of the covariate-assisted tensorized HRMSM is largely attributed to the use of the auxiliary covariates, which aids us in recovering a more accurate solution in the covariate-related subspace.

6 An application

We apply our proposed method to the Medical Information Mart for Intensive Care (MIMIC) III database. The MIMIC III database is an extensive, publicly available Intensive Care Unit (ICU) database, which consists of de-identified health-related data associated with over 40000 patients who stayed in critical care units of the Beth Israel Deaconess Medical Center between 2001 and 2012 (Goldberger et al., 2000; A. Johnson et al., 2016; A. E. Johnson et al., 2016). After removing the erroneous entries due to missingness and duplication, we extract $N = 4006$ patients with trajectories up to $T = 20$ timestamps every four hours. Next, we consider the mechanical ventilation status as

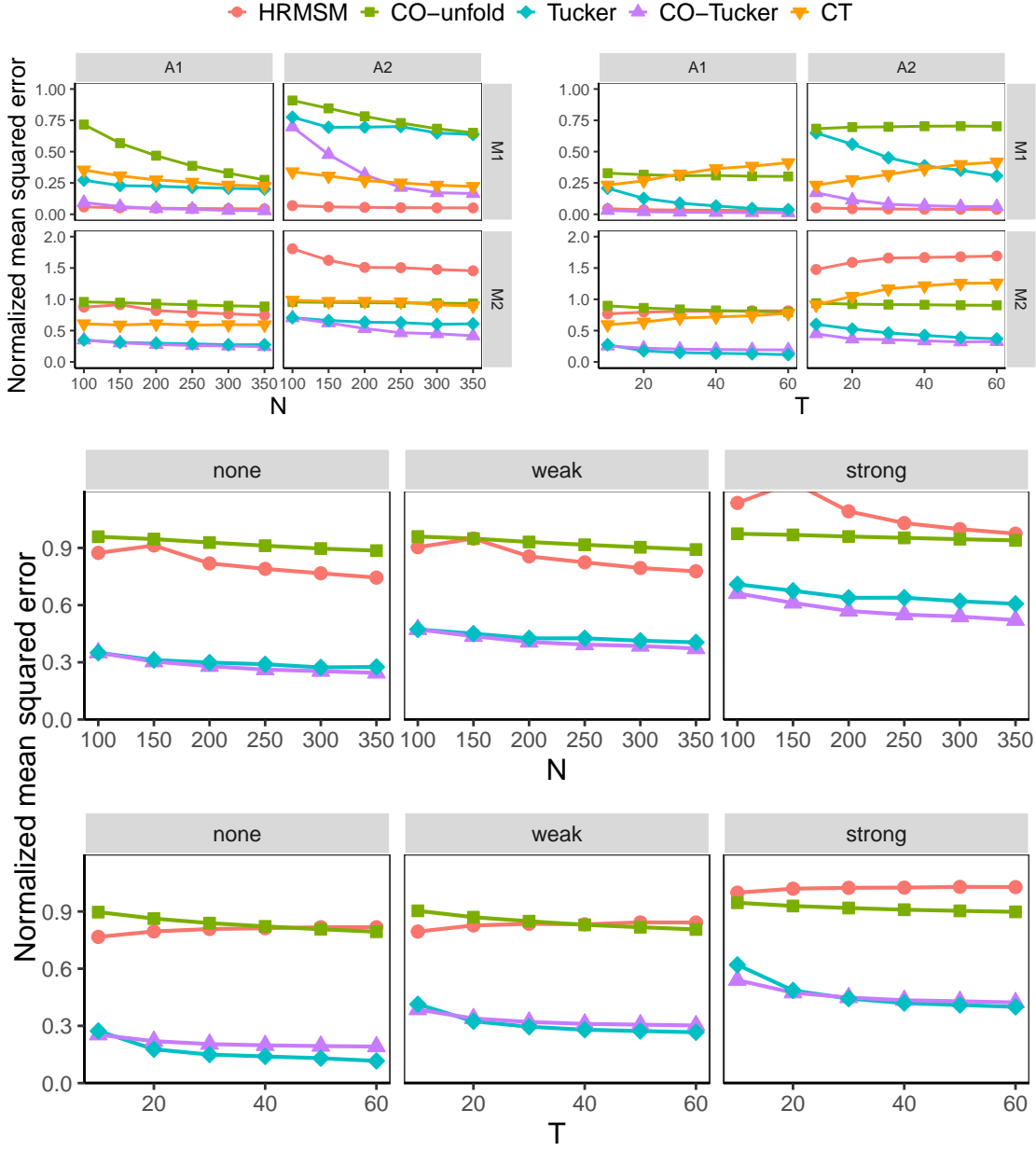


Figure 4: Averaged normalized mean squared tensor error when $T = 10$, $N = 100, 150, \dots, 350$, and $N = 300$, $T = 10, 20, \dots, 60$ under (Top panel) outcome models (M1) and (M2) and treatment assignments (A1) and (A2), and (Bottom panel) none, weak and strong noises due to the covariate-orthogonal factor $\Gamma_{i,j}$; HRMSM is the history-restricted marginal structural model, CO-UNFOLD is the matrix factor model based on unfolded tensor, TUCKER is the *vanilla* tensorized HRMSM, CO-TUCKER is the covariate-assisted tensorized HRMSM, and CT is the Causal Transformer.

the treatment A with 1 as the presence of mechanical ventilation and 0 otherwise. The outcome of interest Y is the Sequential Organ Failure Assessment (SOFA) score, which measures the severity of organ dysfunction for a patient in ICU in terms of pulmonary, renal, hepatic, cardiovascular, hematologic, and neurologic systems. Each organ system gives a score ranging from 0 to 4, and the total score is from 0 to 24 with 0 as the lowest level of morbidity and 24 as the highest level of

morbidity (Vincent et al., 1996). Given the rapidly changing conditions of ICU patients, most of the effects of mechanical ventilation can be captured within a day; thus, we consider the treatment regimes for each patient as his/her previous $k = 6$ binary treatment histories.

In that way, the potential outcomes tensor \mathcal{Y} can be formed accordingly in the dimensions of $4006 \times 20 \times 2^6$. Following the previous studies (Purushotham et al., 2018), we select the baseline covariates $\mathbf{X}_0 \in \mathbb{R}^{N \times 11}$ and the time-varying covariates $\mathbf{X}_t \in \mathbb{R}^{N \times 7}, t = 1, \dots, T$ as listed in Table A1 for our subsequent analyses. We normalize each covariate to have a unit L_2 norm at each timestamp, and construct the basis functions $\Phi(\cdot)$ by the Legendre polynomial functions up to order 10.

Our purpose is to emphasize the flexibility of our low-rank tensor framework and highlight the advantages of including the baseline covariate in recovering the counterfactuals. Particularly, we randomly split the MIMIC III dataset into V folds, denoted by $\mathcal{I}_1, \dots, \mathcal{I}_V$. For each \mathcal{I}_v , the models are trained over the other folds \mathcal{I}_v^c , that is, the complement of \mathcal{I}_v and are evaluated on \mathcal{I}_v for testing. The averaged training error and the testing error are

$$\ell_2(\hat{\mathcal{Y}})_{\text{train}} = \frac{1}{V} \sum_{v=1}^V \frac{\|\mathbf{P}_{\Omega_{\mathcal{I}_v^c}}(\hat{\mathcal{Y}}_{\mathcal{I}_v^c} - \mathcal{Y}_{\mathcal{I}_v^c})\|_F}{\|\mathbf{P}_{\Omega_{\mathcal{I}_v^c}}(\mathcal{Y}_{\mathcal{I}_v^c})\|_F}, \quad \ell_2(\hat{\mathcal{Y}})_{\text{test}} = \frac{1}{V} \sum_{v=1}^V \frac{\|\mathbf{P}_{\Omega_{\mathcal{I}_v}}(\hat{\mathcal{Y}}_{\mathcal{I}_v} - \mathcal{Y}_{\mathcal{I}_v})\|_F}{\|\mathbf{P}_{\Omega_{\mathcal{I}_v}}(\mathcal{Y}_{\mathcal{I}_v})\|_F},$$

where $\mathbf{P}_{\Omega_{\mathcal{I}_v^c}}(\cdot)$ and $\mathbf{P}_{\Omega_{\mathcal{I}_v}}(\cdot)$ are the projections of any tensor onto the observed entries within the training dataset \mathcal{I}_v^c and the testing dataset \mathcal{I}_v ; $\hat{\mathcal{Y}}_{\mathcal{I}_v^c}$ and $\hat{\mathcal{Y}}_{\mathcal{I}_v}$ are the estimated sub-tensor for the sub-samples \mathcal{I}_v^c and \mathcal{I}_v , respectively. Under our framework in (5), we can predict the sub-tensor $\mathcal{Y}_{\mathcal{I}_v}$ using the held-out baseline covariate $\mathbf{X}_{0,\mathcal{I}_v}$ by $\hat{\mathcal{Y}}_{\mathcal{I}_v} = \hat{\mathcal{G}}_{\mathcal{I}_v^c} \times_1 \Phi(\mathbf{X}_{0,\mathcal{I}_v}) \hat{\mathbf{B}}_{\mathcal{I}_v^c} \times_2 \hat{\mathbf{U}}_{2,\mathcal{I}_v^c} \times_3 \hat{\mathbf{U}}_{3,\mathcal{I}_v^c}$, where $\hat{\mathbf{B}}_{\mathcal{I}_v^c} = \{\Phi(\mathbf{X}_{0,\mathcal{I}_v^c})^\top \Phi(\mathbf{X}_{0,\mathcal{I}_v^c})\}^{-1} \Phi(\mathbf{X}_{0,\mathcal{I}_v^c})^\top \hat{\mathbf{U}}_{1,X,\mathcal{I}_v^c}$ and $(\hat{\mathcal{G}}_{\mathcal{I}_v^c}, \hat{\mathbf{U}}_{1,X,\mathcal{I}_v^c}, \hat{\mathbf{U}}_{2,\mathcal{I}_v^c}, \hat{\mathbf{U}}_{3,\mathcal{I}_v^c})$ are the minimizer of the loss function (5) over the sub-sample \mathcal{I}_v^c . For the other methods, the simple kernel smoothing over the first mode is used with $\mathbf{X}_{0,\mathcal{I}_v}$ and $\mathbf{X}_{0,\mathcal{I}_v^c}$ for obtaining the prediction. In specific, the kernel weight matrix $\mathbf{H}_v \in \mathbb{R}^{|\mathcal{I}_v| \times |\mathcal{I}_v^c|}$ is

$$H_{v,i,j} = \frac{\kappa(\|X_{j,0,\mathcal{I}_v^c} - X_{i,0,\mathcal{I}_v}\|^2)}{\sum_{j=1}^{|\mathcal{I}_v^c|} \kappa(\|X_{j,0,\mathcal{I}_v^c} - X_{i,0,\mathcal{I}_v}\|^2)},$$

where $\kappa(\cdot, \cdot)$ is a user-specified kernel distance function and the Gaussian kernel distance is chosen with the kernel variance parameter $\sigma_\kappa = 1$. Then, we can predict the sub-tensor $\mathcal{Y}_{\mathcal{I}_v}$ using $\mathbf{X}_{0,\mathcal{I}_v}$ based on kernel smoothing as $\hat{\mathcal{Y}}_{\mathcal{I}_v} = \hat{\mathcal{Y}}_{\mathcal{I}_v^c} \times_1 \mathbf{H}_v$, which is the best feasible linear predictor under the tensor factor model (E. Y. Chen et al., 2020).

Table 1 presents the training and testing errors averaged over the cross-validation folds with varying V . We find that tensorized HRMSMs (both the *vanilla* and covariate-assisted) achieve comparable performance as the traditional HRMSM over the training sets. However, the covariate-assisted tensorized HRMSM outperforms when evaluated on the testing sets by leveraging the baseline covariates in completing the missing entries, whereas the *vanilla* tensorized HRMSM suffers the issue of overfitting as it does not constrain the low-rank factors to be in a certain functional space spanned by the sieve basis.

In addition, we report the estimated ATE $\hat{\tau}_{\text{ATE}}$ for the full-day presence of mechanical ventilation on the SOFA score. Based on the recovered potential outcome tensor $\hat{\mathcal{Y}}$, $\hat{\tau}_{\text{ATE}}$ over the training set \mathcal{I}_v^c and testing set \mathcal{I}_v can be computed easily by

$$\hat{\tau}_{\text{ATE,train}} = \sum_{i \in \mathcal{I}_v^c, t} \frac{\hat{\mathcal{Y}}_{i,t,(\mathbf{1}_6)_{(10)}} - \hat{\mathcal{Y}}_{i,t,(\mathbf{0}_6)_{(10)}}}{|\mathcal{I}_v^c|T}, \quad \hat{\tau}_{\text{ATE,test}} = \sum_{i \in \mathcal{I}_v, t} \frac{\hat{\mathcal{Y}}_{i,t,(\mathbf{1}_6)_{(10)}} - \hat{\mathcal{Y}}_{i,t,(\mathbf{0}_6)_{(10)}}}{|\mathcal{I}_v|T}. \quad (11)$$

Table 1: Averaged normalized mean squared training $\ell_2(\hat{\mathcal{Y}})_{\text{train}} (\times 10^{-2})$, testing errors $\ell_2(\hat{\mathcal{Y}})_{\text{test}} (\times 10^{-2})$ over cross-validation folds $V = 2, 3, 5, 10$

	V	HRMSM	CO-unfold	Tucker	CO-Tucker
$\ell_2(\hat{\mathcal{Y}})_{\text{train}}$	2	39.02	62.74	33.91	45.91
	3	38.96	59.44	31.62	45.79
	5	38.98	58.00	30.57	45.74
	10	39.01	57.266	29.95	45.70
$\ell_2(\hat{\mathcal{Y}})_{\text{test}}$	2	56.63	60.70	51.11	46.08
	3	160.0	123.58	95.19	45.93
	5	397.64	322.83	258.08	45.83
	10	1001.1	838.66	686.03	45.79

Table 2: Averaged ATE on the training sets $\hat{\tau}_{\text{ATE,train}}$ and the testing sets $\hat{\tau}_{\text{ATE,test}}$ over cross-validation folds $V = 2, 3, 5, 10$

	V	HRMSM	CO-unfold	Tucker	CO-Tucker
$\hat{\tau}_{\text{ATE,train}}$	2	1.12	3.03	2.05	0.39
	3	1.12	3.01	2.04	0.37
	5	1.11	2.78	2.02	0.36
	10	1.11	2.56	2.00	0.37
$\hat{\tau}_{\text{ATE,test}}$	2	1.53	4.12	2.92	0.39
	3	3.05	8.20	5.82	0.37
	5	6.07	15.2	11.5	0.36
	10	13.6	31.5	25.5	0.37

Table 2 reports the estimated ATE, averaged over the folds with various V . As expected, the covariate-assisted tensorized HRMSM yields a stable estimation of the ATE when evaluated on the sets \mathcal{I}_v^C and \mathcal{I}_v across all the number of folds, similar to the phenomena observed from Table 1. However, other methods are subject to the over-fitting issue, indicated by the unstable predictions when the number of folds increases (i.e., more training samples and fewer testing samples). Therefore, it demonstrates the potential benefit of using the flexible tensor representation in conjunction with the sieve approximation for robust prediction. According to our analysis, mechanical ventilation may increase the SOFA score of the treated patients and is therefore harmful to critically ill patients in ICU, which agrees with the findings in Mutlu & Factor (2000) that mechanical ventilation can bring substantial risks to ICU patients and result in various complications, such as ventilator-associated pneumonia (Society et al., 2005; Kalil et al., 2016).

7 Discussion

In this paper, we explore the flexibility introduced by the low-rank tensorized HRMSMs to estimate the unobserved potential outcome via the IPTW, which extends the history-restricted marginal structural models and exploits the full structure of the potential outcomes tensor for completion. Moreover, we adopt the semi-parametric framework to include the baseline covariates in the tensor completion while suppressing the impact of the covariate-independent components by the projected gradient descent algorithm.

The tensor completion framework can be readily adapted for multi-level or cluster treatments by expanding the treatment mode of the tensor to include potential outcomes under treatments of varying levels or structures. Additionally, leveraging the generalized propensity score (Yang et al., 2016) and cluster calibration (Yang, 2018) facilitates confounding adjustment through weighting. Most existing causal models use a discrete-time setup, which requires all subjects to be followed at the same pre-fixed time points but can be restrictive in many practical situations. In practice, the number of observations and observation times differ from subject to subject (Yang, 2022), yielding irregularly-spaced observation times. The proposed tensor completion framework can adapt to such situations by refining and expanding the time mode of the tensor. We can further include additional weighting to adjust for informative observation times. The tensor completion procedure remains the same. Extending the proposed framework for general outcomes such as survival outcomes (Yang et al., 2018; Yang, Pieper, & Cools, 2020) is an important future work. Instead of assuming a low-rank structure on the data tensor, one can impose low-rankness on the model parameter tensor from canonical exponential distributions (Mao et al., 2024). Another intriguing direction is to de-confound the sequential treatments along the lines of Bica et al. (2020), as the key assumption underpinning our framework is the unmeasured confounding condition, whose plausibility relies on collecting a rich set of auxiliary covariates from the observational studies. Lastly, it would be interesting to develop an inferential framework for the tensorized HRMSMs since it is hardly explored in the current tensor completion literature (Xia et al., 2022). A promising approach would be to integrate our method as the outcome model within a doubly robust framework (Kennedy et al., 2023). The statistical inference is valid under the upper bound for the estimation errors established in this paper, which can be a valuable tool for decision-making.

References

Abadie, A., Diamond, A., & Hainmueller, J. (2010). Synthetic control methods for comparative case studies: Estimating the effect of California’s tobacco control program. *Journal of the American Statistical Association*, 105, 493–505.

Acar, E., Kolda, T. G., & Dunlavy, D. M. (2011). All-at-once optimization for coupled matrix and tensor factorizations. *arXiv preprint arXiv:1105.3422*.

Agarwal, A., Dahleh, M., Shah, D., & Shen, D. (2023). Causal matrix completion. In *The thirty-sixth annual conference on learning theory* (pp. 3821–3826).

Agarwal, A., & Syrgkanis, V. (2022). Synthetic blip effects: Generalizing synthetic controls for the dynamic treatment regime. *arXiv preprint arXiv:2210.11003*.

Athey, S., Bayati, M., Doudchenko, N., Imbens, G., & Khosravi, K. (2021). Matrix completion methods for causal panel data models. *Journal of the American Statistical Association*, 116, 1–15.

Bai, J., & Li, K. (2012). Statistical analysis of factor models of high dimension. *The Annals of Statistics*, 40, 436–465.

Barak, B., & Moitra, A. (2016). Noisy tensor completion via the sum-of-squares hierarchy. *Journal of Machine Learning Research*, 49, 1–29.

Belloni, A., Chernozhukov, V., Fernandez-Val, I., & Hansen, C. (2017). Program evaluation and causal inference with high-dimensional data. *Econometrica*, 85, 233–298.

Bica, I., Alaa, A., & Van Der Schaar, M. (2020). Time series deconfounder: Estimating treatment effects over time in the presence of hidden confounders. In *International conference on machine learning* (pp. 884–895).

Cai, C., Li, G., Poor, H. V., & Chen, Y. (2021). Nonconvex low-rank tensor completion from noisy data. *Operations Research*, 70, 1–19.

Candès, E. J., & Recht, B. (2009). Exact matrix completion via convex optimization. *Foundations of Computational Mathematics*, 9, 717–772.

Cao, Y., Zhang, A., & Li, H. (2020). Multisample estimation of bacterial composition matrices in metagenomics data. *Biometrika*, 107, 75–92.

Chang, S. Y., & Lin, W.-W. (2022). Convenient tail bounds for sums of random tensors. *Taiwanese Journal of Mathematics*, 26, 571–606.

Chen, E. Y., Xia, D., Cai, C., & Fan, J. (2020). Semiparametric tensor factor analysis by iteratively projected svd. *arXiv preprint arXiv:2007.02404*.

Chen, X. (2007). Large sample sieve estimation of semi-nonparametric models. *Handbook of Econometrics*, 6, 5549–5632.

Derksen, H. (2016). On the nuclear norm and the singular value decomposition of tensors. *Foundations of Computational Mathematics*, 16, 779–811.

Fan, J., & Li, R. (2001). Variable selection via nonconcave penalized likelihood and its oracle properties. *Journal of the American statistical Association*, 96, 1348–1360.

Fan, J., Liao, Y., & Wang, W. (2016). Projected principal component analysis in factor models. *The Annals of Statistics*, 44, 219–254.

Feldman, H. I., Joffe, M., Robinson, B., Knauss, J., Cizman, B., Guo, W., ... Faich, G. (2004). Administration of parenteral iron and mortality among hemodialysis patients. *Journal of the American Society of Nephrology*, 15, 1623–1632.

Gandy, S., Recht, B., & Yamada, I. (2011). Tensor completion and low-n-rank tensor recovery via convex optimization. *Inverse Problems*, 27, 025010.

Gigli, N., & Ledoux, M. (2013). From log sobolev to talagrand: a quick proof. *Discrete and Continuous Dynamical Systems-Series A*, dcds–2013.

Goldberger, A. L., Amaral, L. A., Glass, L., Hausdorff, J. M., Ivanov, P. C., Mark, R. G., ... Stanley, H. E. (2000). Physiobank, physiotoolkit, and physionet: components of a new research resource for complex physiologic signals. *Circulation*, 101, 215–220.

Hamidi, N., & Bayati, M. (2019). On low-rank trace regression under general sampling distribution. *arXiv preprint arXiv:1904.08576*.

Heron, K. E., & Smyth, J. M. (2010). Ecological momentary interventions: incorporating mobile technology into psychosocial and health behaviour treatments. *British Journal of Health Psychology*, 15, 1–39.

Hogben, L. (2013). *Handbook of linear algebra*. CRC press.

Hu, S. (2015). Relations of the nuclear norm of a tensor and its matrix flattenings. *Linear Algebra and its Applications*, 478, 188–199.

Ibriga, H. S., & Sun, W. W. (2022). Covariate-assisted sparse tensor completion. *Journal of the American Statistical Association*, 1–15.

Jain, P., & Oh, S. (2014). Provable tensor factorization with missing data. In *Advances in neural information processing systems* (pp. 1431–1439).

Johnson, A., Pollard, T., & Mark, R. (2016). Mimic-iii clinical database (version 1.4). *PhysioNet*.

Johnson, A. E., Pollard, T. J., Shen, L., Lehman, L.-w. H., Feng, M., Ghassemi, M., ... Mark, R. G. (2016). Mimic-iii, a freely accessible critical care database. *Scientific Data*, 3, 1–9.

Kalil, A. C., Metersky, M. L., Klompas, M., Muscedere, J., Sweeney, D. A., Palmer, L. B., ... others (2016). Management of adults with hospital-acquired and ventilator-associated pneumonia: 2016 clinical practice guidelines by the infectious diseases society of america and the american thoracic society. *Clinical Infectious Diseases*, 63, 61–111.

Kennedy, E. H., et al. (2023). Towards optimal doubly robust estimation of heterogeneous causal effects. *Electronic Journal of Statistics*, 17.

Klopp, O. (2014). Noisy low-rank matrix completion with general sampling distribution. *Bernoulli*, 20, 282–303.

Kolda, T. G., & Bader, B. W. (2009). Tensor decompositions and applications. *SIAM Review*, 51, 455–500.

Kong, X., Li, J., & Wang, X. (2018). New estimations on the upper bounds for the nuclear norm of a tensor. *Journal of Inequalities and Applications*, 2018, 1–17.

Landsberg, J. M. (2012). Tensors: geometry and applications. *Representation Theory*, 381, 3.

Lee, D., Yang, S., Dong, L., Wang, X., Zeng, D., & Cai, J. (2021). Improving trial generalizability using observational studies. *Biometrics*, doi.org/10.1111/biom.13609.

Li, R., Shahn, Z., Li, J., Lu, M., Chakraborty, P., Sow, D., ... Lehman, L.-w. H. (2021). G-net: a deep learning approach to g-computation for counterfactual outcome prediction under dynamic treatment regimes. *Machine Learning for Health*.

Lim, L.-H., & Comon, P. (2013). Blind multilinear identification. *IEEE Transactions on Information Theory*, 60, 1260–1280.

Liu, J., Musialski, P., Wonka, P., & Ye, J. (2012). Tensor completion for estimating missing values in visual data. *IEEE transactions on pattern analysis and machine intelligence*, 35, 208–220.

Luo, Z., Qi, L., & Toint, P. L. (2020). Tensor bernstein concentration inequalities with an application to sample estimators for high-order moments. *Frontiers of Mathematics in China*, 15, 367–384.

Ma, Z., & Ma, Z. (2017). Exploration of large networks via fast and universal latent space model fitting. *arXiv preprint arXiv:1705.02372*.

Mandal, D., & Parkes, D. (2019). Weighted tensor completion for time-series causal inference. *arXiv preprint arXiv:1902.04646*.

Mao, X., Wang, H., Wang, Z., & Yang, S. (2024). Mixed matrix completion in complex survey sampling under heterogeneous missingness. *Journal of Computational and Graphical Statistics*, 1320–1328.

Massart, P. (2000). About the constants in talagrand’s concentration inequalities for empirical processes. *The Annals of Probability*, 28, 863–884.

Melnychuk, V., Frauen, D., & Feuerriegel, S. (2022). Causal transformer for estimating counterfactual outcomes. In *International conference on machine learning* (pp. 15293–15329).

Mortimer, K. M., Neugebauer, R., Van Der Laan, M., & Tager, I. B. (2005). An application of model-fitting procedures for marginal structural models. *American Journal of Epidemiology*, 162, 382–388.

Mutlu, G., & Factor, P. (2000). Complications of mechanical ventilation. *Respiratory Care Clinics of North America*, 6, 213–252.

Negahban, S., & Wainwright, M. J. (2012). Restricted strong convexity and weighted matrix completion: Optimal bounds with noise. *The Journal of Machine Learning Research*, 13, 1665–1697.

Neugebauer, R., van der Laan, M. J., Joffe, M. M., & Tager, I. B. (2007). Causal inference in longitudinal studies with history-restricted marginal structural models. *Electronic Journal of Statistics*, 1, 119–154.

Nguyen, N. H., Drineas, P., & Tran, T. D. (2015). Tensor sparsification via a bound on the spectral norm of random tensors. *Information and Inference: A Journal of the IMA*, 4, 195–229.

Ning, Y., Sida, P., & Imai, K. (2020). Robust estimation of causal effects via a high-dimensional covariate balancing propensity score. *Biometrika*, 107, 533–554.

Purushotham, S., Meng, C., Che, Z., & Liu, Y. (2018). Benchmarking deep learning models on large healthcare datasets. *Journal of Biomedical Informatics*, 83, 112–134.

Robins, J. (1986). A new approach to causal inference in mortality studies with a sustained exposure period—application to control of the healthy worker survivor effect. *Mathematical Modelling*, 7, 1393–1512.

Robins, J. M. (1994). Correcting for non-compliance in randomized trials using structural nested mean models. *Communications in Statistics-Theory and methods*, 23, 2379–2412.

Robins, J. M. (2000). Marginal structural models versus structural nested models as tools for causal inference. In *Statistical models in epidemiology, the environment, and clinical trials* (Vol. 116, pp. 95–133). Springer.

Robins, J. M., Hernan, M. A., & Brumback, B. (2000). Marginal structural models and causal inference in epidemiology. *Epidemiology*, 11, 550–560.

Rosenbaum, P. R., & Rubin, D. B. (1983). The central role of the propensity score in observational studies for causal effects. *Biometrika*, 70, 41–55.

Semerci, O., Hao, N., Kilmer, M. E., & Miller, E. L. (2014). Tensor-based formulation and nuclear norm regularization for multienergy computed tomography. *IEEE Transactions on Image Processing*, 23, 1678–1693.

Society, A. T., of America, I. D. S., et al. (2005). Guidelines for the management of adults with hospital-acquired, ventilator-associated, and healthcare-associated pneumonia. *American Journal of Respiratory and Critical Care Medicine*, 171, 388–416.

Tomioka, R., Hayashi, K., & Kashima, H. (2010). Estimation of low-rank tensors via convex optimization. *arXiv preprint arXiv:1010.0789*.

Tropp, J. A., et al. (2015). An introduction to matrix concentration inequalities. *Foundations and Trends® in Machine Learning*, 8, 1–230.

Tucker, L. R. (1966). Some mathematical notes on three-mode factor analysis. *Psychometrika*, 31, 279–311.

Van der Laan, M. J., Laan, M., & Robins, J. M. (2003). *Unified methods for censored longitudinal data and causality*. Springer Science & Business Media.

van der Laan, M. J., Petersen, M. L., & Joffe, M. M. (2005). History-adjusted marginal structural models and statically-optimal dynamic treatment regimens. *The International Journal of Biostatistics*, 1.

Vershynin, R. (2018). *High-dimensional probability: An introduction with applications in data science* (Vol. 47). Cambridge university press.

Vincent, J.-L., Moreno, R., Takala, J., Willatts, S., De Mendonça, A., Bruining, H., ... Thijs, L. G. (1996). *The sofa (sepsis-related organ failure assessment) score to describe organ dysfunction/failure*. Springer-Verlag.

Wang, M., & Li, L. (2020). Learning from binary multiway data: Probabilistic tensor decomposition and its statistical optimality. *Journal of Machine Learning Research*, 21(154).

Xia, D., & Yuan, M. (2017). On polynomial time methods for exact low rank tensor completion. *arXiv preprint arXiv:1702.06980*.

Xia, D., Yuan, M., & Zhang, C.-H. (2021). Statistically optimal and computationally efficient low rank tensor completion from noisy entries. *The Annals of Statistics*, 49, 76–99.

Xia, D., Zhang, A. R., & Zhou, Y. (2022). Inference for low-rank tensors—no need to debias. *The Annals of Statistics*, 50, 1220–1245.

Xie, W., Zhu, F., Jiang, J., Lim, E.-P., & Wang, K. (2016). Topicsketch: Real-time bursty topic detection from twitter. *IEEE Transactions on Knowledge and Data Engineering*, 28, 2216–2229.

Xu, Y., & Yin, W. (2013). A block coordinate descent method for regularized multiconvex optimization with applications to nonnegative tensor factorization and completion. *SIAM Journal on Imaging Sciences*, 6, 1758–1789.

Yang, S. (2018). Propensity score weighting for causal inference with clustered data. *Journal of Causal Inference*, 6, 20170027.

Yang, S. (2022). Semiparametric estimation of structural nested mean models with irregularly spaced longitudinal observations. *Biometrics*, 78, 937–949.

Yang, S., Imbens, G. W., Cui, Z., Faries, D. E., & Kadziola, Z. (2016). Propensity score matching and subclassification in observational studies with multi-level treatments. *Biometrics*, 72, 1055–1065.

Yang, S., Kim, J. K., & Song, R. (2020). Doubly robust inference when combining probability and non-probability samples with high dimensional data. *Journal of the Royal Statistical Society: Series B (Statistical Methodology)*, 82, 445–465.

Yang, S., Pieper, K., & Cools, F. (2020). Semiparametric estimation of structural failure time models in continuous-time processes. *Biometrika*, 107, 123–136.

Yang, S., Tsiatis, A. A., & Blazing, M. (2018). Modeling survival distribution as a function of time to treatment discontinuation: A dynamic treatment regime approach. *Biometrics*, 74, 900–909.

Yu, Z., & van der Laan, M. (2006). Double robust estimation in longitudinal marginal structural models. *Journal of Statistical Planning and Inference*, 136, 1061–1089.

Yuan, M., & Zhang, C.-H. (2016). On tensor completion via nuclear norm minimization. *Foundations of Computational Mathematics*, 16, 1031–1068.

Yuan, M., & Zhang, C.-H. (2017). Incoherent tensor norms and their applications in higher order tensor completion. *IEEE Transactions on Information Theory*, 63, 6753–6766.

Zhang, A. (2019). Cross: Efficient low-rank tensor completion. *The Annals of Statistics*, 47, 936–964.

Zhen, Y., & Wang, J. (2024). Nonnegative tensor completion for dynamic counterfactual prediction on covid-19 pandemic. *The Annals of Applied Statistics*, 18(1), 224–245.

Zhou, H., Li, L., & Zhu, H. (2013). Tensor regression with applications in neuroimaging data analysis. *Journal of the American Statistical Association*, 108(502), 540–552.

Zhou, J., Sun, W. W., Zhang, J., & Li, L. (2021). Partially observed dynamic tensor response regression. *Journal of the American Statistical Association*, 1–25.

Zhou, T., Qian, H., Shen, Z., Zhang, C., & Xu, C. (2017). Tensor completion with side information: A riemannian manifold approach. In *Proceedings of the twenty-sixth international joint conference on artificial intelligence* (pp. 3539–3545).

Zhou, Y., Wong, R. K., & He, K. (2024). Broadcasted nonparametric tensor regression. *Journal of the Royal Statistical Society Series B: Statistical Methodology*, 86(5), 1197–1220.

A1 Additional illustrations

A1.1 Details for simulation

A1.1.1 Tensor representation for the outcomes

Let the time-varying covariate $X_{i,t}^{a_{i,(t-2):t}} = \mathbf{1}_{d_0}^\top X_{i,0} + \eta_1 a_{i,t} + \eta_2 a_{i,t-1} + \eta_3 a_{i,t-2}$, the generative models for $\mathcal{Y}_{i,t,l} = \mathcal{Y}_{i,t,\{a_{i,(t-k+1):t}\}_{(10)}}$ with $l = \{a_{i,(t-k+1):t}\}_{(10)}$ under (M1) and (M2) will be

$$(M1) \quad \mathcal{Y}_{i,t,\{a_{i,(t-k+1):t}\}_{(10)}} = 4 \cdot \mathbf{1}_{d_0}^\top X_{i,0} + \beta_1 X_{i,t}^{a_{(t-2):t}} + \beta_2 X_{i,t-1}^{a_{(t-3):(t-1)}} + \gamma_1 a_{i,t} + \gamma_2 a_{i,t-1} + \mathcal{E}_{i,t,l}.$$

$$(M2)$$

$$\begin{aligned} \mathcal{Y}_{i,t,\{a_{i,(t-k+1):t}\}_{(10)}} &= 4 \sum_{j=1}^{J^*} d_0^{-1} \mathbf{1}_{d_0}^\top \Upsilon_j(X_{i,0}) + 4 \cdot \mathbf{1}_{d_0}^\top X_{i,0} \cdot 2^{-t} \\ &+ 3 \cdot \mathbf{1}_k^\top a_{(t-k+1):t} \cdot \mathbf{1}_{d_0}^\top X_{i,0} + 2 a_{i,t} \cdot \mathbf{1}_{d_0}^\top X_{i,0} + a_{i,t-1} \cdot \mathbf{1}_{d_0}^\top X_{i,0} \\ &+ \mathbf{1}_k^\top a_{(t-k+2):t} \cdot \mathbf{1}_{d_0}^\top X_{i,0} \cdot X_{i,t}^{a_{(t-2):t}} + \mathbf{1}_k^\top a_{(t-k+1):(t-1)} \cdot \mathbf{1}_{d_0}^\top X_{i,0} \cdot X_{i,t-1}^{a_{(t-3):(t-1)}} \\ &+ 5\beta_1 X_{i,t}^{a_{(t-2):t}} \cdot \mathbf{1}_{d_0}^\top X_{i,0} + 3\beta_2 X_{i,t-1}^{a_{(t-3):(t-1)}} \cdot \mathbf{1}_{d_0}^\top X_{i,0} \\ &+ \beta_1 X_{i,t}^{a_{(t-2):t}} + \beta_2 X_{i,t-1}^{a_{(t-3):(t-1)}} + \gamma_1 a_{i,t} + \gamma_2 a_{i,(t-1)} + \mathcal{E}_{i,t,l}, \end{aligned}$$

where $\mathcal{E}_{i,t,l}$ is generated with independent standard normal distribution $\mathcal{N}(0, 1)$, $\beta_1 = \beta_2 = 1$, $\gamma_1 = \gamma_2 = 3$, $\Upsilon_j(\cdot)$ is the j -th Legendre polynomial function defined by

$$\Upsilon_0(X) = 1, \quad \Upsilon_1(X) = X, \quad \Upsilon_j(X) = \frac{(2j-1) \cdot \Upsilon_{j-1}(X)X - (j-1)\Upsilon_{j-1}(X)}{j},$$

and $J^* = 2$ is the highest order of the Legendre polynomial function. Note that our low-rank model formulation in (4) encompasses the generative models of $\mathcal{Y}_{i,t,l}$ in both (M1) and (M2) with the potential outcomes tensor defined as $\mathcal{Y}_{i,t,l} = \mathcal{G} \times_1 \mathbf{U}_{1,i}^\top \times_2 \mathbf{U}_{2,t}^\top \times_3 \mathbf{U}_{3,l}^\top + \mathcal{E}_{i,t,l}$ with \mathcal{G} representing the loading coefficients for the associated factors $(\mathbf{U}_{1,i}, \mathbf{U}_{2,t}, \mathbf{U}_{3,l})$. For (M1), we have

$$\mathbf{U}_{1,i} = \{1, \mathbf{1}_{d_0}^\top X_{i,0}\}^\top \in \mathbb{R}^{2 \times 1}, \quad \mathbf{U}_{2,t} = (1) \in \mathbb{R}^{1 \times 1}, \quad \mathbf{U}_{3,l} = (1, l_{(b),1}, \dots, l_{(b),k}) \in \mathbb{R}^{(k+1) \times 1},$$

For (M2), let the basis functions $\Phi(\mathbf{X}_0) = \{1, \Upsilon_1(\mathbf{X}_0), \Upsilon_2(\mathbf{X}_0)\} \in \mathbb{R}^{N \times (2d_0+1)}$, we have

$$\begin{aligned} \mathbf{U}_{1,i} &= \{1, \sum_{j=1}^{J^*} \mathbf{1}_{d_0}^\top \Upsilon_j(X_{i,0}), \mathbf{1}_{d_0}^\top X_{i,0}, (\mathbf{1}_{d_0}^\top X_{i,0})^2\}^\top \in \mathbb{R}^{4 \times 1}, \quad \mathbf{U}_{2,t} = (1, 2^{-t}) \in \mathbb{R}^{2 \times 1}, \\ \mathbf{U}_{3,l} &= (1, l_{(b),1}, \dots, l_{(b),k}, \mathbf{1}_k^\top l_{(b)}, u_3^l) \in \mathbb{R}^{(k+3) \times 1}, \\ u_3^l &= \eta_1 a_{i,t} \mathbf{1}_{k-1}^\top a_{(t-k+2):t} + \eta_2 a_{i,t-1} \mathbf{1}_{k-1}^\top a_{(t-k+2):t} + \eta_3 a_{i,t-2} \mathbf{1}_{k-1}^\top a_{(t-k+2):t} \\ &+ \eta_1 a_{i,t-1} \mathbf{1}_{k-1}^\top a_{(t-k+1):(t-1)} + \eta_2 a_{i,t-2} \mathbf{1}_{k-1}^\top a_{(t-k+1):(t-1)} + \eta_3 a_{i,t-3} \mathbf{1}_{k-1}^\top a_{(t-k+1):(t-1)}, \end{aligned}$$

where the factor u_3^l is induced by $X_{i,t}^{a_{(t-2):t}} \mathbf{1}_{k-1}^\top a_{(t-k+2):t} + X_{i,t-1}^{a_{(t-3):(t-1)}} \mathbf{1}_{k-1}^\top a_{(t-k+1):(t-1)}$. For (M2) with covariate-orthogonal component $\mathbf{\Gamma}$, the potential outcome tensor admits the same low-rank model formulation as (M2) with the tensor factors of mode-1 modified to $\mathbf{U}_{1,i} = \{1, \sum_{j=1}^{J^*} \mathbf{1}_{d_0}^\top \Upsilon_j(X_{i,0}) +$

$\sum_{j=1}^{J^*} \Gamma_{i,j}, \mathbf{1}_{d_0}^\top X_{i,0}, (\mathbf{1}_{d_0}^\top X_{i,0})^2 \} \in \mathbb{R}^4$, where $\mathcal{Y}_{i,t,\{a_{i,(t-k+1):t}\}_{(10)}}$ is defined by

$$\begin{aligned} \mathcal{Y}_{i,t,\{a_{i,(t-k+1):t}\}_{(10)}} = & 4 \sum_{j=1}^{J^*} \{ d_0^{-1} \mathbf{1}_{d_0}^\top \Upsilon_j(X_{i,0}) + \Gamma_{i,j} \} + 4 \cdot \mathbf{1}_{d_0}^\top X_{i,0} \cdot 2^{-t} \\ & + 3 \cdot \mathbf{1}_k^\top a_{(t-k+1):t} \cdot \mathbf{1}_{d_0}^\top X_{i,0} + 2 a_{i,t} \cdot \mathbf{1}_{d_0}^\top X_{i,0} + a_{i,t-1} \cdot \mathbf{1}_{d_0}^\top X_{i,0} \\ & + \mathbf{1}_k^\top a_{(t-k+1):t} \cdot \mathbf{1}_{d_0}^\top X_{i,0} \cdot X_{i,t}^{a_{(t-2):t}} + \mathbf{1}_k^\top a_{(t-k+1):t} \cdot \mathbf{1}_{d_0}^\top X_{i,0} \cdot X_{i,t-1}^{a_{(t-3):(t-1)}} \\ & + 5\beta_1 X_{i,t}^{a_{(t-2):t}} \cdot \mathbf{1}_{d_0}^\top X_{i,0} + 3\beta_2 X_{i,t-1}^{a_{(t-3):(t-1)}} \cdot \mathbf{1}_{d_0}^\top X_{i,0} \\ & + \beta_1 X_{i,t}^{a_{(t-2):t}} + \beta_2 X_{i,t-1}^{a_{(t-3):(t-1)}} + \gamma_1 a_{i,t} + \gamma_2 a_{i,t-1} + \mathcal{E}_{i,t,l}. \end{aligned}$$

A1.1.2 Hyperparameter tuning

In this subsection, we examine the effect of the tuning process for the hyperparameters. First, we generate $(A_{i,t}, \mathcal{Y}_{i,t,l})$ following the same data generating procedures as (A1) and (M2) with fixed multi-linear ranks and covariate-orthogonal noises $\Gamma_{i,j}$ (none or strong) as defined in Section 5.2. Instead of perceiving the multi-linear ranks as known in Sections 5.1 and 5.2, we use the BIC criterion in (7) to sequentially tune these hyperparameters. In particular, we first randomly draw the parameter candidates r_1^\dagger and r_2^\dagger from their tuning ranges, and tune the remaining rank r_3 via (7) with fixed r_1^\dagger and r_2^\dagger . Next, given the tuned rank r_3 , we tune the other two ranks in a similar vein. We set the tuning range for rank r_1 to be $\{1, 3, 5, 7\}$, r_2 to be $\{2, 4, 6\}$ and r_3 to be $\{6, 8, 10\}$.

Figures A1 presents the normalized mean squared error $\ell_2(\hat{\mathcal{Y}})$ when the data-adaptive tuning process is adopted. It can be seen that the BIC-based tuning procedure is subject to a minor quality drop in the absence of covariate-independent components $\Gamma_{i,j}$ when compared to the oracle estimator with known multi-linear ranks. But when the covariate-orthogonal noise $\Gamma_{i,j}$ is strong, BIC-tuned estimators achieve comparable normalized mean squared errors $\ell_2(\hat{\mathcal{Y}})$ as the oracle estimators over the varying amounts of N and T . These findings highlight the practicality of the BIC-based tuning scheme in real-world setups, where covariate-orthogonal noises are ubiquitous and inevitable.

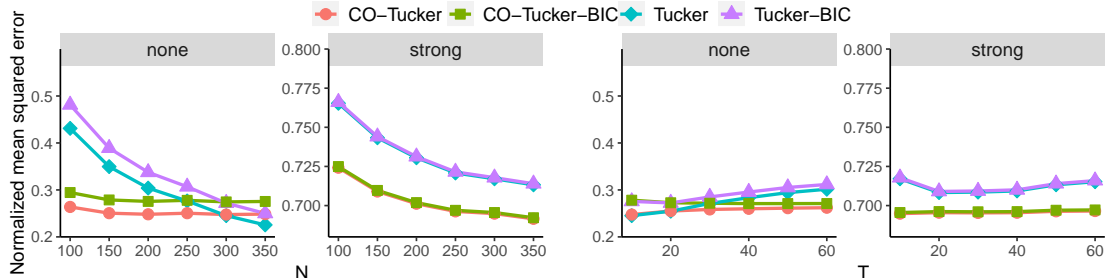


Figure A1: Averaged normalized mean squared tensor error, when $T = 10$, $N = 100, 150, \dots, 350$ (left), and $N = 300$, $T = 10, 20, \dots, 60$ (right) under none, and strong noises due to the covariate-orthogonal component $\Gamma_{i,j}$; TUCKER and CO-TUCKER are the *vanilla* and the covariate-assisted tensorized HRMSMs with known multi-linear ranks (r_1, r_2, r_3) , CO-TUCKER-BIC and TUCKER-BIC are the estimators with adaptively tuned multi-linear ranks (r_1, r_2, r_3) .

A1.1.3 Additional simulation studies for ATE estimation

Considering the estimation error of the average treatment effect $\tau_{\text{ATE}}^{l,l'}$ defined in Section 3.2.1, the Frobenius norm error in Theorem 1 ensures the convergence of the ATE estimation:

$$|\tau_{\text{ATE}}^{l,l'} - \hat{\tau}_{\text{ATE}}^{l,l'}| = (\mathcal{Y}^* - \hat{\mathcal{Y}}) \times_1 \frac{\mathbf{1}_N}{N} \times_2 \frac{\mathbf{1}_T}{T} \times_3 \{e_l(K) - e_{l'}(K)\} \lesssim \frac{\|\mathcal{Y}^* - \hat{\mathcal{Y}}\|}{\sqrt{NT}},$$

where the right-hand side converges to zero as N and T grow. To provide empirical evidence, we present the estimated ATE comparing the fully active regime $\mathbf{1}_k$ and the baseline regime $\mathbf{0}_k$ using the same data-generating procedures outlined in Section 5.

Figure A2 illustrates that HRMSM can identify the ATE in the presence of time-varying confounding when the outcome follows a simple linear model (M1). However, when the outcome model follows the complex additive model (M2), HRMSM exhibits substantial bias in ATE estimation. In addition, the CT exhibits a non-negligible bias across all settings, which does not diminish as N or T increases. This appears to stem both from the accumulation of autoregressive prediction errors and its inability to update time-varying balanced representations under counterfactual interventions. In contrast, our tensorized HRMSMs demonstrate robustness and satisfactory performance regardless of the complexity of the outcome model. In cases where propensity scores present increased variability, as in (A2), the covariate-assisted tensorized HRMSM is preferable as it leverages additional information from the baseline covariates to impute the missing potential outcomes.

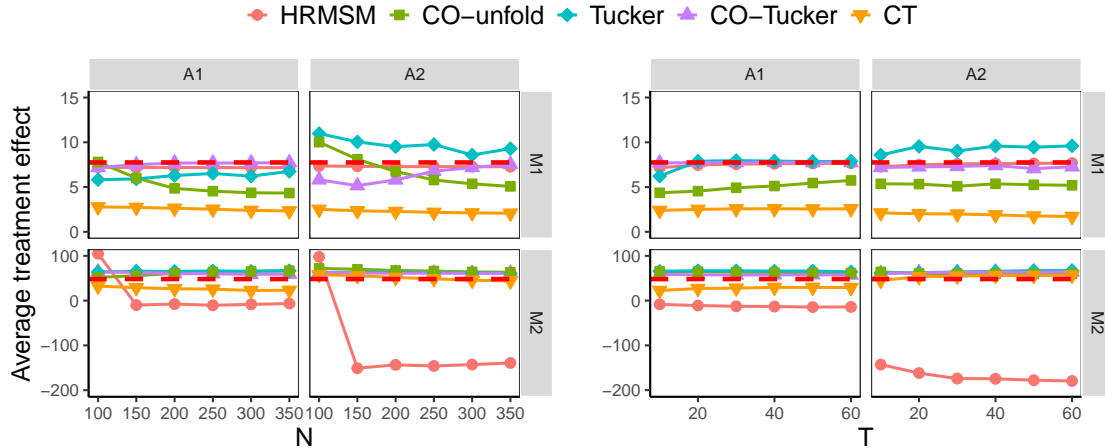


Figure A2: Estimations of the averaged treatment effect $\tau_{\text{ATE}}^{K,0}$ when $T = 10$, $N = 100, 150, \dots, 350$ (left), and $N = 300$, $T = 10, 20, \dots, 60$ (right) under outcome models (M1) and (M2) and treatment assignments (A1) and (A2); HRMSM is the history-restricted marginal structural model, CO-UNFOLD is the matrix factor model based on unfolded tensor, TUCKER is the *vanilla* tensorized HRMSM, CO-TUCKER is the covariate-assisted tensorized HRMSM, and CT is the Causal Transformer; the red solid line stands for the true average treatment effect.

A1.2 Details for application

A1.2.1 Comparisons with matrix completion

In this subsection, we numerically compare our proposed method with the matrix completion method via nuclear norm minimization (MC-NNM) (Athey et al., 2021) and the synthetic nearest

neighbors (SNN) algorithm (Agarwal et al., 2023). In theory, both methods require that the expected number of control units be large enough to recover the post-treatment entries. They also implicitly assume that the potential outcomes are indexed only by the contemporaneous treatment for that unit and not by its past treatment. Hence, we set the length of the treatment regime k to be 1. The outcome of interest here is the potential outcomes matrix $Y(0)$, and the goal is to impute the missing entries of $Y(0)$ under staggered adoption.

We consider the California smoking data studied in Abadie et al. (2010) with $N = 39$ states over $T = 31$ years, including 38 controls units and one treated unit (i.e., California) which will be removed from our experiment. Next, we randomly selected $N_t = 35$ control units and consider them to be treated at some point after T_0 years. The random selection procedure is repeated 10 times and Figure A3 displays the averaged root mean squared error for the post-treatment entries against different ratios T_0/T . Our method utilizes the post-treatment outcomes by storing them in $Y(1)$ and stacks $Y(1)$ with the observed $Y(0)$ to form the observed outcomes tensor. By leveraging additional information from $Y(1)$, it achieves desirable performances in predicting the post-treatment outcomes across all the scenarios even when T_0 is small (i.e., the data presents a large proportion of missingness in the control group). Therefore, our method achieves stable numerical results regardless of the time that subjects are first exposed to the treatment.

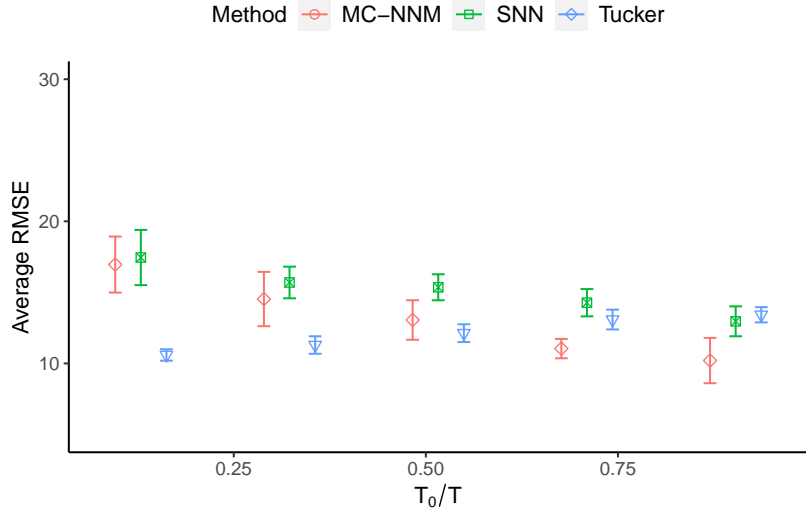


Figure A3: Averaged root mean squared error for different ratios T_0/T ; MC-NNM is the matrix completion via nuclear norm minimization (Athey et al., 2021), SNN is the matrix completion via synthetic nearest neighbors (Agarwal et al., 2023), TUCKER is the *vanilla* tensorized HRMSM with $k = 1$.

A1.2.2 MIMIC III dataset

Table A1 lists the selected baseline covariates $\mathbf{X}_0 \in \mathbb{R}^{N \times 11}$ and the time-varying covariates $\mathbf{X}_t \in \mathbb{R}^{N \times 7}, t = 1, \dots, T$ for the Medical Information Mart for Intensive Care (MIMIC) database.

Table A1: Selected baseline and time-varying covariates for the MIMIC III database with units in parentheses for continuous variables and number of levels in parentheses for categorical variables. A detailed summary of the covariates is given in A. Johnson et al. (2016).

	Covariate	Type
Baseline	gender (2, 0=female, 1=male)	Categorical
	age (years)	
	admission weight (kg)	
	admission temperature (Celsius)	
	glucose amount (mg/dL)	
	blood urea nitrogen amount (mg/dL)	Continuous
	creatinine amount (mg/dL)	
	white blood cell count (E9/L)	
	Glasgow Coma Score (0-15)	
	sodium amount (mEq/L)	
	total input amount (mL)	
	SOFA score at baseline (0-24)	
Time-varying	heart rate (bpm)	Continuous
	respiratory rate (cpm)	
	systolic blood pressure (mmHg)	
	diastolic blood pressure (mmHg)	
	oxygen saturation (%)	
	PaO ₂ / FiO ₂ ratio (%)	
	dose of vasopressin administration (unit)	

A2 Proofs

A2.1 Proof of Theorem 1

A2.1.1 Upper bounds of (8) and (10) under penalized logistic modeling

Under Assumption 3, $\mathcal{W}_{i,t,l} = \mathbb{P}(A_{i,(t-k+1):t} = l_{(b)} \mid H_{i,t})^{-1}$, and we assume that the propensity score at time t follows a logistic model with covariate $H_{i,t}$. The estimation error of $\widehat{\mathcal{W}}_{i,t,l}$ can be bounded by

$$\begin{aligned} |\widehat{\mathcal{W}}_{i,t,l} - \mathcal{W}_{i,t,l}| &= \left| \prod_{j=t-k+1}^t \text{expit}(\widehat{\alpha}^\top H_{i,j}) - \prod_{j=t-k+1}^t \text{expit}(\alpha^{*\top} H_{i,j}) \right| \\ &\leq C_0 \sup_{j=t-k+1, \dots, t} |\text{expit}(\widehat{\alpha}^\top H_{i,j}) - \text{expit}(\alpha^{*\top} H_{i,j})|. \end{aligned}$$

Further, we have

$$\begin{aligned} &\mathbb{P}(\sup_{t=1, \dots, T} |\text{expit}(\widehat{\alpha}^\top H_{i,t}) - \text{expit}(\alpha^{*\top} H_{i,t})| \geq \nu) \\ &\leq \mathbb{P}(\sup_{t=1, \dots, T} \{\text{expit}(\widehat{\alpha}^{*\top} H_{i,t}) + o_{\mathbb{P}}(1)\} H_{i,t}^\top (\widehat{\alpha}_t - \alpha_t^*) \geq \nu) \\ &\leq \sum_{t=1}^T \mathbb{P} \left\{ C_0(1-\delta) \sum_{j \in \mathcal{J}_t} N^{1/2} (\widehat{\alpha}_{t,j} - \alpha_{t,j}^*) \geq N^{1/2} \nu \right\} \\ &\leq 2 \sum_{t=1}^T \exp \left\{ -\frac{cN\nu^2}{|\mathcal{J}_t|^2 C_0^2 (1-\delta)^2} \right\}, \end{aligned}$$

where $\tilde{\alpha}^*$ lies between $\widehat{\alpha}_t$ and α_t^* , the second inequality uses Assumptions A2 (a) and 4, and the third inequality uses the concentration inequality for sub-Gaussian where $N^{1/2}(\widehat{\alpha}_{t,j} - \alpha_{t,j}^*)$, $j \in \mathcal{J}_t$ is sub-Gaussian and $\widehat{\alpha}_{t,j} \rightarrow 0$, $j \in \mathcal{J}_t^c$ by Lemma A3. Therefore, we have

$$\begin{aligned} \sup_{t=1, \dots, T} |\widehat{\mathcal{W}}_{i,t,l} - \mathcal{W}_{i,t,l}| &\leq C_0 \sup_{t=1, \dots, T} |\text{expit}(\widehat{\alpha}^\top H_{i,t}) - \text{expit}(\alpha^{*\top} H_{i,t})| \\ &\leq C \max_{t=1, \dots, T} |\mathcal{J}_t| \log^{1/2}(N+T+K) N^{-1/2}, \end{aligned} \tag{A1}$$

for some constant C with a probability greater than $1 - (N+T+K)^{-2}$ for any $\alpha \geq 1$. The remaining terms require to bound the first- and second-moment of a sub-Gaussian error, that is, $\|\mathcal{Y}_{i,t,l} - \mathcal{Y}_{i,t,l}^*\|_{\psi_1}^2 = \|\mathcal{Y}_{i,t,l} - \mathcal{Y}_{i,t,l}^*\|_{\psi_2}^2 = \sigma^2$ (Vershynin, 2018),

$$\mathbb{P} \left\{ \sum_{\Omega_{i,t,l}=1} (\mathcal{Y}_{i,t,l} - \mathcal{Y}_{i,t,l}^*)^2 \geq t \right\} \leq 2 \exp \left\{ -c \min \left(\frac{t^2}{NT\sigma^4}, \frac{t}{\sigma^2} \right) \right\} = 2 \exp \left\{ -\frac{ct^2}{NT\sigma^4} \right\}.$$

By matching the tail probabilities under Assumption 6, we have

$$\sum_{\Omega_{i,t,l}=1} (\mathcal{Y}_{i,t,l} - \mathcal{Y}_{i,t,l}^*)^2 \leq C\sigma^2 \sqrt{NT \log(N+T+K)},$$

with probability higher than $1 - (N + T + K)^{-2}$. Combine with the bound (A1), we have

$$\begin{aligned} & \sum_{\Omega_{i,t,l}=1} (\widehat{\mathcal{W}}_{i,t,l} - \mathcal{W}_{i,t,l})(\mathcal{Y}_{i,t,l} - \widehat{\mathcal{Y}}_{i,t,l})^2 \\ & \leq C^2 \max_{t=1,\dots,T} |\mathcal{J}_t| N^{-1/2} \log^{1/2}(N + T + K) \left\{ \sigma^2 \sqrt{NT \log(N + T + K)} + \|\mathcal{Y}^* - \widehat{\mathcal{Y}}\|_F^2 \right\} \end{aligned}$$

with probability greater than $1 - 2(N + T + K)^{-2}$ since $\sum_{\Omega_{i,t,l}=1} (\mathcal{Y}_{i,t,l} - \widehat{\mathcal{Y}}_{i,t,l})^2 \leq 2\{\sum_{\Omega_{i,t,l}=1} (\mathcal{Y}_{i,t,l} - \mathcal{Y}_{i,t,l}^*) + \sum_{\Omega_{i,t,l}=1} (\mathcal{Y}_{i,t,l}^* - \widehat{\mathcal{Y}}_{i,t,l})\}$. Therefore,

$$|I_1| + |I_3| \leq C_1 \max_{t=1,\dots,T} |\mathcal{J}_t| N^{-1/2} \log^{1/2}(N + T + K) \left\{ \sigma^2 \sqrt{NT \log(N + T + K)} + \|\mathcal{Y}^* - \widehat{\mathcal{Y}}\|_F^2 \right\},$$

for some constant C_1 .

A2.1.2 Upper bound of (9)

Denote $L_{N,T}(\mathcal{Y}; \mathcal{W}) = \sum_{i,t} \mathcal{W}_{i,t,l} \{Y_{i,t} - \mathcal{Y}(i, t, l)\}^2 / (NT)$, $L_{N,T}(\mathcal{Y}) = \mathbb{E}\{L_{N,T}(\mathcal{Y}; \mathcal{W})\}$. Consider the restricted tensor space, which requires an upper bound on the incoherence of the loading matrices and the spectral norm of each matricization of the core tensor \mathcal{G} . Let

$$\begin{aligned} \mu(\mathbf{U}_1) &= \frac{N}{r_1} \|\mathbf{U}_1\|_{2,\infty}^2, \mu(\mathbf{U}_2) = \frac{T}{r_2} \|\mathbf{U}_2\|_{2,\infty}^2, \mu(\mathbf{U}_3) = \frac{K}{r_3} \|\mathbf{U}_3\|_{2,\infty}^2, \\ \mu(\mathcal{X}) &= \max\{\mu(\mathbf{U}_1), \mu(\mathbf{U}_2), \mu(\mathbf{U}_3)\}, \end{aligned}$$

and the restricted tensor space $\mathfrak{C}(r_1, r_2, r_3, \mu_0, L_0)$ is defined as

$$\begin{aligned} & \mathfrak{C}(r_1, r_2, r_3, \mu_0, L_0) \\ &= \left\{ \mathcal{X} = \mathcal{G} \times_1 \mathbf{U}_1 \times_2 \mathbf{U}_2 \times_3 \mathbf{U}_3, \quad \mu(\mathcal{X}) \leq \mu_0, \quad \max_{k \in \{1,2,3\}} \|\mathcal{M}_k(\mathcal{G})\| \leq L_0 \sqrt{\frac{NTK}{\mu_0^{3/2} (r_1 r_2 r_3)^{1/2}}} \right\}. \end{aligned}$$

Now, using the definition of $\widehat{\mathcal{Y}}$, i.e., $L_{N,T}(\widehat{\mathcal{Y}}; \widehat{\mathcal{W}}) \leq L_{N,T}(\mathcal{Y}^*; \mathcal{W})$, we have

$$\begin{aligned} & \frac{1}{NT} \sum_{i,t} \mathcal{W}_{i,t,l} (\mathcal{Y}_{i,t,l}^* - \widehat{\mathcal{Y}}_{i,t,l})^2 \leq -\frac{2}{NT} \sum_{i,t} \mathcal{W}_{i,t,l} \mathcal{E}_{i,t,l} (\mathcal{Y}_{i,t,l}^* - \widehat{\mathcal{Y}}_{i,t,l}) - \frac{I_1 + I_3}{NT} \\ & \leq -\frac{2}{NT} \langle \mathcal{E}_\Omega^w, \mathcal{Y}^* - \widehat{\mathcal{Y}} \rangle - \frac{I_1 + I_3}{NT} \\ & \leq -\frac{2}{NT} \langle \mathcal{E}_\Omega^w, (\mathcal{Y}^* - \widehat{\mathcal{Y}}) \times_1 \mathbf{P}_{\Phi(\mathbf{X})} + (\mathcal{Y}^* - \widehat{\mathcal{Y}}) \times_1 \mathbf{P}_{\Phi(\mathbf{X})}^\perp \rangle \\ & \quad + \frac{1}{NT} (\|I_1\| + \|I_3\|) \\ & \leq \frac{2}{NT} \|\mathcal{E}_\Omega^w\| \left\{ \|(\mathcal{Y}^* - \widehat{\mathcal{Y}}) \times_1 \mathbf{P}_{\Phi(\mathbf{X})}\|_* + \|(\mathcal{Y}^* - \widehat{\mathcal{Y}}) \times_1 \mathbf{P}_{\Phi(\mathbf{X})}^\perp\|_* \right\} \\ & \quad + \frac{1}{NT} (\|I_1\| + \|I_3\|), \end{aligned} \tag{A2}$$

where $\mathcal{E}_\Omega^w = \sum_{(i,t) \in \mathcal{O}} \mathcal{W}_{i,t,l} \mathcal{E}_{i,t,l} \cdot e_i(N) \otimes e_j(T) \otimes e_l(K)$ whose entries are all zero except its (i, t, l) -th entry and the fourth inequality is derived by Lemma A6. The boundary of (A2) is challenging and can be solved in the following steps.

Step 1 Obtain an upper bound for $\|\mathcal{E}_\Omega^w\|$. Previous literature mainly focuses on independent sampling (Negahban & Wainwright, 2012; Klopp, 2014; Hamidi & Bayati, 2019), but it is not applicable in our setup since the entries in Ω tie to the received treatment regimes and are correlated by nature. To curb the impact of dependence between $\Omega_{i,t,l}$ and $\Omega_{i,t',l'}$ for any $t' \neq t$ and $l' \neq l$, an additional assumption is needed.

Assumption A1. *For any $t' \geq t + k$ and some constant $c_0 > 0$, the treatment regimes $A_{i,(t-k+1):t}$ and $A_{i,(t'-k+1):t'}$ satisfy*

$$1 - c_0 \leq \frac{\mathbb{P}(A_{i,(t'-k+1):t'} = a_{(t-k+1):t} \mid \mathbb{V}_{i,t}, A_{i,(t-k+1):t})}{\mathbb{P}(A_{i,(t'-k+1):t'} = a_{(t'-k+1):t'})} \leq 1 + c_0,$$

where $a_{(t-k+1):t}, a_{(t'-k+1):t'} \in \mathbb{A}_k$.

Assumption A1 implies that two treatment regimes assigned at time points far apart are almost independent (Mandal & Parkes, 2019). Under Assumption A1, we consider separating the sum of tensors \mathcal{E}_Ω^w by computing t modulo k

$$\mathcal{E}_\Omega^{[h]} = \sum_{i=1}^N \sum_{\text{mod}(t,k)=h} \mathcal{W}_{i,t,l} \mathcal{E}_{i,t,(A_{i,(t-k+1):t})_{(10)}} \cdot e_i(N) \otimes e_t(T) \otimes e_{(A_{i,(t-k+1):t})_{(10)}}(K),$$

for $h = 0, \dots, k-1$, where $\text{mod}(t,k)$ returns the remainder of t divided by k , and $\mathcal{E}_\Omega^{[h]}$ is the sum of several (nearly) independent random tensors under Assumption A1. Therefore, it reduces the likelihood where the mass of observation pattern Ω is concentrated on one or two particular slices. For example, if all the patients have always been treated during the study period, the observation pattern Ω will not be well-conditioned since its one-values shall concentrate on one particular slice of Ω , causing its spectral norm to be abnormally large. Together with Assumption A1, they collectively entail a similar sparse structure on Ω as implied by the uniform sampling design in Klopp (2014), Cai et al. (2021), and Xia et al. (2021). Therefore, the spectral norm of \mathcal{E}_Ω^w can be well-controlled by the Bernstein-type inequality in Lemma A1. Similar results are presented in Nguyen et al. (2015).

Lemma A1. *(Tensor Bernstein Inequality (Theorem 4.3, Luo et al., 2020)) Let Z_1, \dots, Z_N be independent tensor in $\mathbb{R}^{d \times d \times d}$, such that $\mathbb{E}(Z_i) = 0$ and $\|Z_i\| \leq D_Z$ for all $i \in [N]$. Let σ_Z be such that*

$$\sigma_Z^2 \geq \max \left\{ \left\| \mathbb{E} \left(\sum_{i=1}^N Z_i \overline{\square} \sum_{i=1}^N Z_i \right) \right\|, \left\| \mathbb{E} \left(\sum_{i=1}^N Z_i \underline{\square} \sum_{i=1}^N Z_i \right) \right\| \right\}.$$

Then for any $\alpha \geq 0$

$$\mathbb{P} \left(\left\| \sum_{i=1}^N Z_i \right\| \overline{\square} \geq \alpha \right) \leq d^2 \exp \left\{ \frac{-\alpha^2}{2\sigma_Z^2 + (2D_Z\alpha)/3} \right\},$$

where $\overline{\square}$ and $\underline{\square}$ are two generalized Einstein products of tensors, which are defined in Section A2.4.1.

Define the sequence of independent random tensors as $\mathcal{E}_{\Omega_1}^w, \dots, \mathcal{E}_{\Omega_N}^w$. For subject $i \in [N]$, define

$$\begin{aligned} \mathcal{E}_{\Omega_i}^w &= \sum_{t \in \mathcal{O}_i} \mathcal{W}_{i,t,l} \mathcal{E}_{i,t,l} \cdot e_i(N) \otimes e_j(T) \otimes e_l(K) \\ &= \sum_{t=1}^T \mathcal{W}_{i,t,l} \mathcal{E}_{i,t,(A_{i,(t-k+1):t})_{(10)}} \cdot e_i(N) \otimes e_t(T) \otimes e_{(A_{i,(t-k+1):t})_{(10)}}(K), \end{aligned}$$

where $\mathcal{O}_i = \{t : \Omega_{i,t,l} = 1, t = 1, \dots, T\}$ and $\mathcal{E}_\Omega^w = \sum_{i=1}^N \mathcal{E}_{\Omega_i}^w$, and $\mathbb{E}\{\mathcal{E}_{\Omega_i}^w\} = 0$. By the dilation arguments in Chang & Lin (2022), we define an operator $D(\cdot)$ that dilate the non-square tensor to a square tensor. For example, $D(\mathcal{E}_\Omega^w) \in \mathbb{R}^{(N+T+K) \times (N+T+K) \times (N+T+K)}$ and $\|D(\mathcal{E}_\Omega^w)\| = \|\mathcal{E}_\Omega^w\|$ follows by the definition of norm. To resolve the dependence of $(A_{i,(t-k+1):t})_{(10)}$ with i and t , the summation of $D(\mathcal{E}_{\Omega_i,t}^{w,[h]})$ over t modulo k and define

$$\begin{aligned} D(\mathcal{E}_{\Omega_i}^{w,[h]}) &= \sum_{\text{mod } (t,k)=h} D(\mathcal{E}_{\Omega_i,t}^{w,[h]}) \\ &= \sum_{\text{mod } (t,k)=h} \mathcal{W}_{i,t,l} \mathcal{E}_{i,t,(A_{i,(t-k+1):t})_{(10)}} \cdot e_i(N) \otimes e_t(T) \otimes e_{(A_{i,(t-k+1):t})_{(10)}}(K). \end{aligned}$$

By Lemma A1 and union bound, we have

$$\mathbb{P}(\max_i \|D(\mathcal{E}_{\Omega_i}^{w,[h]})\| \geq \alpha) \leq N(N+T+K)^2 \exp \left\{ -\frac{\alpha^2}{2p_{\min}^{-2} k^{-1} T \|D(\mathcal{E}_{\Omega_i,t}^{w,[h]})\|_\psi^2 + (2D_Z^{[h]} \alpha)/3} \right\},$$

where $\|D(\mathcal{E}_{\Omega_i,t}^{w,[h]})\|_\psi^2 = \sigma^2$ and $D_Z^{[h]} \leq p_{\min}^{-1} \sigma^2 \log(N+T+K)$ with probability greater than $1 - (N+T+K)^{-2}$. Hence, it implies that

$$\max_i \|D(\mathcal{E}_{\Omega_i}^{w,[h]})\| = \max_i \left\| \sum_{\text{mod } (t,k)=h} D(\mathcal{E}_{\Omega_i,t}^{w,[h]}) \right\| \leq C \sigma p_{\min}^{-1} k^{-1/2} T^{1/2} \log(N+T+K) \cdot \log(N),$$

with probability greater $1 - (N+T+K)^{-2}$. For the upper bound of the variance, the iterated expectation technique can be used and we have

$$\begin{aligned} \left\| \sum_{i=1}^N \mathbb{E}\{\mathcal{E}_{\Omega_i}^{w,[h]} \square \mathcal{E}_{\Omega_i}^{w,[h]}\} \right\| &= \left\| \sum_{i=1}^N \mathbb{E} \left\{ \sum_{\text{mod } (t,k)=h} \sum_{\text{mod } (t',k)=h} \mathcal{E}_{\Omega_i,t}^{w,[h]} \square \mathcal{E}_{\Omega_i,t'}^{w,[h]} \right\} \right\| \\ &= \left\| \sum_{i=1}^N \mathbb{E} \left\{ \sum_{\text{mod } (t,k)=h} \mathcal{E}_{\Omega_i,t}^{w,[h]} \square \mathcal{E}_{\Omega_i,t}^{w,[h]} + \sum_{t \neq t'} \mathcal{E}_{\Omega_i,t}^{w,[h]} \square \mathcal{E}_{\Omega_i,t'}^{w,[h]} \right\} \right\| \\ &= \left\| \sum_{i=1}^N \sum_{\text{mod } (t,k)=h} \mathbb{E} \left\{ \mathcal{E}_{\Omega_i,t}^{w,[h]} \square \mathcal{E}_{\Omega_i,t}^{w,[h]} \right\} \right\| \\ &\leq \max_{t,l} \sum_i \mathcal{W}_{i,t,l}^2 \sigma^2 \lesssim N p_{\min}^{-2} \sigma^2 \log(N+T+K), \end{aligned}$$

and

$$\begin{aligned} \left\| \sum_{i=1}^N \mathbb{E}\{\mathcal{E}_{\Omega_i}^{w,[h]} \square \mathcal{E}_{\Omega_i}^{w,[h]}\} \right\| &= \left\| \sum_{i=1}^N \mathbb{E} \left\{ \sum_{\text{mod } (t,k)=h} \sum_{\text{mod } (t',k)=h} \mathcal{E}_{\Omega_i,t}^{w,[h]} \square \mathcal{E}_{\Omega_i,t'}^{w,[h]} \right\} \right\| \\ &\leq \max_i \sum_{t,l} \mathcal{W}_{i,t,l}^2 \sigma^2 \lesssim T p_{\min}^{-2} \sigma^2 \log(N+T+K), \end{aligned}$$

with probability greater than $1 - (N+T+K)^{-2}$, where $\mathbb{E}\{\mathcal{E}_{\Omega_i,t}^{w,[h]} \square \mathcal{E}_{\Omega_i,t'}^{w,[h]}\} = 0$ for $t \neq t'$ since $\mathbb{E}\{\mathcal{E}_{i,t,(a_{i,(t-k+1):t})_{(10)}} \mid a_{i,(t-k+1):t}, \mathcal{E}_{i,t',(a_{i,(t-k+1):t})_{(10)}}\} = 0$ under Assumption A1.

Let $D_Z = \sigma p_{\min}^{-1} k^{-1/2} T^{1/2} \log(N + T + K) \log(N)$ and $\sigma_Z^2 = p_{\min}^{-2} (N \vee T) \sigma^2 \log(N + T + K)$, we obtain the upper bound for $\|\mathcal{E}_\Omega^w\|$ by applying Lemma A1 as

$$\begin{aligned} \mathbb{P}(\|\sum_{i=1}^N D(\mathcal{E}_{\Omega_i}^{w,[h]})\|^{\bar{\square}} \geq \alpha) &\leq (N + T + K)^2 \exp\left\{-\frac{\alpha^2}{2\sigma_Z^2 + (2D_Z\alpha)/3}\right\} \\ &\leq (N + T + K)^2 \\ &\times \exp\left[-\frac{3}{4} \min\left\{\frac{\alpha^2}{p_{\min}^{-2} (N \vee T) \sigma^2 \log(N + T + K)}, \frac{\alpha}{\sigma p_{\min}^{-1} k^{-1/2} T^{1/2} \log(N + T + K) \log(N)}\right\}\right], \end{aligned}$$

which holds with probability greater $1 - 2(N + T + K)^{-2}$. By union bound over h , we have with probability greater than $1 - 3(N + T + K)^{-2}$

$$\begin{aligned} \|\sum_{i=1}^N \mathcal{E}_{\Omega_i}^w\| &= \|\sum_{i=1}^N D(\mathcal{E}_{\Omega_i}^w)\| \leq \|\sum_{i=1}^N D(\mathcal{E}_{\Omega_i}^w)\|^{\bar{\square}} \leq \sum_{h=1}^k \|\sum_{i=1}^N D(\mathcal{E}_{\Omega_i}^{w,[h]})\|^{\bar{\square}} \\ &\leq C_3 k \sigma p_{\min}^{-1} \sqrt{(N \vee T) \log(N + T + K)}, \end{aligned}$$

for a constant C_3 , where the first inequality is shown in Luo et al. (2020).

Step 2 We aim to bound the term $\|\mathcal{Y}^* - \hat{\mathcal{Y}}\|_*$. First, we can decompose it into two parts: $\mathcal{Y}^* - \hat{\mathcal{Y}} = (\mathcal{Y}^* - \hat{\mathcal{Y}}) \times_1 \mathbf{P}_{\Phi(\mathbf{X}_0)} + (\mathcal{Y}^* - \hat{\mathcal{Y}}) \times_1 \mathbf{P}_{\Phi(\mathbf{X}_0)}^\perp$, where $\mathbf{P}_{\Phi(\mathbf{X}_0)}$ is the projection matrix onto the column spaces of $\Phi(\mathbf{X}_0)$, and $\mathbf{P}_{\Phi(\mathbf{X}_0)}^\perp$ is the projection matrix onto the orthogonal space of $\Phi(\mathbf{X}_0)$. For the first term, we have

$$\begin{aligned} \|(\mathcal{Y}^* - \hat{\mathcal{Y}}) \times_1 \mathbf{P}_{\Phi(\mathbf{X})}\|_* &= \sup_{\|\mathcal{Z}\| \leq 1} \langle (\mathcal{Y}^* - \hat{\mathcal{Y}}) \times_1 \mathbf{P}_{\Phi(\mathbf{X})}, \mathcal{Z} \rangle \\ &= \sup_{\|\mathcal{Z}\| \leq 1} \langle (\mathcal{Y}^* - \hat{\mathcal{Y}}) \times_1 \Phi(\mathbf{X})^\top, \mathcal{Z} \times_1 \Phi(\mathbf{X})^\top \rangle \\ &\leq \sup_{\|\mathcal{Z}\| \leq 1} \langle (\mathcal{Y}^* - \hat{\mathcal{Y}}) \times_1 \Phi(\mathbf{X})^\top, \mathcal{Z} \rangle \\ &\leq \|(\mathcal{Y}^* - \hat{\mathcal{Y}}) \times_1 \Phi(\mathbf{X})^\top\|_* \\ &\leq 2 \sqrt{\frac{(r_1 \wedge d_\Phi) r_2 r_3}{\max\{(r_1 \wedge d_\Phi), r_2, r_3\}}} \|(\mathcal{Y}^* - \hat{\mathcal{Y}}) \times_1 \Phi(\mathbf{X})^\top\|_F \\ &\leq 2 \sqrt{\frac{(r_1 \wedge d_\Phi) r_2 r_3}{\max\{(r_1 \wedge d_\Phi), r_2, r_3\}}} \|(\mathcal{Y}^* - \hat{\mathcal{Y}})\|_F, \end{aligned}$$

where the last two inequalities are based on Lemma A7, which are adapted from Theorem 1.2 in Kong et al. (2018) and Lemma 5.1 in Hu (2015). For the second term, we have

$$\begin{aligned}
\|(\mathcal{Y}^* - \widehat{\mathcal{Y}}) \times_1 \mathbf{P}_{\Phi(\mathbf{X})}^\perp\|_* &= \|\mathcal{Y}^* \times_1 \mathbf{P}_{\Phi(\mathbf{X})}^\perp\|_* \\
&= \|\mathcal{G}^* \times_1 \{\mathbf{P}_{\Phi(\mathbf{X})}^\perp \cdot (\mathbf{R} + \boldsymbol{\Gamma})\} \times_2 \mathbf{U}_2^* \times_3 \mathbf{U}_3^*\|_* \\
&= \sup_{\|\mathcal{Z}\| \leq 1} \langle \mathcal{G}^* \times_1 \{\mathbf{P}_{\Phi(\mathbf{X})}^\perp \cdot (\mathbf{R} + \boldsymbol{\Gamma})\} \times_2 \mathbf{U}_2^* \times_3 \mathbf{U}_3^*, \mathcal{Z} \rangle \\
&= \sup_{\|\mathcal{Z}\| \leq 1} \langle \{\mathbf{P}_{\Phi(\mathbf{X})}^\perp \cdot (\mathbf{R} + \boldsymbol{\Gamma})\} \mathcal{M}_1(\mathcal{G}^*)(\mathbf{U}_3^* \otimes \mathbf{U}_2^*)^\top, \mathcal{M}_1(\mathcal{Z}) \rangle \\
&= \sup_{\|\mathcal{Z}\| \leq 1} \langle \mathcal{M}_1(\mathcal{G}^*), \{(\mathbf{R}^\top + \boldsymbol{\Gamma}^\top) \mathbf{P}_{\Phi(\mathbf{X})}^\perp\} \mathcal{M}_1(\mathcal{Z})(\mathbf{U}_3^* \otimes \mathbf{U}_2^*) \rangle \\
&= \sup_{\|\mathcal{Z}\| \leq 1} \langle \mathcal{G}^*, \mathcal{Z} \times_1 \{(\mathbf{R}^\top + \boldsymbol{\Gamma}^\top) \mathbf{P}_{\Phi(\mathbf{X})}^\perp\} \times_2 \mathbf{U}_2^{*\top} \times_3 \mathbf{U}_3^{*\top} \rangle \\
&\leq \sup_{\|\mathcal{Z}\| \leq 1} \langle \mathcal{G}^*, \mathcal{Z} \rangle \|\mathbf{P}_{\Phi(\mathbf{X})}^\perp(\mathbf{R} + \boldsymbol{\Gamma})\| \|\mathbf{U}_2^*\| \|\mathbf{U}_3^*\| \\
&\leq \|\mathcal{G}^*\|_* \{\|\mathbf{R}\|_F + \|\boldsymbol{\Gamma}\|\} \\
&\leq C_2 r_3 \sqrt{r_1 \wedge r_2} \max_{k=1,2,3} \|\mathcal{M}_k(\mathcal{G}^*)\| \{\sqrt{Nr_1} \cdot d_\Phi^{-\tau/2} \vee \|\boldsymbol{\Gamma}\|\} \quad (A3) \\
&\leq C_2 r_3 \sqrt{r_1 \wedge r_2} L_0 \sqrt{\frac{NTK}{\mu_0^3 r_1 r_2 r_3}} \{\sqrt{Nr_1} \cdot d_\Phi^{-\tau/2} \vee \|\boldsymbol{\Gamma}\|\},
\end{aligned}$$

where the tensor nuclear norm is the dual norm to the tensor spectral norm (Lim & Comon, 2013; Derksen, 2016), (A3) is based on Lemma A8, $\mathbf{P}_{\Phi(\mathbf{X})}\Phi(\mathbf{X}_0) = \Phi(\mathbf{X}_0)$, $\mathbf{P}_{\Phi(\mathbf{X})}^\perp\boldsymbol{\Gamma} = \boldsymbol{\Gamma}$, $\mathbf{P}_{\Phi(\mathbf{X})}\boldsymbol{\Gamma} = 0$ by definition, and $\|\mathbf{R}\|_F = O(\sqrt{Nr_1} \cdot d_\Phi^{-\tau/2})$ under Assumption A3. Thus, we are able to prove that:

$$\begin{aligned}
&\frac{1}{NT} \sum_{i,t} \mathcal{W}_{i,t,l} (\mathcal{Y}_{i,t,l}^* - \widehat{\mathcal{Y}}_{i,t,l})^2 \\
&\leq \frac{2}{NT} \|\mathcal{E}_\Omega^w\| \left\{ \|(\mathcal{Y}^* - \widehat{\mathcal{Y}}) \times_1 \mathbf{P}_{\Phi(\mathbf{X})}\|_* + \|(\mathcal{Y}^* - \widehat{\mathcal{Y}}) \times_1 \mathbf{P}_{\Phi(\mathbf{X})}^\perp\|_* \right\} \\
&+ \frac{1}{NT} (\|I_1\| + \|I_3\|) \\
&\leq \frac{4C_3 k \sigma}{NT} p_{\min}^{-1} \sqrt{(N \vee T)} \log(N + T + K) \cdot \sqrt{\frac{(r_1 \wedge d_\Phi) r_2 r_3}{\max\{(r_1 \wedge d_\Phi), r_2, r_3\}}} \|(\mathcal{Y}^* - \widehat{\mathcal{Y}})\|_F \\
&+ \frac{2C_2 k \sigma}{NT} p_{\min}^{-1} \sqrt{(N \vee T)} \log(N + T + K) \cdot r_3 \sqrt{r_1 \wedge r_2} L_0 \sqrt{\frac{NTK}{\mu_0^3 r_1 r_2 r_3}} \left\{ \sqrt{Nr_1} \cdot d_\Phi^{-\tau/2} \vee \|\boldsymbol{\Gamma}\| \right\} \\
&+ \frac{1}{NT} (\|I_1\| + \|I_3\|).
\end{aligned}$$

Notice that if $\|\Delta\|_F^2 \leq 4L_0^2 T \log(N + T + K)/p_{\min}$, then the bound in Theorem holds. Hence, our focus now is the error bound conditional on the event where $\|\Delta\|_F^2 \geq 4L_0^2 T \log(N + T + K)/p_{\min}$.

A2.1.3 Restricted strong convexity

We now aim to prove the restricted strong convexity of the loss function, that is $\|\mathcal{Y}^* - \widehat{\mathcal{Y}}\|_F^2$ is larger than a constant fraction of $\|\mathbf{P}_\Omega(\mathcal{Y}^* - \widehat{\mathcal{Y}})\|_F^2$ up to an additive term. A summary of the

proof adapted to our setting. For starter, we can provide an entry-wise upper bound for any $\mathcal{X} \in \mathfrak{C}(r_1, r_2, r_3, \mu_0, L_0)$. Let the maximum entry of \mathcal{X} be $\|\mathcal{X}\|_{\max}$ and

$$\begin{aligned}
\|\mathcal{X}\|_{\max} &= \max_{i,t,l} |\langle \mathcal{X}, e_i \otimes e_t \otimes e_l \rangle| \\
&= \max_{i,t,l} |\langle \mathcal{G} \times_1 \mathbf{U}_1 \times_2 \mathbf{U}_2 \times_3 \mathbf{U}_3, e_i \otimes e_t \otimes e_l \rangle| \\
&= \max_{i,t,l} |\langle \mathcal{G}, (\mathbf{U}_1^\top e_i) \otimes (\mathbf{U}_2^\top e_t) \otimes (\mathbf{U}_3^\top e_l) \rangle| \\
&\leq \max_{k \in \{1,2,3\}} \|\mathcal{M}_k(\mathcal{G})\| \max_i \|\mathbf{U}_1^\top e_i\|_F \max_t \|\mathbf{U}_2^\top e_t\|_F \max_l \|\mathbf{U}_3^\top e_l\|_F \\
&\leq \max_{k \in \{1,2,3\}} \|\mathcal{M}_k(\mathcal{G})\| \|\mathbf{U}_1\|_{2,\infty} \|\mathbf{U}_2\|_{2,\infty} \|\mathbf{U}_3\|_{2,\infty} \\
&\leq L_0 \sqrt{\frac{NTK}{\mu_0^{3/2} (r_1 r_2 r_3)^{1/2}}} \cdot \mu_0^{3/2} (r_1 r_2 r_3)^{1/2} (NTK)^{-1/2} \leq L_0,
\end{aligned}$$

which implies the entry-wise upper bound. Next, Lemma A2 proves the restricted strong convexity by the Massart's inequality (Massart, 2000) and peeling arguments in Lemma 14, Klopp (2014).

Lemma A2. *Let $\Delta = \mathcal{Y}^* - \widehat{\mathcal{Y}}$ and $\|\Delta\|_{L^2(\Omega)} = \sqrt{\mathbb{E}_{\mathcal{A}}(\|P_{\Omega}(\Delta)\|_F^2)}$, if $\Delta \in \mathfrak{C}(r_1, r_2, r_3, \mu_0, L_0)$ and $\|\Delta\|_F^2 \geq L_0^2 \theta / p_{\min}$ for $\theta = C'' T \log(N + T + K)$, we have for small enough constant C_4 (e.g., $C_4 = 0.005$),*

$$\mathbb{P}_{\mathcal{A}} \left\{ \frac{p_{\min}}{2} \|\Delta\|_F^2 \geq \|P_{\Omega}(\Delta)\|_F^2 + 2 \|\Delta\|_{\max}^2 \vartheta \right\} \leq 2 \exp \left(- \frac{C_4 \theta}{T} \right)$$

where $p_{\min} = \delta^k \leq \mathbb{P}(A_{i,t-k+1:t} = a_{(t-k+1):t} \mid H_{i,t}) \leq (1 - \delta)^k = p_{\max}$ by Lemma A10,

$$\vartheta = C'' \frac{(r_1 \wedge d_{\Phi}) r_2 r_3}{\max\{(r_1 \wedge d_{\Phi}), r_2, r_3\} p_{\min}} k^2 (N \vee T) \log(N + T + K),$$

and $\mathbb{P}_{\mathcal{A}}, \mathbb{E}_{\mathcal{A}}$ are taken with respect to the marginal distribution of the treatment assignments.

Combing Lemma A2 with the previous steps and the upper bound on I_1 and I_3 , we have for $\mathcal{Y}^*, \widehat{\mathcal{Y}} \in \mathfrak{C}(r_1, r_2, r_3, \mu_0, L_0)$ and $\|\Delta\|_F^2 \geq L_0^2 \theta / p_{\min}$,

$$\begin{aligned}
\frac{p_{\min}}{2p_{\max}} \|\mathcal{Y}^* - \widehat{\mathcal{Y}}\|_F^2 &\leq \frac{p_{\min}}{4p_{\max}} \|\mathcal{Y}^* - \widehat{\mathcal{Y}}\|_F^2 \\
&+ C_1 \max_{t=1, \dots, T} |\mathcal{J}_t| \log^{1/2}(N + T + K) N^{-1/2} \|\mathcal{Y}^* - \widehat{\mathcal{Y}}\|_F^2
\end{aligned} \tag{A4}$$

$$\begin{aligned}
&+ 16C_2^2 \frac{(r_1 \wedge d_{\Phi}) r_2 r_3}{\max\{(r_1 \wedge d_{\Phi}), r_2, r_3\}} \sigma^2 p_{\min}^{-2} k^2 (N \vee T) \log(N + T + K) p_{\min}^{-1} p_{\max} \\
&+ 2C_2 C_3 p_{\min}^{-1} k \{\log(N + T + K)\}^{1/2} \sigma L_0 \sqrt{\frac{r_3 (r_1 \wedge r_2) (N \vee T) NTK}{\mu^3 r_1 r_2}} \{\sqrt{Nr_1} \cdot d_{\Phi}^{-\tau/2} \vee \|\boldsymbol{\Gamma}\|\} \tag{A5}
\end{aligned}$$

$$\begin{aligned}
&+ 8C_2 C_6 L_0^2 \frac{(r_1 \wedge d_{\Phi}) r_2 r_3}{\max\{(r_1 \wedge d_{\Phi}), r_2, r_3\} p_{\min} p_{\max}} k^2 (N \vee T) \log(N + T + K) \\
&+ C_1 \max_{t=1, \dots, T} |\mathcal{J}_t| \log^{1/2}(N + T + K) N^{-1/2} \sigma^2 \sqrt{NT \log(N + T + K)}, \tag{A6}
\end{aligned}$$

with probability greater than $1 - 7(N + T + K)^{-2}$. Under Assumption 5, (A5) and (A6) are negligible compared to the rest terms. Therefore, it completes the proof of Theorem 1 by rearranging the

terms as follows:

$$\begin{aligned} \frac{\|\mathcal{Y}^* - \widehat{\mathcal{Y}}\|_F^2}{NT} &\leq \frac{CL_0^2}{p_{\min}} \frac{\log(N+T+K)}{N} \\ &\vee \frac{C'k^2(r_1 \wedge d_\Phi)r_2r_3}{\max\{(r_1 \wedge d_\Phi), r_2, r_3\}p_{\min}^2} \frac{(N \vee T)}{NT} \log(N+T+K) \left\{ \sigma^2 \left(\frac{p_{\max}}{p_{\min}} \right)^2 \vee L_0^2 \right\}, \end{aligned}$$

with probability greater than $1 - 7(N+T+K)^{-2}$ for some constants C and C' , where (A4) is negligible to $\|\mathcal{Y}^* - \widehat{\mathcal{Y}}\|_F^2$ under Assumption A2(e).

A2.2 Additional Lemmas

In this section, we include technical proof for all the lemmas.

A2.3 Proof of Lemma A3

Lemma A3. *Under Assumption 1-4 and regularity conditions in Assumption A2 of the Appendix, let $p_{\lambda_\alpha}(\cdot)$ be the SCAD penalty function*

$$p_{\lambda_\alpha}(|\alpha_{1,t}|) = \begin{cases} \lambda_\alpha |\alpha_{1,t}| & \text{if } |\alpha_{1,t}| < \lambda_\alpha \\ \frac{\epsilon \lambda_\alpha |\alpha_{1,t}| - \alpha_{1,t}^2 - \lambda_\alpha^2}{\epsilon - 1} & \text{if } \lambda_\alpha < |\alpha_{1,t}| \leq \epsilon \lambda_\alpha, \\ \frac{\lambda_\alpha^2(\epsilon + 1)}{2} & \text{if } |\alpha_{1,t}| > \epsilon \lambda_\alpha \end{cases}$$

with $\epsilon = 3.7$ as suggested in Fan & Li (2001), there exists an approximate penalized minimizer $\widehat{\alpha}_t$ to (6) at each time point, such that

$$\widehat{\alpha}_{t,\mathcal{J}_t} - \alpha_{t,\mathcal{J}_t}^* = O_{\mathbb{P}}(\sqrt{|\mathcal{J}_t|/N}), \quad \mathbb{P}(\widehat{\alpha}_{t,\mathcal{J}_t^c} = 0) \rightarrow 1 \text{ as } N \rightarrow \infty,$$

where α_{t,\mathcal{J}_t} is a sub-vector of α_t formed by its elements whose indexes are in \mathcal{J}_t , and \mathcal{J}_t^c is the complement of \mathcal{J}_t .

We request the following regularity conditions to hold.

Assumption A2. (a) $\|X_{i,t}\|$ are bounded uniformly by C_0 for $i = 1, \dots, N$ and $t = 1, \dots, T$.
(b) Let α_t^* lies in the interior of the compact ball and

$$Z_{i,t} = \left\{ \frac{\exp(\alpha_{0,t}^* + \alpha_{1,t}^* H_{i,t})}{1 + \exp(\alpha_{0,t}^* + \alpha_{1,t}^* H_{i,t})} - A_{i,t} \right\}.$$

Assume $\mathbb{E}(Z_{i,t}) = 0$ for $i = 1, \dots, N, t = 1, \dots, T$ and there exists constant C_1 such that $\mathbb{E}(|Z_{i,t}|^{2+\delta}) \leq C_1$ for some $\delta > 0$.

(c) Let $\Sigma_{Z_{i,t}} = \mathbb{E}\{\partial Z_{i,t}/\partial \alpha_t^\top \cdot (1, H_{i,t})\}$, that is

$$\Sigma_{Z_{i,t}} = \mathbb{E} \left\{ (1, H_{i,t})^\top \frac{\exp(\alpha_{0,t}^* + \alpha_{1,t}^* H_{i,t})}{\{1 + \exp(\alpha_{0,t}^* + \alpha_{1,t}^* H_{i,t})\}^2} (1, H_{i,t}) \right\}.$$

Assume $\|\Sigma_{Z_{i,t}}\|$ is bounded and satisfied the restricted eigenvalue condition, that is, for any b

$$C_2 \|b\|_2^2 \leq b^\top \Sigma_{Z_{i,t}} b \leq C_3 \|b\|_2^2,$$

for some constants C_2 and C_3 .

(d) For any $t = 1, \dots, T$, there exist constants C_4 and C_5 such that

$$C_4 < \sigma_{\min} \left(\frac{1}{N} \sum_{i=1}^N H_{i,t} H_{i,t}^\top \right) < \sigma_{\max} \left(\frac{1}{N} \sum_{i=1}^N H_{i,t} H_{i,t}^\top \right) < C_5,$$

where $\sigma_{\min}(\cdot)$ and $\sigma_{\max}(\cdot)$ return the minimum and the maximum eigenvalue of a symmetric matrix, respectively.

(e) $|\mathcal{J}_t| = O(1)$ for any $t = 1, \dots, T$. The tuning parameter satisfies that $\lambda_\alpha \rightarrow 0$ and $\sqrt{N}\lambda_\alpha \rightarrow \infty$ as $N \rightarrow \infty$.

Assumptions A2 (a)-(d) are typical regularity conditions in the penalization literature (Fan & Li, 2001; Yang, Kim, & Song, 2020). Assumption A2(e) specifies the restrictions on the dimension of the true nonzero coefficients and places an asymptotic nature for the tuning parameter. Strictly speaking, a weaker sparsity assumption can be imposed on the number of nonzero coefficients for the propensity score model. Assume that $\max_{t=1, \dots, T} |\mathcal{J}_t| \log^{1/2}(N + T + k)N^{-1/2} = o(1)$, our non-asymptotic analysis in Theorem 1 remains valid as shown in Section A2.1.3. Similar conditions can be found in Belloni et al. (2017) and Ning et al. (2020).

Proof of Lemma A3. For each time point t , we aim to prove that there exists a large constant τ for any given $\varepsilon > 0$ such that

$$\mathbb{P} \left\{ \sup_{\alpha_t \in \partial \mathfrak{M}_\tau} Q(\alpha_t) > Q(\alpha_t^*) \right\} \geq 1 - \varepsilon, \quad \mathfrak{M}_\tau = \{ \alpha_t : \|\alpha_t - \alpha_t^*\| \leq \tau \sqrt{|\mathcal{J}_t|/N} \}, \quad (\text{A7})$$

and $\partial \mathfrak{M}_\tau$ means that α_t attains the boundary of the restricted set, i.e., $\|\alpha_t - \alpha_t^*\| = \tau \sqrt{|\mathcal{J}_t|/N}$. (A7) implies that there exists a local minimum $\hat{\alpha}_t$ in the ball \mathfrak{M}_τ as continuous function must have a local minimum within a compact subset, i.e., \mathfrak{M}_r . Using $p_{\lambda_\alpha}(|\alpha_{1,t,j}|) = 0, j \in \mathcal{J}_t^c$, we have

$$\begin{aligned} Q(\alpha_t) - Q(\alpha_t^*) &= L(\alpha_t) - L(\alpha_t^*) + p_{\lambda_\alpha}(|\alpha_{1,t}|) - p_{\lambda_\alpha}(|\alpha_{1,t}^*|) \\ &\geq \frac{\partial L(\alpha_t^*)}{\partial \alpha_t^\top} (\alpha_t - \alpha_t^*) + (\alpha_t - \alpha_t^*)^\top \frac{\partial L(\hat{\alpha}_t^*)}{\partial \alpha_t \partial \alpha_t^\top} (\alpha_t - \alpha_t^*) + \sum_{j \in \mathcal{J}_t} \{ p_{\lambda_\alpha}(|\alpha_{1,t,j}|) - p_{\lambda_\alpha}(|\alpha_{1,t,j}^*|) \} \\ &= \mathcal{T}_1 + \mathcal{T}_2 + \mathcal{T}_3, \end{aligned} \quad (\text{A8})$$

where $\hat{\alpha}_t^*$ is between α_t and α_t^* . Considering the first term \mathcal{T}_1 , by Cauchy-Schwarz inequality, we have

$$|\mathcal{T}_1| \leq \tau \sqrt{|\mathcal{J}_t|/N} \left\| \frac{\partial L(\alpha_t^*)}{\partial \alpha_t^\top} \right\| \leq \tau \sqrt{C_1 C_5} |\mathcal{J}_t|/N,$$

where

$$\begin{aligned} \mathbb{E} \left\{ \left\| \frac{\partial L(\alpha_t^*)}{\partial \alpha_t^\top} \right\|^2 \right\} &= \mathbb{E} \left\{ \left\| \frac{1}{N} \sum_{i=1}^N \left\{ \frac{\exp(\alpha_{0,t} + \alpha_{1,t} H_{i,t})}{1 + \exp(\alpha_{0,t} + \alpha_{1,t} H_{i,t})} - A_{i,t} \right\} (1, H_{i,t}) \right\|^2 \right\} \\ &= \mathbb{E} \left\{ \left\| \frac{1}{N} \sum_{i=1}^N Z_{i,t}(1, H_{i,t}) \right\|^2 \right\} \\ &= \frac{1}{N^2} \text{trace} \left\{ \sum_{i=1}^N \mathbb{E} (Z_{i,t}^2) H_{i,t} H_{i,t}^\top \right\} \\ &\leq \frac{C_1}{N^2} |\mathcal{J}_t| \sigma_{\max} \left(\sum_{i=1}^N H_{i,t} H_{i,t}^\top \right) \leq C_1 C_5 |\mathcal{J}_t|/N, \end{aligned}$$

under Assumptions A2 (b) and (d). Considering \mathcal{T}_2 , we have

$$\begin{aligned}
\mathcal{T}_2 &= (\alpha_t - \alpha_t^*)^\top \frac{\partial L(\hat{\alpha}_t^*)}{\partial \alpha_t \partial \alpha_t^\top} (\alpha_t - \alpha_t^*) \\
&= (\alpha_t - \alpha_t^*)^\top \Sigma_{Z_{i,t}} (\alpha_t - \alpha_t^*) \\
&\quad + (\alpha_t - \alpha_t^*)^\top \left\{ \frac{\partial L(\hat{\alpha}_t^*)}{\partial \alpha_t \partial \alpha_t^\top} - \frac{\partial L(\alpha_t^*)}{\partial \alpha_t \partial \alpha_t^\top} \right\} (\alpha_t - \alpha_t^*) \\
&= \mathcal{T}_{21} + \mathcal{T}_{22}.
\end{aligned}$$

For \mathcal{T}_{21} ,

$$\begin{aligned}
\mathcal{T}_{21} &= (\alpha_t - \alpha_t^*)^\top \Sigma_{Z_{i,t}} (\alpha_t - \alpha_t^*) \\
&\leq C_3 \|\alpha_t - \alpha_t^*\|^2 \leq C_3 \tau^2 |\mathcal{J}_t| / N,
\end{aligned}$$

under Assumptions A2 (c). For \mathcal{T}_{22} ,

$$\begin{aligned}
\mathcal{T}_{22} &= (\alpha_t - \alpha_t^*)^\top \left\{ \frac{\partial L(\hat{\alpha}_t^*)}{\partial \alpha_t \partial \alpha_t^\top} - \frac{\partial L(\alpha_t^*)}{\partial \alpha_t \partial \alpha_t^\top} \right\} (\alpha_t - \alpha_t^*) \\
&= B \|\alpha_t - \alpha_t^*\|^2 \|\hat{\alpha}_t^* - \alpha_t^*\| \cdot \sigma_{\max} \left(\frac{1}{N} \sum_{i=1}^N H_{i,t,\mathcal{J}_t} H_{i,t,\mathcal{J}_t}^\top \right) \\
&= B \cdot (\tau \sqrt{|\mathcal{J}_t|/N})^3 = o(|\mathcal{J}_t|/N),
\end{aligned}$$

where

$$\begin{aligned}
&\frac{\partial L(\hat{\alpha}_t^*)}{\partial \alpha_t \partial \alpha_t^\top} - \frac{\partial L(\alpha_t^*)}{\partial \alpha_t \partial \alpha_t^\top} \\
&= \frac{1}{N} \sum_{i=1}^N \left\{ \frac{\exp(\hat{\alpha}_{0,t}^* + \hat{\alpha}_{1,t}^* H_{i,t})}{\{1 + \exp(\hat{\alpha}_{0,t}^* + \hat{\alpha}_{1,t}^* H_{i,t})\}^2} - \frac{\exp(\alpha_{0,t}^* + \alpha_{1,t}^* H_{i,t})}{\{1 + \exp(\alpha_{0,t}^* + \alpha_{1,t}^* H_{i,t})\}^2} \right\} (1, H_{i,t})(1, H_{i,t})^\top \\
&= \frac{1}{N} \sum_{i=1}^N B \cdot (\hat{\alpha}_t^* - \alpha_t^*)(1, H_{i,t})(1, H_{i,t})^\top,
\end{aligned}$$

where

$$B = \sup_{\alpha_t \in \mathfrak{M}_\tau} \left\{ \frac{\exp(\hat{\alpha}_{0,t}^* + \hat{\alpha}_{1,t}^* H_{i,t})}{\{1 + \exp(\hat{\alpha}_{0,t}^* + \hat{\alpha}_{1,t}^* H_{i,t})\}^2} - \frac{\exp(\alpha_{0,t}^* + \alpha_{1,t}^* H_{i,t})}{\{1 + \exp(\alpha_{0,t}^* + \alpha_{1,t}^* H_{i,t})\}^2} \right\} \|H_{i,t}\|_{\max},$$

which is bounded by Assumptions A2 (a). Considering the third term \mathcal{T}_3

$$\begin{aligned}
\mathcal{T}_3 &= \sum_{j \in \mathcal{J}_t} \{p_{\lambda_\alpha}(|\alpha_{1,t,j}|) - p_{\lambda_\alpha}(|\alpha_{1,t,j}^*|)\} \\
&= \sum_{j \in \mathcal{J}_t} p'_{\lambda_\alpha}(|\alpha_{1,t,j}^*|) \text{sgn}(\alpha_{1,t,j}^*) (\alpha_{1,t,j} - \alpha_{1,t,j}^*) \\
&\quad + \sum_{j \in \mathcal{J}_t} p''_{\lambda_\alpha}(|\hat{\alpha}_{1,t,j}^*|) (\alpha_{1,t,j} - \alpha_{1,t,j}^*)^2 \\
&= \sqrt{|\mathcal{J}_t|} \max \{|p'_{\lambda_\alpha}(|\alpha_{1,t,j}^*|)| : j \in \mathcal{J}_t\} \cdot \tau \sqrt{|\mathcal{J}_t|/N} \\
&\quad + \max \{|p''_{\lambda_\alpha}(|\alpha_{1,t,j}^*|)| : j \in \mathcal{J}_t\} \cdot \tau^2 |\mathcal{J}_t|/N,
\end{aligned}$$

where $\widehat{\alpha}_{1,t,j}^*$ is between $\alpha_{1,t,j}$ and $\alpha_{1,t,j}^*$. If $p_{\lambda_\alpha}(x)$ be the SCAD penalty function, we have

$$\begin{aligned} p'_\lambda(|\theta|) &= \lambda \left\{ I(|\theta| < \lambda) + \frac{(a\lambda - |\theta|)_+}{(a-1)\lambda} I(|\theta| \geq \lambda) \right\}, \\ p''_\lambda(|\theta|) &= \frac{-1}{(a-1)\lambda} I(\lambda \leq |\theta| \leq a\lambda). \end{aligned}$$

Therefore, under Assumption A2(e), \mathcal{T}_3 is dominated by \mathcal{T}_2 with a proper choice of λ_α . In addition, by choosing a sufficiently large τ , \mathcal{T}_{21} dominates the right-hand side of (A8) in the ball \mathfrak{M}_τ . Since \mathcal{T}_{21} is positive for sufficiently large N , (A7) holds and hence $\widehat{\alpha}_t - \alpha_t^* = O(\sqrt{|\mathcal{J}_t|/N})$.

For proving (A3), it is sufficient to show that for any $j \in \mathcal{J}_t^c$, we have

$$\begin{aligned} \frac{\partial Q(\alpha_t)}{\partial \alpha_{t,j}} &< 0, \quad \alpha_{t,j} < 0, \\ \frac{\partial Q(\alpha_t)}{\partial \alpha_{t,j}} &> 0, \quad \alpha_{t,j} > 0, \end{aligned}$$

where $\alpha_{t,j} \in \mathfrak{M}_\tau$. To show this, by Taylor's expansion, we have

$$\begin{aligned} \frac{\partial Q(\alpha_t)}{\partial \alpha_{t,j}} &= \frac{\partial L(\alpha_t)}{\partial \alpha_{t,j}} + p'_{\lambda_\alpha}(|\alpha_{t,j}|) \text{sgn}(\alpha_{t,j}) \\ &= \frac{\partial L(\alpha_t^*)}{\partial \alpha_{t,j}} + \sum_l \frac{\partial L(\alpha_t^*)}{\partial \alpha_{t,j} \partial \alpha_{t,l}} (\alpha_{t,l} - \alpha_{t,l}^*) \\ &\quad + \sum_{l,k} \frac{\partial L(\widehat{\alpha}_t^*)}{\partial \alpha_{t,j} \partial \alpha_{t,l} \partial \alpha_{t,k}} \times (\alpha_{t,l} - \alpha_{t,l}^*)(\alpha_{t,k} - \alpha_{t,k}^*) + p'_{\lambda_\alpha}(|\alpha_{t,j}|) \text{sgn}(\alpha_{t,j}) \end{aligned}$$

where $\widehat{\alpha}_t^*$ lies between α_t and α_t^* . Under Assumptions A2 (a), (b) and (c),

$$\frac{\partial L(\alpha_t^*)}{\partial \alpha_{t,j}} = O(N^{-1/2}), \quad \frac{\partial L(\alpha_t^*)}{\partial \alpha_{t,j} \partial \alpha_{t,l}} = \mathbb{E} \left\{ \frac{\partial L(\alpha_t^*)}{\partial \alpha_{t,j} \partial \alpha_{t,l}} \right\} + o(1).$$

As $\alpha_t \in \mathfrak{M}_r$, we have

$$\frac{\partial Q(\alpha_t)}{\partial \alpha_{t,j}} = \lambda_\alpha \{ \lambda_\alpha^{-1} p'_{\lambda_\alpha}(|\alpha_{t,j}|) \text{sgn}(\alpha_{t,j}) + O(N^{-1/2}/\lambda_\alpha) \}.$$

where $\lambda_\alpha^{-1} p'_{\lambda_\alpha}(|\alpha_{t,j}|) > 0$ under the SCAD penalty and $N^{-1/2}/\lambda_\alpha \rightarrow 0$ by Assumption A2(e). Therefore, the sign of derivative is completely determined by $\alpha_{t,j}$ and hence completes the proof. \square

A2.4 Proof of Lemma A4

Lemma A4. *Under Assumptions 1-4 and regularity conditions in Assumption A3 of the Appendix, we have for $r = 1, \dots, r_1$*

$$\sup_{i=1, \dots, N} |G_r^*(X_{0,i}) - \sum_{j=1}^{d_\Phi} b_{j,r} \Phi_j(X_{0,i})|^2 = O(d_\Phi^{-\tau}),$$

where $\tau = 2(q + \beta) \geq 4$ for (q, β) defined in (A9), and the sieve coefficients $b_{j,r}$ satisfy that $\max_{j,r} b_{j,r}^2 < \infty$.

Assumption A3. (a) $\mathbf{U}_1^{*\top} \mathbf{U}_1^* = I_{r_1} = G^*(\mathbf{X}_0)^\top G^*(\mathbf{X}_0) + \mathbf{\Gamma}^\top \mathbf{\Gamma}$ and $G^*(\mathbf{X}_0)^\top \mathbf{\Gamma} = 0$.

(b) For the basis functions, there exist constants $C_1, C_2 > 0$ such that

$$C_0 < \frac{1}{N} \sigma_{\min} \{ \Phi(\mathbf{X}_0)^\top \Phi(\mathbf{X}_0) \} < \frac{1}{N} \sigma_{\max} \{ \Phi(\mathbf{X}_0)^\top \Phi(\mathbf{X}_0) \} < C_1,$$

and $\max_{i=1,\dots,N} \|\Phi(X_{i,0})\| < C_2$.

(c) Let $G^*(X_{i,0}) = \{G_1^*(X_{i,0}), \dots, G_{r_1}^*(X_{i,0})\}^\top$, the functions $G_r^*(X), r = 1, \dots, r_1$ belong to a Hölder class \mathfrak{G} defined by

$$\mathfrak{G} = \{G \in \mathfrak{G}^q : \sup_{\mathbf{u}, \mathbf{v}} |G^{(q)}(\mathbf{u}) - G^{(q)}(\mathbf{v})| \leq C_3 \|\mathbf{u} - \mathbf{v}\|_2^\beta\}, \quad (\text{A9})$$

for some positive number C_3 . Here, \mathfrak{G}^q is the space of all q -times continuously differentiable real-value functions, and $G^{(q)}$ is the q -th derivative of the function G .

Assumption (a) is the identification assumption used in factor analysis (Bai & Li, 2012) and implies that the residual loading component $\mathbf{\Gamma}$ is bounded. Assumption (b) ensures that $\Phi(\mathbf{X}_0)^\top \Phi(\mathbf{X}_0)$ is well-conditioned and this condition can be achieved by common basis functions, such as polynomial basis functions or B-splines under proper normalization. Assumption (c) imposes mild smoothness on the unknown function $G^*(\mathbf{X}_0)$, which is critical for sieve approximation (X. Chen, 2007).

Proof of Lemma A4. Under Assumptions A3, the sieve approximation is well-controlled and its accuracy is guaranteed; see X. Chen (2007) for more details. \square

A2.4.1 Proof of Lemma A1

Proof. Let \mathcal{A} and \mathcal{B} be two real tensors in $\mathbb{R}^{I_1 \times \dots \times I_M}$. Define two generalized Einstein products $\mathcal{A} \bar{\square} \mathcal{B}$ and $\mathcal{A} \underline{\square} \mathcal{B}$ be

$$(\mathcal{A} \bar{\square} \mathcal{B})_{i_1, \dots, i_m, j_1, \dots, j_m} = \sum_{k_1, \dots, k_{M-m}} a_{i_1 \dots i_m k_1 \dots k_{M-m}} b_{j_1 \dots j_m k_1 \dots k_{M-m}}$$

and

$$(\mathcal{A} \underline{\square} \mathcal{B})_{k_1, \dots, k_{N-m}, k'_1, \dots, k'_{N-m}} = \sum_{i_1, \dots, i_m} a_{i_1 \dots i_m, k_1 \dots k_{N-m}} b_{i_1 \dots i_m, k'_1 \dots k'_{M-m}},$$

where $m = [M/2]$, $\mathcal{A} \bar{\square} \mathcal{B} \in \mathbb{R}^{I_1 \times \dots \times I_m \times I_1 \times \dots \times I_m}$ and $\mathcal{A} \underline{\square} \mathcal{B} \in \mathbb{R}^{I_{m+1} \times \dots \times I_M \times I_{m+1} \times \dots \times I_M}$. Similarly, we define the spectral norm of \mathcal{A} by $\|\mathcal{A}\| \bar{\square} = \sqrt{\|\mathcal{A} \bar{\square} \mathcal{A}\| \bar{\square}}$, and it has been shown by Lemma 4.2 and 4.3 in Luo et al. (2020) that $\|\mathcal{A}\| \bar{\square} = \|D(\mathcal{A})\| \bar{\square} = \|D(\mathcal{A})\| \bar{\square}$, where $D(\cdot)$ is the dilation operator.

By applying Theorem 6.1.1 in Tropp et al. (2015) to $\bar{f}(\mathcal{A})$, where $\bar{f}(\cdot)$ is a bijective linear transformation:

$$\bar{f} : \mathbb{R}^{I_1 \times \dots \times I_M} \rightarrow \mathbb{R}^{\prod_{k=1}^m I_k \times \prod_{k=1}^{M-m} I_{k+m}}$$

such that for any tensor $\mathcal{A} \in \mathbb{R}^{I_1 \times \dots \times I_M}$,

$$(\bar{f}(\mathcal{A}))_{ij} = a_{i_1 \dots i_m, j_1 \dots j_{M-m}},$$

where

$$i = i_1 + \sum_{k=2}^m \left((i_k - 1) \prod_{l=1}^{k-1} I_l \right), \quad j = j_1 + \sum_{k=2}^{M-m} \left((j_k - 1) \prod_{l=1}^{k-1} I_{l+m} \right),$$

the results of Lemma A1 follow. \square

A2.4.2 Proof of Lemma A2

Proof. We aim to prove that

$$\sum_{\Omega_{i,t,l}=1} \Delta_{i,t,l}^2 \geq \frac{p_{\min}}{2} \sum_{i,t,l} \Delta_{i,t,l}^2 - 2\|\Delta\|_{\max}^2 \vartheta$$

with high probability. Let for any $\Delta \in \mathfrak{C}(r_1, r_2, r_3, \mu_0, L_0)$:

$$\|\Delta\|_{L^2(\Omega)}^2 \geq p_{\min} \|\Delta\|_F^2 \geq L_0^2 \theta, \quad \|\Delta\|_{\max} \leq 2L_0,$$

where the first inequality is shown in Lemma A10 and the second inequality by definition. By Lemma A11, we have for small enough C_4 (e.g., $C_4 = 0.005$)

$$\begin{aligned} & \mathbb{P}_{\mathcal{A}} \left\{ \frac{p_{\min}}{2} \sum_{i,t,l} (\mathcal{Y}_{i,t,l}^* - \hat{\mathcal{Y}}_{i,t,l})^2 \geq \sum_{\Omega_{i,t,l}=1} (\mathcal{Y}_{i,t,l}^* - \hat{\mathcal{Y}}_{i,t,l})^2 + 2\|\Delta\|_{\max}^2 \vartheta \right\} \\ &= \mathbb{P}_{\mathcal{A}} \left\{ \frac{p_{\min}}{2} \|\Delta\|_F^2 \geq \|P_{\Omega}(\Delta)\|_F^2 + 2\|\Delta\|_{\max}^2 \vartheta \right\} \\ &\leq \mathbb{P}_{\mathcal{A}} \left\{ \frac{1}{2} \left\| \frac{\Delta}{L_0} \right\|_{L^2(\Omega)}^2 \geq \|P_{\Omega} \frac{\Delta}{L_0}\|_F^2 + 2\left\| \frac{\Delta}{L_0} \right\|_{\max}^2 \vartheta \right\} \\ &\leq 2 \exp \left(-\frac{C_4 \theta}{T} \right)^{\theta=C''T \log(N+T+K)} \leq \frac{1}{(N+T+K)^2}, \end{aligned}$$

which completes the proof. \square

A2.4.3 Proof of Lemma A5

Lemma A5. Let $\mathcal{X} \in \mathbb{R}^{p_1 \times p_2 \times p_3}$, we have

$$\|\mathcal{X}\|_* = \left\{ \min \sum_{i=1}^r |\lambda_i| : \mathcal{X} = \sum_{i=1}^r \lambda_i \mathbf{a}_i \otimes \mathbf{b}_i \otimes \mathbf{c}_i, \|\mathbf{a}_i\| = \|\mathbf{b}_i\| = \|\mathbf{c}_i\| = 1, i = 1, \dots, r \right\}.$$

Proof. see (Hogben, 2013) for proofs. Note that the nuclear matrix norm has a similar characterization as well. \square

A2.4.4 Proof of Lemma A6

Lemma A6. Let $\mathcal{X} \in \mathbb{R}^{p_1 \times p_2 \times p_3}$ and $\mathcal{Y} \in \mathbb{R}^{p_1 \times p_2 \times p_3}$, then, $|\langle \mathcal{X}, \mathcal{Y} \rangle| \leq \|\mathcal{X}\| \|\mathcal{Y}\|_*$.

Proof. By Lemma A5, we know that $\mathcal{Y} = \sum_{i=1}^r \lambda_i \mathbf{a}_i \otimes \mathbf{b}_i \otimes \mathbf{c}_i$ with $\|\mathbf{a}_i\| = \|\mathbf{b}_i\| = \|\mathbf{c}_i\| = 1$ and $\|\mathcal{Y}\|_* = \sum_{i=1}^r \lambda_i$. Therefore, we have

$$|\langle \mathcal{X}, \mathcal{Y} \rangle| = \left| \langle \mathcal{X}, \sum_{i=1}^r \lambda_i \mathbf{a}_i \otimes \mathbf{b}_i \otimes \mathbf{c}_i \rangle \right| \leq \sum_{i=1}^r |\lambda_i| |\langle \mathcal{X}, \mathbf{a}_i \otimes \mathbf{b}_i \otimes \mathbf{c}_i \rangle| \leq \|\mathcal{X}\| \|\mathcal{Y}\|_*.$$

\square

A2.4.5 Proof of Lemma A7

Lemma A7. Let $\mathcal{X} \in \mathfrak{C}(r_1, r_2, r_3, L_0)$, then

$$\|\mathcal{X}\|_* \leq \sqrt{\frac{(r_1 \wedge d_\Phi)r_2r_3}{\max\{(r_1 \wedge d_\Phi), r_2, r_3\}}} \|\mathcal{X}\|_F.$$

Proof. Similar to the proof of Lemma 2 in Wang & Li (2020). Let $\mathbf{e}_N, \mathbf{e}_T$, and \mathbf{e}_K be the standard orthonormal basis of the three modes of \mathcal{X} . Then

$$\begin{aligned} \mathcal{X} &= \sum_{i \in [N], t \in [T]} \lambda_{K,i,t}^* \otimes \mathbf{e}_{N,i} \otimes \mathbf{e}_{T,t} \\ &= \sum_{i \in \mathcal{I}_1, t \in \mathcal{I}_2} \lambda_{K,i,t} \otimes \mathbf{e}_{N,i} \otimes \mathbf{e}_{T,t}, \end{aligned}$$

where $\lambda_{K,i,t}^*$ and $\lambda_{K,i,t}$ are two third-mode vectors of \mathcal{X} , the second inequality is based on $\mathcal{X} \in \mathfrak{C}(r_1, r_2, r_3, \mu_0, L_0)$ and $(\mathcal{I}_1, \mathcal{I}_2)$ are two appropriate indices of first and second modes with $|\mathcal{I}_1| = d_\Phi \wedge r_1$ and $|\mathcal{I}_2| = r_2$. Then, we have

$$\begin{aligned} \|\mathcal{X}\|_F^2 &= \sum_{i \in \mathcal{I}_1, t \in \mathcal{I}_2} \langle \lambda_{K,i,t} \otimes \mathbf{e}_{N,i} \otimes \mathbf{e}_{T,t}, \lambda_{K,i,t} \otimes \mathbf{e}_{N,i} \otimes \mathbf{e}_{T,t} \rangle = \sum_{i \in \mathcal{I}_1, t \in \mathcal{I}_2} \|\lambda_{K,i,t}\|^2, \\ \|\mathcal{X}\|_* &= \sum_{i \in \mathcal{I}_1, t \in \mathcal{I}_2} \|\lambda_{K,i,t}\|. \end{aligned}$$

By Cauchy-Schwarz inequality, we have

$$\|\mathcal{X}\|_* = \sum_{i \in \mathcal{I}_1, t \in \mathcal{I}_2} \|\lambda_{K,i,t}\| \leq \sqrt{(d_\Phi \wedge r_1)r_2} \sum_{i \in \mathcal{I}_1, t \in \mathcal{I}_2} \|\lambda_{K,i,t}\|^2 = \sqrt{(d_\Phi \wedge r_1)r_2} \|\mathcal{X}\|_F.$$

Similar inequalities hold for $\lambda_{N,t,l}$ and $\lambda_{T,i,l}$ as the first and second mode vector of \mathcal{X} . Thus, we have

$$\|\mathcal{X}\|_* \leq \sqrt{(d_\Phi \wedge r_1)r_3} \|\mathcal{X}\|_F, \quad \|\mathcal{X}\|_* \leq \sqrt{r_2r_3} \|\mathcal{X}\|_F.$$

To sum up, the upper bound of the nuclear norm of a tensor $\mathcal{X} \in \mathfrak{C}(r_1, r_2, r_3, L_0)$ is

$$\|\mathcal{X}\|_* \leq \sqrt{\frac{(r_1 \wedge d_\Phi)r_2r_3}{\max\{(r_1 \wedge d_\Phi), r_2, r_3\}}} \|\mathcal{X}\|_F,$$

which completes the proof. \square

A2.4.6 Proof of Lemma A8

Lemma A8. For any core tensor $\mathcal{G} \in \mathbb{R}^{r_1 \times r_2 \times 3}$ and $\mathcal{M}_1(\mathcal{G}) = \sum_{i=1}^{r_1} \sigma_i \mathbf{x}_i \otimes \mathbf{z}_i$ being its singular value decomposition, we have

$$\|\mathcal{G}\|_* \leq r_1 \sqrt{r_2 \wedge r_3} \|\mathcal{M}_1(\mathcal{G})\|.$$

Similar results hold for matrix flattening in modes 2 and 3. The inequality becomes equality when $r_1 = 1$.

Let $Z_i \in \mathbb{R}^{r_2 \times r_3}$ be the matrix reformulation of $\mathbf{z}_i \in \mathbb{R}^{r_2 r_3}$, which has the singular value decomposition as

$$Z_i = \sum_{j=1}^{r_2 \wedge r_3} \mu_{i,j} \mathbf{v}_{i,j} \otimes \mathbf{w}_{i,j}, \quad i = 1, \dots, r_1.$$

Since $\mathcal{M}_1(\mathcal{G}) = \sum_{i=1}^{r_1} \sigma_i \mathbf{x}_i \otimes \mathbf{z}_i$, under the isomorphism with the matricization in mode 1 (Lemma 3.1 in Hu (2015)), we have

$$\mathcal{G} = \sum_{i=1}^{r_1} \sigma_i \mathbf{x}_i \otimes \left\{ \sum_{j=1}^{r_2 \wedge r_3} \mu_{i,j} \mathbf{v}_{i,j} \otimes \mathbf{w}_{i,j} \right\}.$$

Then, followed by the definition of nuclear norm, we have

$$\begin{aligned} \|\mathcal{G}\|_* &\leq \sum_{i=1}^{r_1} \sigma_i \sum_{j=1}^{r_2 \wedge r_3} \mu_{i,j} \leq \left(r_1 \max_i \sigma_i \right) \left(\max_i \sum_{j=1}^{r_2 \wedge r_3} \mu_{i,j} \right) \\ &\leq r_1 \|\mathcal{M}_1(\mathcal{G})\| \|\mathbf{z}_i\|_* \leq r_1 \sqrt{r_2 \wedge r_3} \|\mathcal{M}_1(\mathcal{G})\|, \end{aligned}$$

where $\|\mathbf{z}_i\|_* = \max\{\|Z_i\|_* : 1 \leq i \leq r_1\}$. The last inequality is based on Lemma A9 and $1 = \mathbf{z}_i^\top \mathbf{z}_i = \text{trace}(Z_i^\top Z_i) = \|Z_i\|_F^2$ for any $i = 1, \dots, r_1$.

A2.4.7 Proof of Lemma A9

Lemma A9. *Let $Z \in \mathbb{R}^{r_2 \times r_3}$, we have $\|Z\|_* \leq \sqrt{r_2 \wedge r_3} \|Z\|_F$.*

Let $Z = \sum_{i=1}^{r_2 \wedge r_3} \sigma_i \mathbf{u}_i \otimes \mathbf{v}_i$ be the singular value decomposition of Z , we know that

$$\|Z\|_* = \sum_{i=1}^{r_2 \wedge r_3} \sigma_i, \quad \|Z\|_F = \sqrt{\sum_{i=1}^{r_2 \wedge r_3} \sigma_i^2}.$$

By Cauchy-Schwarz inequality, we have

$$\frac{\|Z\|_*}{r_2 \wedge r_3} \leq \sqrt{\frac{\|Z\|_F^2}{r_2 \wedge r_3}},$$

which completes the proof after rearrangement.

A2.4.8 Proof of Lemma A10

Lemma A10. $p_{\min} < \mathbb{P}(A_{i,(t-k+1):t} = a_{(t-k+1):t} \mid H_{i,t}) \leq p_{\max}$ and $p_{\min} < \mathbb{P}(A_{i,(t-k+1):t} = a_{(t-k+1):t}) \leq p_{\max}$, where $p_{\min} = \delta^k$ and $p_{\max} = (1 - \delta)^k$.

Proof. The first statement is straightforward under Assumption 4. For the second one, we have by the law of expectation

$$\begin{aligned} \mathbb{P}(A_{i,t-k+1:t} = a) &= \mathbb{E}\{\mathbb{P}(A_{i,t-k+1:t} = a \mid H_{i,t})\} \\ &= \int_{H_{i,t}} \mathbb{P}(A_{i,t-k+1:t} = a \mid H_{i,t}) dF(H_{i,t}), \end{aligned}$$

where $F(H_{i,t})$ is the joint cumulative probability function of $H_{i,t}$. Under the positivity assumption in Assumption 4 with constant δ , we have $\delta^k < \mathbb{P}(A_{i,t-k+1:t} = a \mid H_{i,t}) < (1 - \delta)^k$ for any $a \in \mathbb{A}$ and the desired bound follows. \square

A2.4.9 Proof of Lemma A11

Lemma A11. Define the constraint set

$$\mathfrak{B}(\theta, \tau) = \{\Delta \in \mathbb{R}^{N \times T \times K} : \|\Delta\|_{L^2(\Omega)}^2 \geq \theta, \|\Delta\|_* \leq \sqrt{\tau} \|\Delta\|_F, \|\Delta\|_{\max} \leq 1\}$$

Define

$$\vartheta = \frac{(r_1 \wedge d_\Phi) r_2 r_3}{\max\{(r_1 \wedge d_\Phi), r_2, r_3\} p_{\min}} k^2 (N \vee T) \log(N + T + K).$$

Whenever $\Delta \in \mathfrak{B}(\theta, \tau)$ and there exist small enough constant C_4 (e.g., $C_4 = 0.005$) s.t. $C_4 \theta > T$

$$\mathbb{P}_{\mathcal{A}} \left\{ \frac{1}{2} \|\Delta\|_{L^2(\Omega)}^2 \geq \|P_\Omega \Delta\|_F^2 + 2\vartheta \right\} \leq 2 \exp \left(-\frac{C_4 \theta}{T} \right).$$

Proof. Our proof is based on the standard peeling argument. Let ξ be a constant larger than 1 (e.g., $\xi = 2$) and define for every $\rho \geq 0$

$$\mathfrak{B}_\rho(\theta, \tau) = \{\Delta \in \mathfrak{B}(\theta, \tau) : \rho \leq \|\Delta\|_{L^2(\Omega)}^2 \leq \rho \xi\}.$$

And we have $\mathfrak{B}(\theta, \tau) = \bigcup_{l=1}^{\infty} \mathfrak{B}_{\theta \xi^{l-1}}(\theta, \tau)$, therefore, for some $l \geq 1$ and $\Delta \in \mathfrak{B}_{\theta \xi^{l-1}}(\theta, \tau)$, we have

$$\|\Delta\|_{L^2(\Omega)}^2 - \|P_\Omega \Delta\|_F^2 \geq \frac{1}{2} \|\Delta\|_{L^2(\Omega)}^2 + 2\vartheta \geq \frac{1}{2\xi} \theta \xi^l + 2\vartheta.$$

Define this as the bad event

$$\mathcal{E}(\Omega)_l = \left\{ \exists \Delta \in \mathfrak{B}_{\theta \xi^{l-1}}(\theta, \tau) \mid \left| \|P_\Omega \Delta\|_F^2 - \|\Delta\|_{L^2(\Omega)}^2 \right| \geq \frac{1}{2\xi} \theta \xi^l + 2\vartheta \right\},$$

and $\mathcal{E}(\Omega) = \left\{ \exists \Delta \in \mathfrak{B}(\theta, \tau) \mid \|\Delta\|_{L^2(\Omega)}^2 - \|P_\Omega \Delta\|_F^2 \geq \frac{1}{2} \|\Delta\|_{L^2(\Omega)}^2 + 2\vartheta \right\} \subset \bigcup_{l=1}^{\infty} \mathcal{E}(\Omega)_l$, that is, if $\mathcal{E}(\Omega)$ holds for some tensor Δ , then this Δ must belong to $\mathfrak{B}_{\theta \xi^{l-1}}(\theta, \tau)$ for some l . Hence, by Lemma A12, we have

$$\mathbb{P}_{\mathcal{A}} \{ \mathcal{E}(\Omega)_l \} \leq \exp \left(-\frac{C_3 \xi^l \theta}{T} \right) \leq \exp \left(-\frac{C_3 l \log(\xi) \theta}{T} \right) \leq \exp \left(-\frac{0.5 C_3 l \theta}{T} \right),$$

since $\xi^l \geq l \log(\xi)$ for $\xi = 2$. Then, let $C_4 = 0.5 C_3$ and by union bound, we have

$$\mathbb{P}_{\mathcal{A}} \{ \mathcal{E}(\Omega) \} \leq \sum_{l=1}^{\infty} \left\{ \exp \left(-\frac{C_4 \theta}{T} \right) \right\}^l = \frac{\exp \left(-\frac{C_4 \theta}{T} \right)}{1 - \exp \left(-\frac{C_4 \theta}{T} \right)} \leq 2 \exp \left(-\frac{C_4 \theta}{T} \right),$$

if $C_4 \theta > T$ and

$$\mathbb{P}_{\mathcal{A}} \left\{ \frac{1}{2} \|\Delta\|_{L^2(\Omega)}^2 \geq \|P_\Omega \Delta\|_F^2 + 2\vartheta \right\} \leq \mathbb{P}_{\mathcal{A}}(\mathcal{B}) \leq 2 \exp \left(-\frac{C_4 \theta}{T} \right),$$

which completes the proof. \square

A2.4.10 Proof of Lemma A12

Lemma A12. *Let*

$$\tilde{\mathcal{Z}}_\rho = \sup_{\Delta \in \mathfrak{B}_\rho(\theta, \tau)} \left| \|P_\Omega \Delta\|_F^2 - \|\Delta\|_{L^2(\Omega)}^2 \right| = \sup_{\Delta \in \mathfrak{B}_\rho(\theta, \tau)} \left| \sum_{i=1}^N \|\Delta_\Omega^{(i)}\|_F^2 - \|\Delta\|_{L^2(\Omega)}^2 \right|.$$

where $\Delta_\Omega^{(i)} = \sum_{t=1}^T \Delta_{i,t, (A_{i,(t-k+1):t})_{(10)}} \cdot e_i(N) \otimes e_j(T) \otimes e_{(A_{i,(t-k+1):t})_{(10)}}(K) \in \mathbb{R}^{N \times T \times K}$. Then, there exists a small enough constant C (e.g., $C = 0.01$) s.t.

$$\mathbb{P}_{\mathcal{A}}(\tilde{\mathcal{Z}}_\rho \geq \frac{1}{2\xi} \rho \xi + 2\vartheta) \leq \exp\left(-\frac{C\rho\xi}{T}\right),$$

for any $\Delta \in \mathfrak{B}_\rho(\theta, \tau) = \{\Delta \in \mathfrak{B}(\theta, \tau) : \rho \leq \|\Delta\|_{L^2(\Omega)}^2 \leq \rho\xi\}$.

Proof. We know

$$\begin{aligned} \sigma^2 &= \sup_{\Delta \in \mathfrak{B}_\rho(\theta, \tau)} \sum_{i=1}^N \text{var}(\|\Delta_\Omega^{(i)}\|_F^2) \leq \sup_{\Delta \in \mathfrak{B}_\rho(\theta, \tau)} \sum_{i=1}^N \mathbb{E}(\|\Delta_\Omega^{(i)}\|_F^4) \\ &\leq \sup_{\Delta \in \mathfrak{B}_\rho(\theta, \tau)} \sum_{i=1}^N \left\{ \mathbb{E}(\|\Delta_\Omega^{(i)}\|_F^2) \cdot \mathbb{E}(\|\Delta_\Omega^{(i)}\|_F^2) \right\} \\ &\leq T \sup_{\Delta \in \mathfrak{B}_\rho(\theta, \tau)} \sum_{i=1}^N \mathbb{E}(\|\Delta_\Omega^{(i)}\|_F^2) \\ &= T \sup_{\Delta \in \mathfrak{B}_\rho(\theta, \tau)} \|\Delta\|_{L^2(\Omega)}^2 \leq T\rho\xi, \end{aligned}$$

where the second inequality is by Cauchy–Schwarz inequality, the third inequality is by $\|\Delta\|_{\max} \leq 1$, $\|\Delta_\Omega^{(i)}\|_F^2 \leq T$ as each subject must be observed once at each time, and the last inequality is derived by $\|\Delta\|_{L^2(\Omega)}^2 \leq \rho\xi$. By the symmetrization argument in Lemma 6.3 of Gigli & Ledoux (2013) and Lemma 14, Klopp (2014)

$$\begin{aligned} \mathbb{E}_{\mathcal{A}}(\tilde{\mathcal{Z}}_\rho) &\leq 2\mathbb{E}_{\mathcal{A}, \zeta} \left\{ \sup_{\Delta \in \mathfrak{B}_\rho(\theta, \tau)} \left| \sum_{i=1}^N \zeta_i \|\Delta_\Omega^{(i)}\|_F^2 \right| \right\} \\ &= 2\mathbb{E}_{\mathcal{A}, \zeta} \left\{ \sup_{\Delta \in \mathfrak{B}_\rho(\theta, \tau)} \left| \left\langle \sum_{i=1}^N \zeta_i \Delta_\Omega^{(i)}, \Delta \right\rangle \right| \right\} \\ &\leq 2\mathbb{E}_{\mathcal{A}, \zeta} \left\{ \sup_{\Delta \in \mathfrak{B}_\rho(\theta, \tau)} \left\| \sum_{i=1}^N \zeta_i \Delta_\Omega^{(i)} \right\| \|\Delta\|_* \right\} \\ &\leq 4 \sqrt{\frac{(r_1 \wedge d_\Phi) r_2 r_3}{\max\{(r_1 \wedge d_\Phi), r_2, r_3\}}} \mathbb{E}_{\mathcal{A}, \zeta} \left\{ \sup_{\Delta \in \mathfrak{B}_\rho(\theta, \tau)} \left\| \sum_{i=1}^N \zeta_i \Delta_\Omega^{(i)} \right\| \|\Delta\|_F \right\} \\ &\leq 4 \sqrt{\frac{(r_1 \wedge d_\Phi) r_2 r_3}{\max\{(r_1 \wedge d_\Phi), r_2, r_3\} p_{\min}}} \mathbb{E}_{\mathcal{A}, \zeta} \left\{ \sup_{\Delta \in \mathfrak{B}_\rho(\theta, \tau)} \left\| \sum_{i=1}^N \zeta_i \Delta_\Omega^{(i)} \right\| \|\Delta\|_{L^2(\Omega)} \right\} \\ &\leq 4 \sqrt{\frac{(r_1 \wedge d_\Phi) r_2 r_3 \rho \xi}{\max\{(r_1 \wedge d_\Phi), r_2, r_3\} p_{\min}}} \mathbb{E}_{\mathcal{A}, \zeta} \left\{ \sup_{\Delta \in \mathfrak{B}_\rho(\theta, \tau)} \|\Delta_\Omega^{\text{Rad}}\| \right\} \\ &\leq C_1 \rho \xi + \frac{(r_1 \wedge d_\Phi) r_2 r_3 U_{\text{Rad}}^2}{C_1 \max\{(r_1 \wedge d_\Phi), r_2, r_3\} p_{\min}}, \end{aligned}$$

where $\{\zeta_i\}_{i=1}^N$ are i.i.d. Rademacher random variables, $U_{\text{Rad}} = \mathbb{E}_{\mathcal{A}, \zeta} \left\{ \sup_{\Delta \in \mathfrak{B}_\rho(\theta, \tau)} \|\Delta_\Omega^{\text{Rad}}\| \right\}$ is the Rademacher complexity, and $\Delta_\Omega^{\text{Rad}} = \sum_{i=1}^N \zeta_i \Delta_\Omega^{(i)}$, with its (i, t, l) -entry as $\zeta_i \Delta_{i,t,l}$ if $\Omega_{i,t,l} = 1$ and zero otherwise. By Lemma A13, we invoke the Theorem 3 in Massart (2000) with $\varepsilon = 1$:

$$\mathbb{P}_{\mathcal{A}} \left\{ \tilde{\mathcal{Z}}_\rho \geq 2\mathbb{E}_{\mathcal{A}}(\tilde{\mathcal{Z}}_\rho) + 2\sigma\sqrt{x} + 34.5Tx \right\} \leq \exp(-x),$$

where $\sigma^2 = \sup_{\Delta \in \mathcal{S}_{\theta, \tau, \gamma}(\rho)} \sum_{i=1}^N \text{var}(\|\Delta_\Omega^{(i)}\|_F^2) \leq T\rho\xi$. Let $x = C_3\rho\xi/T$ with small constant C_3, C_4 ,

$$\begin{aligned} & \mathbb{P}_{\mathcal{A}} \left\{ \tilde{\mathcal{Z}}_\rho \geq \frac{1}{2\xi} \rho\xi + 2\vartheta \right\} \\ &= \mathbb{P}_{\mathcal{A}} \left\{ \tilde{\mathcal{Z}}_\rho \geq \frac{1}{2 \times 2} \rho\xi + \frac{2(r_1 \wedge d_\Phi) r_2 r_3}{\max\{(r_1 \wedge d_\Phi), r_2, r_3\} p_{\min}} k^2 (N \vee T) \log(N + T + K) \right\} \\ &\leq \mathbb{P}_{\mathcal{A}} \left\{ \tilde{\mathcal{Z}}_\rho \geq 2\sqrt{C_3\rho\xi} + 34.5C_3\rho\xi + 2C_4\rho\xi + 2 \frac{(r_1 \wedge d_\Phi) r_2 r_3}{\max\{(r_1 \wedge d_\Phi), r_2, r_3\} p_{\min}} U_{\text{Rad}}^2 \right\} \\ &\leq \mathbb{P}_{\mathcal{A}} \left\{ \tilde{\mathcal{Z}}_\rho \geq 2\sqrt{TK\rho\xi} \sqrt{C_3\rho\xi/T} + 34.5T \cdot C_3\rho\xi/T + 2\mathbb{E}_{\mathcal{A}}(\tilde{\mathcal{Z}}_\rho) \right\} \\ &\leq \mathbb{P}_{\mathcal{A}} \left\{ \tilde{\mathcal{Z}}_\rho \geq 2\sigma\sqrt{x} + 34.5Tx + 2\mathbb{E}_{\mathcal{A}}(\tilde{\mathcal{Z}}_\rho) \right\} \\ &\leq \exp \left(-\frac{C_3\rho\xi}{T} \right), \end{aligned}$$

which completed the proof. In order to get a bound in close form, we need to obtain a suitable upper bound on $U_{\text{Rad}} = \mathbb{E} \left\{ \sup_{\Delta \in \mathfrak{B}_\rho(\theta, \tau)} \|\Delta_\Omega^{\text{Rad}}\| \right\}$, which can be obtained in the case of sub-Gaussian noise. Most of the subsequent proof is adapted from Lemma 5 and 6, Klopp (2014). \square

A2.4.11 Proof of Lemma A13

Lemma A13. *For any $\Delta \in \mathfrak{B}_\rho(\theta, \tau)$, we have*

$$\mathbb{E} \left\{ \sup_{\Delta \in \mathfrak{B}_\rho(\theta, \tau)} \|\Delta_\Omega^{\text{Rad}}\| \right\} \leq C_5 k \sqrt{(N \vee T)} \|\Delta\|_{\max} \{\log(N + T + K)\}^{1/2},$$

for large enough constant C_5 .

Proof. For any $\Delta \in \mathfrak{B}_\rho(\theta, \tau)$, we separate the $\Delta_\Omega^{\text{Rad}}$ by $\Delta_\Omega^{\text{Rad}} = \sum_{h=0}^{k-1} \zeta_i \Delta_\Omega^{(i),h}$, where

$$\begin{aligned} \left\| \sum_{i=1}^N \mathbb{E} \{ D(\zeta_i \Delta_\Omega^{(i),h}) \square D(\zeta_i \Delta_\Omega^{(i),h}) \} \right\| &\leq \max_i \sum_{t,l} \Delta_{i,t,l}^2 \lesssim T \|\Delta\|_{\max}^2 \log(N + T + K), \\ \left\| \sum_{i=1}^N \mathbb{E} \{ D(\zeta_i \Delta_\Omega^{(i),h}) \square D(\zeta_i \Delta_\Omega^{(i),h}) \} \right\| &\leq \max_{t,l} \sum_i \Delta_{i,t,l}^2 \lesssim N \|\Delta\|_{\max}^2 \log(N + T + K), \end{aligned}$$

with probability greater than $1 - (N + T + K)^{-2}$ under the restriction for δ . For each $D(\zeta_i \Delta_\Omega^{(i)})$, its spectral norm is

$$\max_i \|D(\zeta_i \Delta_\Omega^{(i),h})\| \leq \max_i \max_{\|a\| = \|b\| = \|c\|} \langle D(\zeta_i \Delta_\Omega^{(i),h}), a \otimes b \otimes c \rangle \leq k^{-1/2} T^{1/2} \|\Delta\|_{\max} \cdot \log(N).$$

Let $Z_i = \zeta_i \Delta_{\Omega}^{(i),h}$ and we know that $\mathbb{E}(Z_i) = 0$, $\max_i \|Z_i\| \leq k^{-1/2} T^{1/2} \|\Delta\|_{\max} \log(N+T+K)$ for all $i \in [D]$, and $\sigma_Z^2 \leq (N \vee T) \|\Delta\|_{\max}^2 \log(N+T+K)$. Then for any $\alpha \geq 0$, we have

$$\begin{aligned} \mathbb{P}(\|D(\Delta_{\Omega}^{\text{Rad},h})\| \geq \alpha) &\leq (N+T+K) \exp \left\{ \frac{-\alpha^2}{2\sigma_Z^2 + (2k^{-1/2} T^{1/2} \|\Delta\|_{\max} \log(N) \alpha) / 3} \right\} \\ &\leq (N+T+K) \exp \left[-\frac{3}{4} \min \left\{ \frac{\alpha^2}{\sigma_Z^2}, \frac{\alpha}{k^{-1/2} T^{1/2} \|\Delta\|_{\max} \log(N)} \right\} \right] \\ &\leq (N+T+K) \exp \left(-\frac{3}{4} \frac{\alpha^2}{(N \vee T) \|\Delta\|_{\max}^2 \log(N+T+K)} \right). \end{aligned}$$

By Hölder's inequality, we get for any $\Delta \in \mathfrak{B}_{\rho}(\theta, \tau)$ and large enough constant C_5 ,

$$\begin{aligned} \mathbb{E} \|D(\Delta_{\Omega}^{\text{Rad},h})\| &\leq \left\{ \mathbb{E} \|D(\Delta_{\Omega}^{\text{Rad}})\|^{2 \log(N+T+K)} \right\}^{1/\{2 \log(N+T+K)\}} \\ &\leq (N+T+K)^{1/\{2 \log(N+T+K)\}} \log(N+T+K) \nu_1^{-1/2} 2^{1/\{2 \log(N+T+K)\}-1/2} \\ &\leq \sqrt{2ek^{-1}(N \vee T)} \|\Delta\|_{\max} \log(N+T+K), \end{aligned}$$

where

$$\begin{aligned} \mathbb{E} \|D(\Delta_{\Omega}^{\text{Rad}}, h)\|^{2 \log(N+T+K)} &\leq \int_0^{+\infty} \mathbb{P}(\|D(\Delta_{\Omega}^{\text{Rad},h})\| > t^{1/\{2 \log(N+T+K)\}}) dt \\ &\leq (N+T+K) \int_0^{+\infty} \exp \left\{ -t^{1/\log(N+T+K)} \nu_1 \right\} dt \\ &\leq (N+T+K) \log(N+T+K) \nu_1^{-\log(N+T+K)} \Gamma\{\log(N+T+K)\} \\ &\leq (N+T+K) \log(N+T+K)^{\log(N+T+K)} \nu_1^{-\log(N+T+K)} 2^{1-\log(N+T+K)}, \end{aligned}$$

where $\nu_1 = 1/\{(N \vee T) \|\Delta\|_{\max}^2 \log(N+T+K)\}$,

$$\int_0^{+\infty} \exp \left\{ -t^{1/\log(N+T+K)} \nu_1 \right\} dt = \log(N+T+K) \nu_1^{-\log(N+T+K)} \Gamma\{\log(N+T+K)\},$$

and $\Gamma(x) \leq (x/2)^{x-1}$ for $x \geq 2$. Therefore,

$$\begin{aligned} \mathbb{E} \left\{ \sup_{\Delta \in \mathfrak{B}_{\rho}(\theta, \tau)} \|\Delta_{\Omega}^{\text{Rad}}\| \right\} &\leq \mathbb{E} \left\{ \sup_{\Delta \in \mathfrak{B}_{\rho}(\theta, \tau)} \sum_{h=0}^{k-1} \|D(\Delta_{\Omega}^{\text{Rad},h})\| \right\} \\ &\leq C_5 k \sqrt{(N \vee T)} \|\Delta\|_{\max} \{\log(N+T+K)\}^{1/2} \end{aligned}$$

for large enough constant C_5 . □